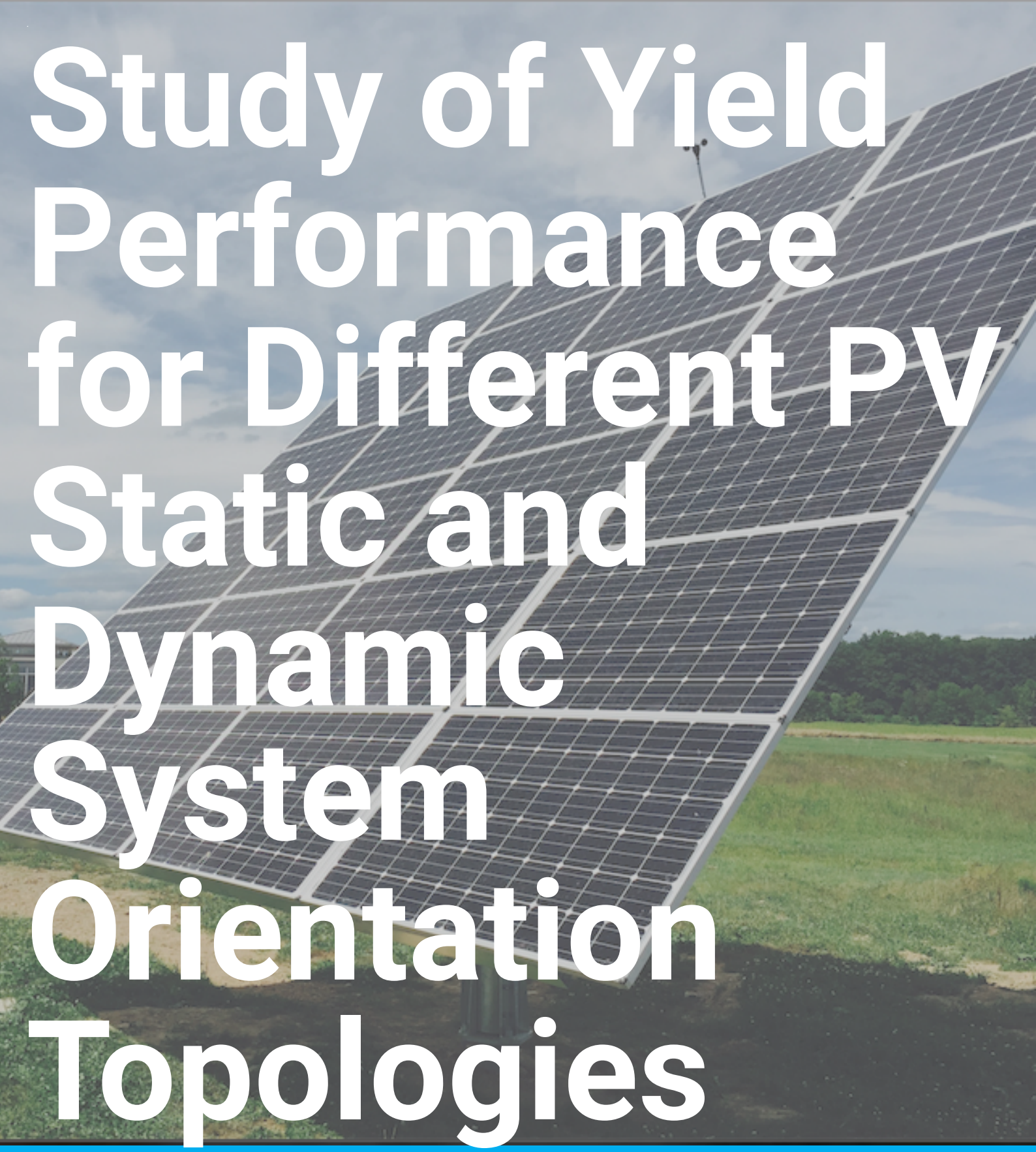

Study of Yield Performance for Different PV Static and Dynamic System Orientation Topologies

J. A. Fuentes Casillas
Student Nr. 4324781

TU Delft

PVMD
Delft University of Technology

Study of Yield Performance for Different PV Static and Dynamic System Orientation Topologies

by

J. A. Fuentes Casillas
Student Nr. 4324781

in partial fulfilment of the requirements for the degree of

Master of Science
in Sustainable Energy Technology

at the Delft University of Technology,
to be defended publicly on Wednesday August 30, 2017 at 10:00 AM.

Supervisor:	Prof. Dr. A. H. M. Smets	TU Delft
Thesis committee:	Prof. Dr. M. Zeman	TU Delft
	Dr. R. Santbergen	TU Delft
	Dr. J. Dong	TU Delft

An electronic version of this thesis is available at http://repository.tudelft.nl/.

TU Delft Delft University of Technology

PVMD Delft University of Technology

Acknowledgements

First of all, I would like to thank the rest of the members of the PVMD group for their suggestions, especially to Dr. R. Santbergen for his patience and support during this process, Prof. A. H. M. Smets for his patience and guidance throughout all these months of hard work, coding, research and that finally were finished after a long time.

Furthermore, I would like to thank my family and friends who have given me their support and companionship during all this time. They are a critical and important part of this achievement. I really want to say thank you very much to you all.

Finally, I would like to thank to the counsellors Leonie Boortman and John Stals for all their support and caring during hard times, without them I would have not been able to achieve the finalization of this Master in Sciences Degree.

J. A. Fuentes Casillas
Student Nr. 4324781
Delft, August 2017

Abstract

One of the most important aspects to consider when a PV system will be mounted, is the PV panel's orientation in order to receive the highest amount of solar radiation and thus produce as much energy as possible. This is achieved by tilting the solar panel to an optimal angle (which depends of the location's latitude) or by tracking systems which follow the Sun to get the maximum of energy from it.

In this project several topologies of PV panels will be analysed and a new one will be introduced: a floating PV module offshore. The irradiance incident on the panels and how much energy reaches the module at several static and tracking topologies. For the statical PV modules, it will be analysed and discussed which is the optimal tilting angle according to its location, (the latitude is the variable to consider in this case) as well as the monthly energy yield generated on each topology.

Finally, a comparison of incident energy yield per topology (including the new offshore one) will be assessed and discussed, indicating what are the results found in this project, which tools were used to get these results and how they were obtained.

Contents

List of Figures

List of Tables

1 Introduction

Humans have always tried to take maximum profit from the Sun throughout history. From greenhouse containers for cultivation to steam water. Today it is used to generate electricity, a crucial energetic power which determines how advanced a small neighbourhood, village, town, city, state or country really is. It is stated that a community with electricity is considered as a developed region, such as the United Nations Development Programme (UNDP) shows in its "Human Development Report" in 2015 [1]. This can be seen in something as simple such a solar lantern: children in rural areas of Africa who study using a solar lamp tend to have better performance in their grades than those who used kerosene lamps or only study when there is sunlight.

This demonstrates that electricity is synonym of development. However not all these zones in developing countries are reached by the national grid and they need to use an alternative to generate their own electricity. This is where sustainable energy technologies play an important role, being the solar photovoltaic one of the most popular technologies implemented to generate electricity at such locations.

The importance of using technologies that generate electricity without emitting CO_2 has been crucial in the last decades due to global warming, which is a serious problem that contributes to climate change. The photovoltaic technology helps to reduce the CO_2 thrown into the atmosphere.

In order to understand better how the PV panels help to fight against global warming, it is necessary to go through several steps before taking a decision about the sizing of the system. This Project will be focused mainly on what is the optimal position and tilting angle for a PV module in order to receive the highest amount of energy [kWh/m^2] during one year. This will be performed on the different static and tracking topologies which tend to be implemented for the photovoltaic systems, besides of the new offshore floating PV topology introduced in this project. Therefore, some important theoretical aspects are necessary to read first in order to have a better understanding of how the PV systems help to reduce the fossil fuels consumption and at the same time, the reduction of the production of greenhouse gases.

1.1. How Does a PV Module Work?

The operation of modern solar cells is based on the so-called "photovoltaic effect" in semiconductor materials (such as silicon). This effect refers to the generation of a potential difference at the junction of two different materials in response to the electromagnetic radiation [2].

The are three basic principles behind the "photovoltaic effect" in semiconductor materials [2]:

- 1.- Generation of the electron-hole pairs due to the absorption of photons in the semiconductor materials that form a junction
- 2.- Separation of the photo-generated electrons and holes in the junction
- 3.- Collection of the photo-generated carriers at the terminals (electrodes) of the junction.

The Figure 1.1 depicts in a simple way how the photovoltaic effect works

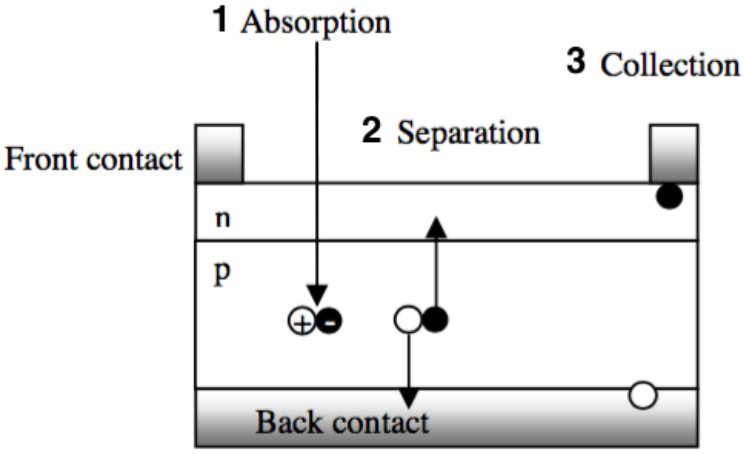

Figure 1.1: The 3 principles that rule the "photovoltaic effect".

1.2. PV Technologies

Generally, the solar cell technologies are categorized in three generations [2]:

- **1st Generation:** technologies that work with “bulk” crystalline silicon; for terrestrial applications
- **2nd Generation:** development of low-cost thin-film solar cells, which belong to this generation. They are aimed to reduce the material costs of the crystalline silicon solar cells. For terrestrial applications.
- **3rd Generation:** ultra high efficiency thin-film solar cells. They use advanced materials and new conversion concepts and processes to achieve this. Used in space applications.

Why PV? Advantages and Drawbacks

It is clear that nothing in this world can be build without consuming or polluting the environment and the fabrication of the PV modules is not the exception to the rule. So why choose them over fossil fuels? The answer would be because there is only a generation of CO_2 to the atmosphere during its fabrication, but when the module is "working" (producing electrical energy from the sunlight) it emits no CO_2 to the atmosphere. Here are some advantages and drawbacks of the pv technology:

Advantages:

- Environmentally friendly
- No emissions of CO_2 when it is working
- No noise, no moving parts (if it is does not have a tracking system)
- Does not use fossil fuels to work
- Long lifespan (25 years)
- Works during cloudy days
- Scalable (its size may change depending on the necessities)
- Minimal maintenance

Drawbacks:

- Large area is needed for large-scale applications
- No sun = no electricity production
- High initial investment costs

- Since they generate DC current, other power electronic devices such as inverters are required to go from DC to AC
- Need of batteries for stand-alone systems, which increases more the initial costs
- More investment needed if a tracking system will be implemented

Nevertheless, in the majority of the cases the payback period (which is the time passed to recover the initial investment costs) tends to be from 5-8 years, depending of how sunny the location is. This means that in average, the owner of the PV system will have 17-20 years of economical profits in terms of electrical consumption.

It is important to stress that in many countries, PV technologies are subventioned by the local governments, which means that they are cheaper for the consumer than they would actually be without this support. In this case, it could probably take longer to reach the payback time.

1.2.1. PV System Components: PV Modules and Balance of System

It is important to know which are the main components that compose a PV system. There are 5 main devices which will be briefly introduced in the next subsections:

- PV Modules
- Cables
- Inverter
- Batteries (for off-grid/stand alone systems)
- Charge controllers (for off-grid/stand alone systems)
- Other components (rack, screws, mountable pieces)

It is denominated "balance of system" to the parts which do not correspond to the PV modules, such as batteries (for off-grid systems) racking, wiring, inverter, the maintenance costs and other components [2].

1.2.2. PV Modules

Considered the main component in a PV system. They generate the electricity by using the previously mentioned "photovoltaic effect": the transformation of light into useful electricity. As it was described before, there are different types of PV modules, in which the most commonly used for households are the polycrystalline and monocrystalline modules made with silicon. Their efficiency goes from 12% up to 19% depending on the fabricator. The figure 1.2 depicts a monocrystalline PV module.

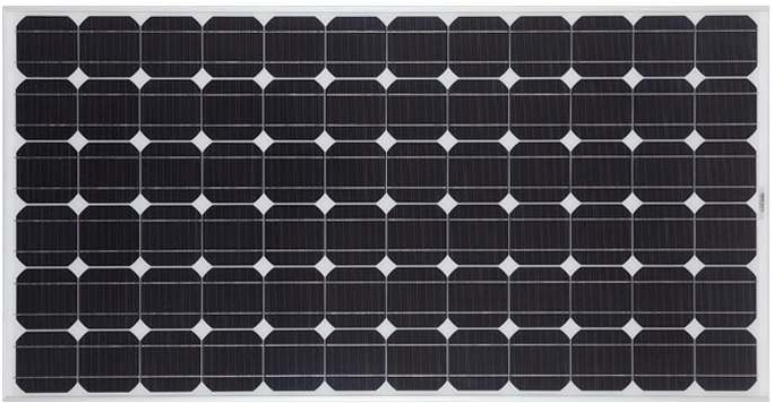

Figure 1.2: Monocrystalline silicon PV Module.

1.2.3. Inverter

All the houses have electric and electronic devices that run with AC power, thus, the use of DC/AC inverters is mandatory in order to convert the power from the PV module (in DC) into AC power. This device is used for both off-grid and on-grid system configurations. Many inverters for grid-connected systems have an internal DC-DC converter to convert the variable voltage generated in the PV array to a constant voltage, which is the input for the actual DC-AC converter.

Stand-alone systems may have an inverter connected to the batteries. The design of such inverters differs considerably from that for a grid-connected system [2]. The off-grid inverters feed the load with the power generated at the PV array and/or the battery bank and supplies a constant frequency and voltage independent of the load conditions [3]. Figure 1.3 depicts a DC-AC inverter.

Figure 1.3: DC-AC inverter.

1.2.4. Charge Controller

It is used in off-grid systems to control the charge and discharge of the battery. This prevents the overcharging (during the day) and the over-discharging (night time) of the battery bank. They count with a DC-DC converter and a maximum power point tracker (MPPT) so that the PV voltage and PV current are independent from the battery bank voltage and battery bank current [2]. Figure 1.4 shows a charge controller for PV systems. The load demand of each PV system requires a specific charge controller that satisfies the needs of the household's load. Otherwise this can lead to failures and accidents.

Figure 1.4: Charge controller for PV systems [4]

1.2.5. Batteries

One of the most important components for a stand-alone configuration. It provides electricity to the system during the night and in periods with weak sunlight. The Figure 1.5 depicts a battery bank for a photovoltaic system. The Depth of Discharge (DoD) is one important aspect to consider when selecting the batteries, since it is the depth until which the battery can be effectively used. The lower the DoD, the higher the battery bank capacity requirement. On the other hand, the higher the battery's DoD, it can be discharged more, and therefore, lower the battery bank capacity needed reducing at the same time the investment costs [2].

Figure 1.5: Battery bank for a PV system [5]

1.2.6. Cables

Another component of the "balance of system". The cables sizing consider two relevant factors [6]: The first is the cable's current carrying capacity; the second is the minimum loss that the cable carries. The sizing correspondent to the cables is divided in five parts:

- Cable from the panels to the PV connector
- From the PV connector to charge controller
- From the charge controller to battery bank
- From the battery bank to inverter
- From the inverter to AC loads

1.3. Motivation of the Thesis

Nowadays there are standards that are ruled worldwide to determine what is the "best" tilting angle for a PV module in order to absorb the highest possible irradiance throughout a year on it. In this project, it will be analysed what is the individual influence of these 3 irradiances: direct irradiance (G_M^{dir}), diffuse irradiance (G_M^{diff}) and the ground/albedo irradiance (G_M^{Ground})). The product of their sum is known as the total global irradiance (G_M). The current existing software have a default estimated tilting angle according to the location where the PV system wants to be built, but it does not automatically provide the exact tilting angle. Therefore, another important goal is to determine what is the best static optimal tilting angle for a PV module at any location in the world.

Moreover, the project is aimed to give a preview of what could be an expected behaviour of a PV module which is constantly moving on the water surface offshore (it moves along with the waves) and make the comparison of the energy yield received with a module on the ground. Nowadays there are floating PV plants, but they all are built on natural/artificial lakes where important parameters (such as the water movement) are controlled. There are no studies about the behaviour of a module onto a more dynamic and unpredictable scenario and how to possibly obtain the best optimal angle to get the highest irradiance under this scenario.

1.4. PV Systems: Static, Tracking and Floating Systems

The incident irradiance on a PV module which is implemented at any of the current topologies that are used in the market (which are: floating, static and tracking) and the new concept of an offshore floating PV module will be studied in this project. The following is a brief explanation of all these topologies:

- **1^{st} Static array:** As its name suggests, the PV array remains static at one unique tilting angle and facing the True South (for northern latitudes, like in the Netherlands) or True North (for southern latitudes, like in New Zealand). They can be divided in 2 sub-categories:
  - Semi-static: Which can be optimally tilted per season or month, depending on the needs. Usually it has to be manually tilted. These changes on the tilting increase the reception of solar radiation per month or season, improving thus the system's energy production yield. See Figure 1.6a
  - Static: this is the most used installation. It does not change its tilting angle throughout the year. From all the configurations (static and trackers), this is the one that receives the smallest amount of solar irradiance. See Figure 1.6b

- **2^{nd} Tracking array:** This configuration tracks the Sun in order to receive the highest possible radiation. It also can be divided in 1-axis or 2-axis tracker, which are:

  - Azimuth-Tilting Tracker (TRAT): 2-axis tracker. The PV module/array acts as a sunflower. It has the highest perception of solar radiation of all the trackers. See Figure 1.7a

  - Azimuth Tracker (TRA): 1-axis tracker. Where the PV module/array is tilted statically at its optimal angle and it makes horizontal movements to follow the sun path. This configuration has the 2^{nd} highest perception of solar radiation. See Figure 1.7b

  - Tilting Tracker (TRT): 1-axis tracker. The PV module/array remains statically facing South or North (according to the location) and it goes up and down during the day throughout the year to get the highest possible solar radiation during the day throughout the year. This has the lowest perception of solar radiation amongst the tracking systems. See Figure 1.7c

- **3^{rd} Floating PV System:** It is a PV array which is floating onto the water's surface. All the known projects of this kind of topology have been developed on small natural and artificial lakes and dams. The objective of this project is to analyse a scenario where the PV module is offshore, how much incident global irradiance falls onto it and what is its difference when compared with a PV module onshore. Figure 1.8 depicts a floating PV system.

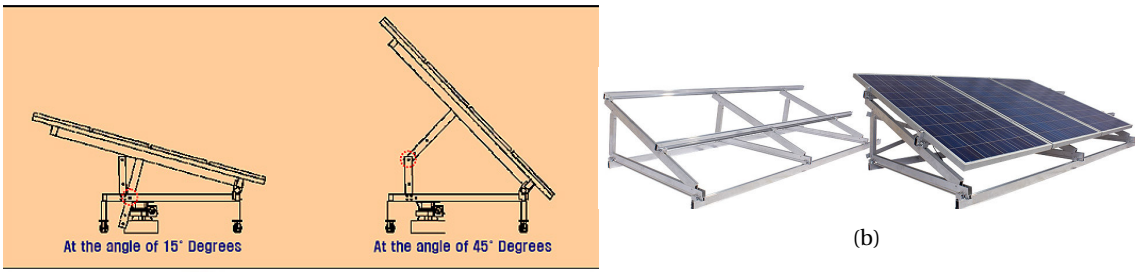

(a) (b)

Figure 1.6: (a)Semi-static Mounting for PV arrays [7] (b)Static Mounting for PV arrays [8]

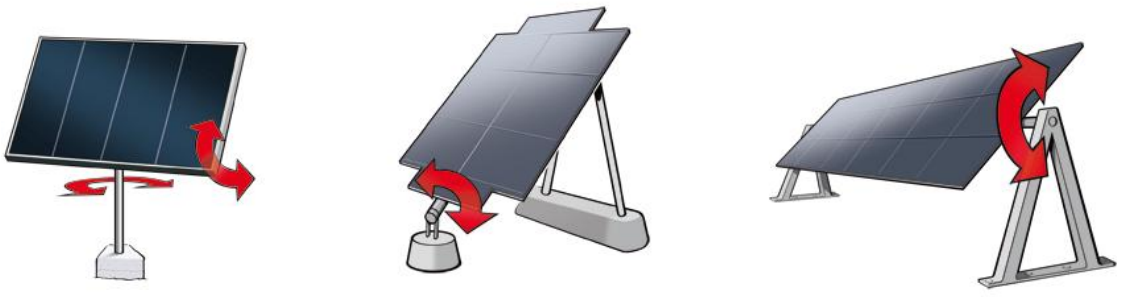

(a) (b) (c)

Figure 1.7: Tracker Systems. 1 and 2 axis [9] (a) Azimuth-Tilting Tracker (TRAT) (b) Azimuth Tracker (TRA) (c) Tilting Tracker (TRT)

Figure 1.8: Floating PV Array [10].

Of course, each topology has its advantages and drawbacks. The next list mentions some of these characteristics for each topology (besides of the standard ones that a PV system has to offer):

Advantages of static/semi-static topologies:

- Easier to install than a tracking topology
- Installation costs significantly lower than a tracking system
- No moving (or barely moving) parts (static/semi-static)
- Sturdier mounting structure due to its immobility
- Minimal maintenance
- Easily scalable

Drawbacks of static/semi-static topologies

- Has the lowest performance ratio compared to any tracking system

Advantages of tracking topologies:

- Depending on the tracking topology implemented, a higher (or the highest possible) performance and energy yield can be obtained from a PV array
- Depending on the location's irradiance, the payback period could be slightly faster than in a static topology
- Any tracking topology has a higher performance than the static/semi-static topologies

Drawbacks of tracking topologies

- Investment costs significantly rise because of the tracking parts
- Mounting structure is less stable than in a static topology, therefore, the system could be seriously damaged when exposed to high wind speeds
- Maintenance costs rise since the mechanical moving parts need periodical attention
- Since there are mechanical pieces, the need of replace them could rise the system costs
- More difficult to escalate
- The mechanical parts need energy in order to track the Sun, thus, not all the energy produced is used by the grid or the edification, but to move the tracking structure

Advantages of floating PV topologies (considering the cases of projects built onshore):

- The PV module has a better performance in terms of temperature, since the water's surface does not heat up as much as if it were on the ground

- It can convert "dead-areas" into useful-areas, since the surface of the water will be used in order to help to generate electricity
- Thanks to the increase of performance due to the cooling of the PV module, the payback period could be slightly faster than in a conventional PV static system on the ground
- Prevents the growth of algae on lakes or dams [11] (algae is considered a weed which can modify the lake's ecosystem)
- Prevents evaporation of water [11] (which could help during a drought season)
- Easily scalable

Drawbacks of floating PV topologies (only considering offshore projects)

- Special equipment needed to keep the PV arrays floating on the water
- Material could be damaged faster due to corrosiveness of the salt water
- The PV System would be exposed to a much more aggressive environment. This rises the risks of damages on the PV system and its components
- Conventional PV modules are not built to endure such extreme humid and salty environments, therefore, it is expected that their lifespan is drastically reduced
- Extremely high investment costs for offshore PV systems
- It is expected to have a lesser performance than a PV system of the same size placed on the ground, due to the constant movement of the PV panel caused by the waves
- The previous point would force to use a wider area in order to achieve the same performance than on the ground. Hence, this would rise even more the investment costs
- Impossible to predict the behaviour of the waves offshore, this increases the difficulty to estimate an accurate sizing of a PV System offshore
- The PV panels contain toxic materials (such as cadmium), if any PV module is severely damaged or destroyed due to a storm or extreme climate conditions, the sea would be heavily polluted with all these highly toxic and dangerous components

1.5. Software Tools Used in This Project

Several existent tools were used in this Thesis Project, which will be seen more in deep detail at Chapter 3. In this section they are briefly introduced so that the reader can start to recognise them.

1.5.1. Meteonorm

This is the first application to be used before any other, since it provides the meteorological data that will be used as the input-data needed to perform the simulations in all the other softwares used in this project. The most important variables for the model created in this thesis are: the global horizontal irradiance, direct normal irradiance and the diffuse horizontal irradiance. This tool provides information of meteorological conditions from thousands of cities in the world, in hourly or minutely time steps.

1.5.2. System Advisor Model: SAM

Created by the National Renewable Energy Laboratories (NREL), SAM is a financial and performance model for all the people involved in the renewable technologies industry. Its simulator for on-grid solar PV systems projects will be used in this thesis project. It can be downloaded and used for free. In the Section 3.2 a deeper analysis of its capabilities is given.

1.5.3. PVSyst

PVSyst is the second tool to be used here. Unlike SAM, PV Syst focuses only on PV Systems projects (both on-grid and off-grid topologies). It has a 30 days free trial version, after that period, a license has to be purchased to keep using it. More about PVSyst is explained at Section 3.3.

1.5.4. MATLAB

This is a high performance programming language for complex and technical computing. This tool will be used in order to create the models proposed for the topologies presented in this project. More about this application is given at Section 3.4.

1.6. Validation of the Models

There will be 7 different models which will be created using MATLAB. These models will be 2 for the PV Static topology, 3 for the current tracking topologies (azimuth,tilting and azimuth-tilting tracking systems) and 2 for the floating PV topologies. The next subsections will briefly introduce the function of each of the previously mentioned topologies.

1.6.1. PV Static Finder

This is the simplest topology of all and the first one that will be used. It will determine the optimal tilting angle for a PV module in which the PV panel will receive the highest incident annual energy yield. The figure 1.9 depicts how the model for the PV Static finder topology works.

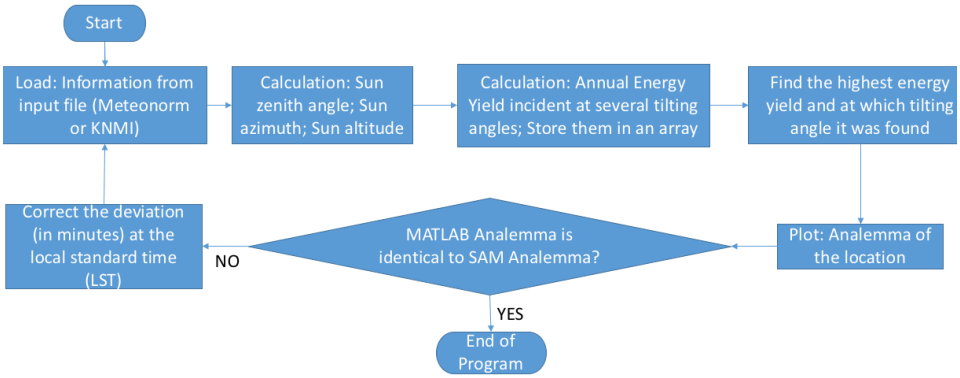

Figure 1.9: Flowchart of the PV Static Finder model.

1.6.2. PV Static Topology

This is the second topology to use and the first of the analysed topologies of this study. The Figure 1.10 describes the function of the model to get the results for the PV Static topology.

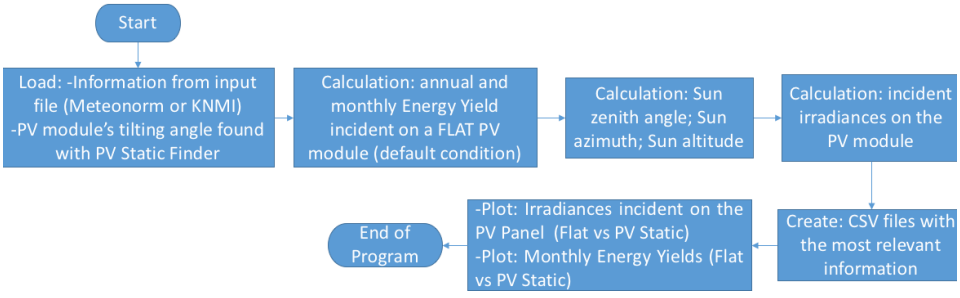

Figure 1.10: Flowchart of the PV Static model.

1.6.3. PV Tracker: Azimuth-Tilting Tracking System (TRAT)

This is the first tracking topology studied in this Project. It is a system with 2-axis which allows the PV module to act as a sunflower: always following the Sun. The algorithm determines what is the best tilting angle in order to achieve the maximum incident irradiance onto the PV module. The algorithm is "smart" enough to put the PV panel at a tilting of 0º (flat) instead of using the standard optimal tilting angle of the location for days of poor solar radiation. This configuration helps to take the maximum profit from the diffuse irradiance, which is dominant on very cloudy days. The Figure 1.11 explains how this topology works.

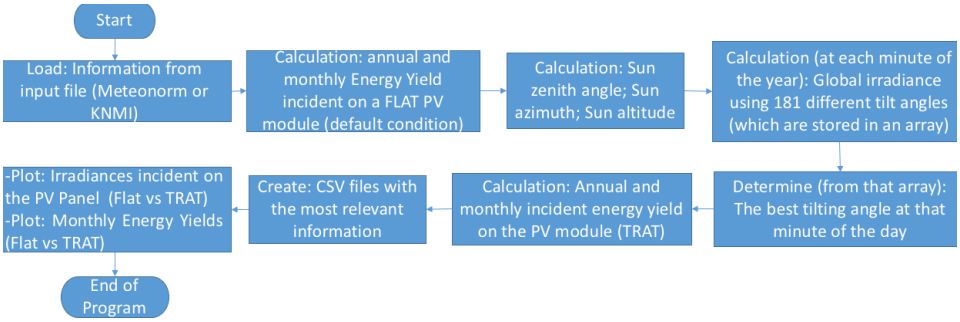

Figure 1.11: Flowchart of the azimuth-tilting tracking model.

1.6.4. PV Tracker: Azimuth Tracking System (TRA)

This second tracking topology counts with only 1-axis to track the Sun from East to West. It has a static tilting angle for all over the year. The Figure 1.12 describes the behaviour of this model. In Chapter 5 a deeper explanation is given regarding this flowchart.

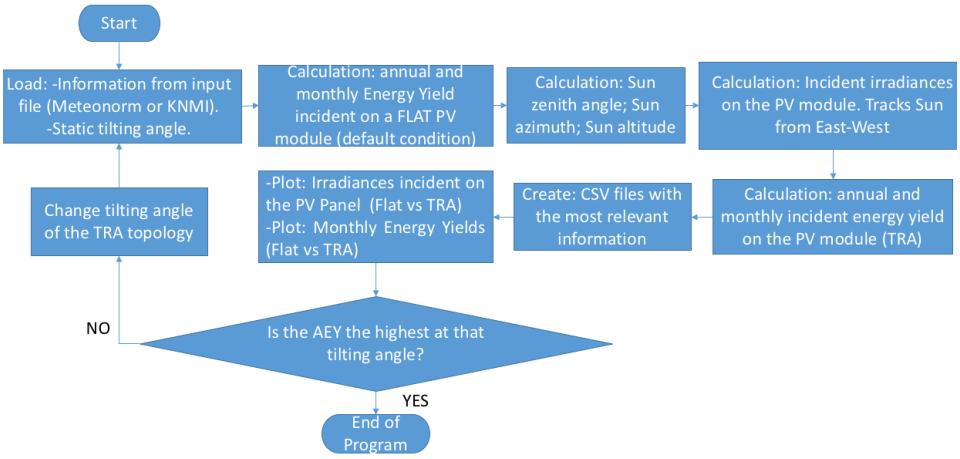

Figure 1.12: Flowchart of the azimuth tracking model.

1.6.5. PV Tracker: Tilting Tracking System (TRT)

This third tracking topology also counts with only 1-axis tracking-system to determine the best tilting angle at every minute of the day throughout one year. The PV module's azimuth remains always static (facing the true South or true North, depending on the location). The Figure 1.13 describes how this model works.

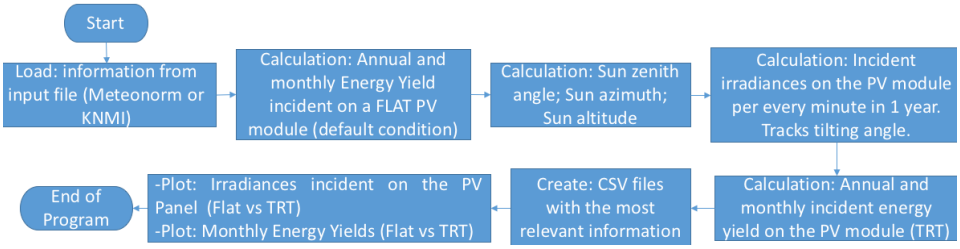

Figure 1.13: Flowchart of the tilting tracking model.

1.6.6. Floating PV Model

This is the new topology in which the incident irradiance onto a PV module will be observed when the panel is offshore. The model also determines what is the energy yield incident on a PV module floating on the sea. Moreover, this model simulates the position of the PV module on a wave. The PV panel will change at every minute its tilting angle going from a positive angle to a negative one and vice versa. This is a "controlled waving" scenario. There is also a version where the behaviour of the waves is completely random and the PV

module's azimuth and tilting angle always change randomly throughout the year. This is called the "random waving" case. The Figure 1.14 describes the model of a controlled waving scenario.

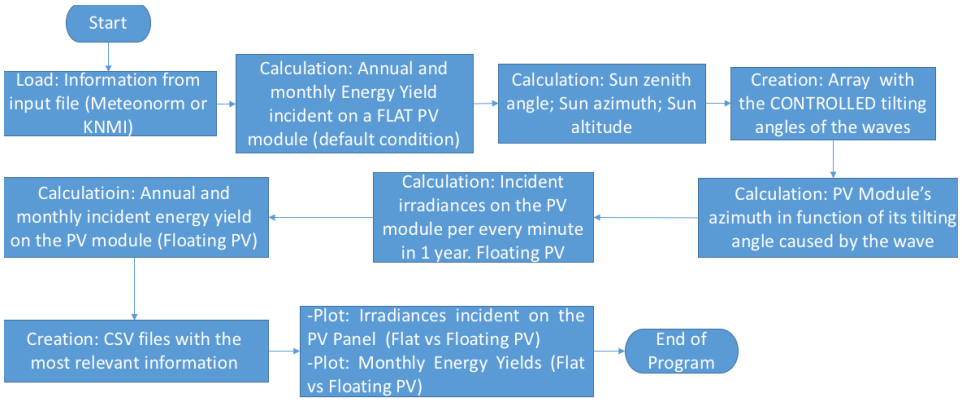

Figure 1.14: Flowchart of the Floating PV model with CONTROLLED waving.

The Figure 1.15 describes the model of a random waving scenario.

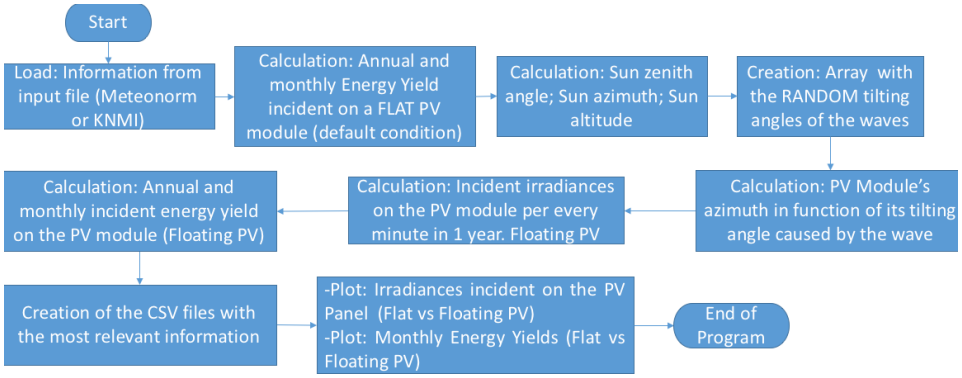

Figure 1.15: Flowchart of the Floating PV model with RANDOM waving.

In Chapter 5 each of these topologies will be deeply analysed. The results of each topology and their final comparison will be also approached. This comparative will help to understand the behaviour of the incident energy yield on the PV panel on each of these topologies and how the tilting angle plays an important role to achieve the highest possible amount of energy coming from the Sun.

1.7. Research Questions

Now that the topologies and the validation of the models have been briefly explained, what comes next in order to get a more specific path which will lead to the desired results, the next research questions and sub-questions have been asked and they will be answered on further chapters of this Thesis Project:

1. Can 2 different softwares calculate the same annual energy yield of a PV System when both use the same setup scenario? *Addressed in chapter 4.*

   (a) Is it possible to use any of these tested softwares as a corrector for systematic errors for the development of the MATLAB models (static, tracking and floating systems)? *Addressed in chapter 4.*

2. Why are these models created and what is the novelty in them that other models do not have? *Addressed in Chapter 5.*

3. What is the energy yield that a PV module can receive on each static and tracking system technologies?

   (a) How much direct, diffuse and ground irradiance the module receives under each topology configuration, what is the relevance of each one of them at a certain location and what is the main radiative contributor under each topology? *Addressed in Chapter 5 and Chapter 6.*

   (b) Are the suggested tilting angles found in literature the same as the ones obtained in these MATLAB models (for static, tracking and floating systems)? *Addressed in chapter 5.*

   (c) What is the influence of the diffuse irradiance on a PV module on a tracking system? *Addressed in Chapter 5 Section 5.12.*

4. What is the irradiance and the AEY incident on a PV module located offshore under a controlled wave scenario and under a random wave scenario?

   (a) What is the optimal tilting angle under each scenario (controlled and random waving) and why? *Addressed in Chapter 6.*

One of the main objectives will be to analyse what is the role played of the different incident irradiances on the modules in the floating, static and tracking configurations. Besides, a stronger analysis will be performed on the new floating PV concept: the reception of irradiance onto a module floating offshore, which presents a dynamic scenario in which the PV module minutely moves in a sinusoidal way. The objectives of analysing such dynamic scenario would be:

- Determine the radiation received by the module when it is flat on the water
- Determine the radiation received by the module when it is tilted on the water
- Determine what is its optimal angle depending of the waves movement
- Compare the energy yield received under a floating and dynamic scenario with the one of a PV module on the ground

All these aspects will be extensively analysed on Chapter 6.

2

Irradiance on the PV Module

This chapter addresses some concepts in order to have a better understanding of how the irradiance reaches a PV module and how it is measured. The necessary steps include the explanation of the meteorological data collection which will be critical for further calculations in order to obtain the direct, diffuse and ground/albedo irradiances incident on the PV module (for the MATLAB model) and to determine the PV System performance for the SAM and PVSyst modellings.

2.1. Meteorological Data

The meteorological data is the most important information needed since it is the core of the calculations. The 2 main sources for this project were acquired using the Royal Netherlands Meteorological Institute (KNMI) [12] to perform the simulations in the Netherlands and the software Meteonorm for the rest of the world, which has an vast meteorological information for 8,000 cities in the world [13]. With Meteonorm a personalised location can be created, with interpolated data from the closest stations in monthly or hourly intervals, this data is generated by using stochastic models [14]. The time steps of all the data extracted from these 2 official sources, was in minutes per year.

The results format was presented in a file of "Comma Separated Values" (CSV) which can be viewed using Excel and that includes Typical Meteorological Year data in minutely values of solar radiation and other weather elements for one year. The resulting dataset simulates normal weather conditions and not extreme ones. The format of the files with the information collected and that will be used as input data for the calculations is the following:

- Year of the information
- Month of the year (from 1 to 12)
- Day of the month (from 1 to 31)
- Hour of the day (from 0 to 23)
- Minute of the hour (from 0 to 59)
- Global Horizontal Irradiance (GHI): Total radiation received by a flat horizontal surface, in W/m^2.
- Direct Normal Irradiance (DNI): Irradiance normal to the direction of the radiation, measured using a device with a narrow solid angle of 5°. Measured in W/m^2
- Diffuse Horizontal Irradiance (DHI): Amount of horizontal radiation due to the scattering in the atmosphere and not the direct irradiance. Measured in W/m^2.
- Latitude: indicates if the place is at the Northern (positive number) or Southern (negative number) hemisphere.
- Longitude: indicates if the place is at the Western (negative value) or Eastern hemisphere (positive)

- Time Zone: difference in hours from the Greenwich line (negative for the Western locations, positive for the Eastern ones). From 0 to -11 or from 0 to +12 [15].

The Figure 2.1 depicts a part of the input file format used in order to determine the irradiance falling onto the PV panel and all the other irradiances incident on the PV module. The other columns will not be explained since they are not necessary for the calculations performed on the MATLAB model. Nevertheless they are there since both SAM and PVSyst use them (in their own different format). Basically one same file was used to make simulations in two different softwares (SAM and MATLAB) and another file with different format was used for PVSyst. Nevertheless, the source for the SAM vs PVSyst simulation was the same: Meteonorm.

	A	B	C	D	E	F	G	H	I	J	K	L	M	N	O
1	Source	Location ID	City	State	Region	Country	Latitude	Longitude	Time Zone	Elevation					
2	MN	Delft	Delft	Delft	Delft	Country	52.01	4.364	1	1					
3	Year	Month	Day	Hour	Minute	GHI	DNI	DHI	Tdry	Tdew	RH	Pres	Wspd	Wdir	Snow Depth
4	2014	1	1	0	1	0	0	0	9.9	8.6	85	1015	3.1	218	10
5	2014	1	1	0	2	0	0	0	9.9	8.6	85	1015	3.1	218	10
6	2014	1	1	0	3	0	0	0	9.9	8.6	85	1015	3.1	218	10
7	2014	1	1	0	4	0	0	0	9.9	8.6	85	1015	3.1	218	10
8	2014	1	1	0	5	0	0	0	9.9	8.6	85	1015	3.1	218	10
9	2014	1	1	0	6	0	0	0	9.9	8.6	85	1015	3.1	218	10
10	2014	1	1	0	7	0	0	0	9.9	8.6	85	1015	3.1	218	10
11	2014	1	1	0	8	0	0	0	9.9	8.6	85	1015	3.1	218	10
12	2014	1	1	0	9	0	0	0	9.9	8.6	85	1015	3.1	218	10
13	2014	1	1	0	10	0	0	0	9.9	8.6	85	1015	3.1	218	10
14	2014	1	1	0	11	0	0	0	9.9	8.6	85	1015	3.1	218	10
15	2014	1	1	0	12	0	0	0	9.9	8.6	85	1015	3.1	218	10
16	2014	1	1	0	13	0	0	0	9.9	8.6	85	1015	3.1	218	10
17	2014	1	1	0	14	0	0	0	9.9	8.6	85	1015	3.1	218	10
18	2014	1	1	0	15	0	0	0	9.9	8.6	85	1015	3.1	218	10
19	2014	1	1	0	16	0	0	0	9.9	8.6	85	1015	3.1	218	10
20	2014	1	1	0	17	0	0	0	9.9	8.6	85	1015	3.1	218	10
21	2014	1	1	0	18	0	0	0	9.9	8.6	85	1015	3.1	218	10
22	2014	1	1	0	19	0	0	0	9.9	8.6	85	1015	3.1	218	10
23	2014	1	1	0	20	0	0	0	9.9	8.6	85	1015	3.1	218	10
24	2014	1	1	0	21	0	0	0	9.9	8.6	85	1015	3.1	218	10

Figure 2.1: Input format used for the SAM and the MATLAB models. For the calculations of the energy yield incident on the PV module (for MATLAB) and to calculate the performance of a PV system (SAM).

This same file was used for the SAM (refer to Chapter 3 for further details) software and for the calculations performed in MATLAB. A more detailed explanation will be given about the software used in this project.

2.2. Position of the Sun in the Sky: Solar Position Formula

In order to correctly calculate the solar energy available in a location, it is important to know the position of the sun in the sky (in this case) per minute throughout the year. The procedure chosen to obtain the solar azimuth and elevation, is the one found in the ASHRAE Handbook 2011 [16]. ASHRAE stands for: "American Society of Heating, Refrigerating and Air-Conditioning Engineers" [17]. This methodology will be extensively treated at Chapter 5. The reason to use this algorithm is because it proofed to be accurate at any location in the world when its results were compared with those from SAM. It was found a small time deviation for locations at Eastern longitudes and Northern latitudes, which was easy to fix and this helped to get the correct result, which was almost identical when compared with SAM's results.

2.2.1. Solar Path: Analemma

The analemma is the "8" shaped figure that is formed in the sky if a picture was taken to the Sun every day at the same time (local time) for one year. The Figure 2.2 describes the dates of an analemma and it shows an example of the Sun's position in Greece throughout one year.

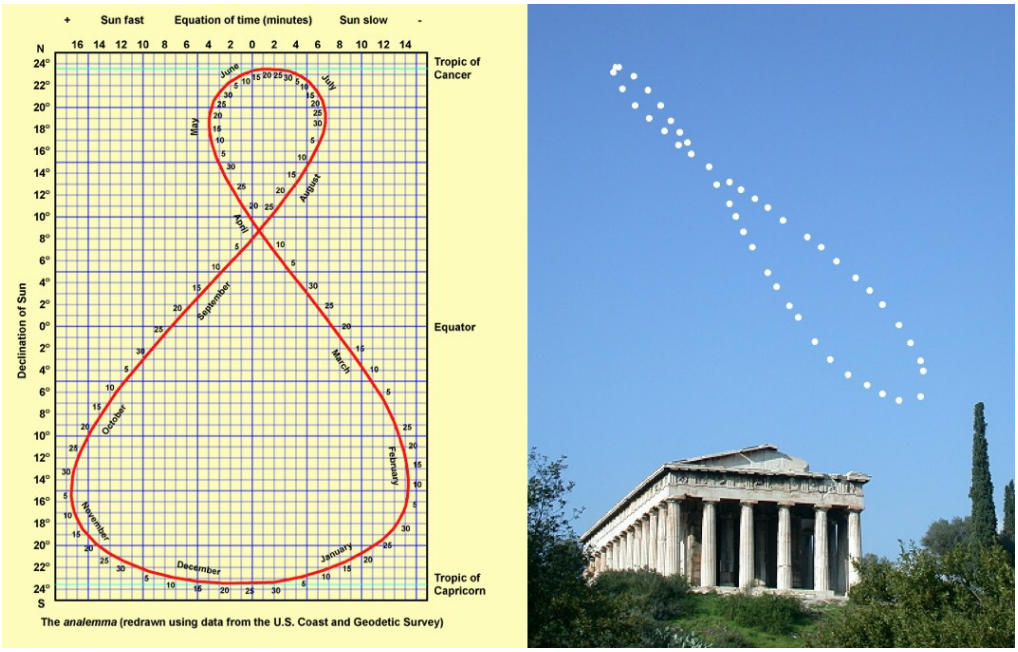

Figure 2.2: Analemma (Sun's position in the sky). Description and example of an analemma [18]

The Figure 2.3 shows the Sun path during the year from 3h00 up to the 23h00 for Delft. The coloured analemma is the one calculated by the model presented in this project created in MATLAB using the ASHRAE's algorithm and the black analemma (inside the coloured analemmas) is the one calculated by the software SAM. The solstice can be found on the top, the spring and autumn equinoxes in the middle of the graph and the winter solstice are at the bottom. This information will be used during the later explanation of how the MATLAB model was setted-up. The analemma helps to determine if the sun is visible in a location at a given time of the year. In Appendix A analemmas of other locations in the world can be consulted.

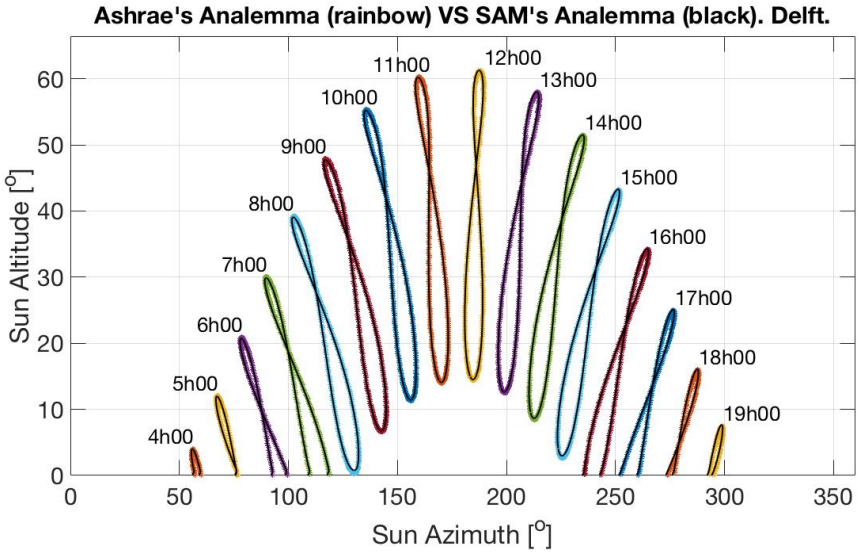

Figure 2.3: Analemma (Sun's position in the sky) in Delft at different times of the year. In the "X" axis (azimuth): 0º = North, 90º = East, 180º = South, 270º = West.

2.3. Irrradiances on the PV Module: Global Irradiance

The global irradiance that a PV module receives is the sum of 3 different irradiances which were already mentioned before in this chapter: the direct normal irradiance G_M^{dir}, the diffuse irradiance G_M^{diff} and the ground or albedo irradiance G_M^{ground} incident on a PV panel. The Figure 2.4 describes this.

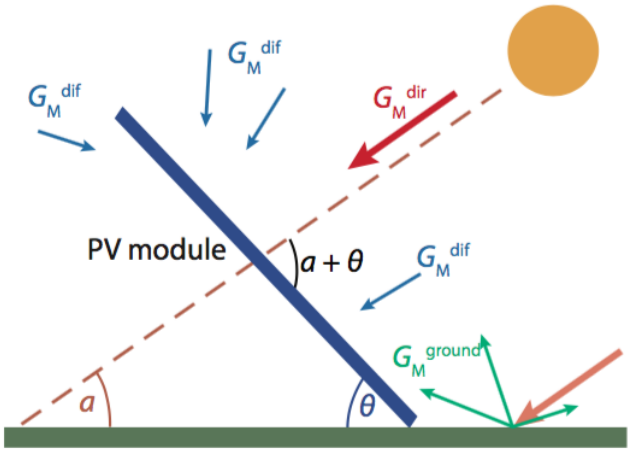

Figure 2.4: Direct, diffuse and ground irradiances on a PV module. Together conform the global irradiance [2].

Where θ in the figure stands for the PV module's tilting angle, α is the angle from the direct irradiance incident onto the module (at 90º). The following equation determines the global irradiance G_M falling onto the module:

$$G_M = G_M^{\text{dir}} + G_M^{\text{diff}} + G_M^{\text{ground}} \tag{2.1}$$

The next subsections deeply describe the formulas used for the calculations to obtain these values.

2.3.1. Direct Normal Irradiance

The direct normal irradiance: is the amount of solar radiation received per unit area by a surface that is perpendicular (or normal) to the sun rays in a straight line from the sun's direction at its current position in the sky [19]. The equation to calculate this parameter is [2] :

$$G_M^{\text{dir}} = DNI \cdot \cos(AOI) \tag{2.2}$$

AOI stands for "angle of incidence". Which value is calculated by [2]:

$$\cos(AOI) = \sin(a_M) \cdot \sin(a_S) + \cos(a_M) \cdot \cos(a_S) \cdot \cos(A_M - A_S) \tag{2.3}$$

Where A_M stands for the "azimuth of the module" and A_S stands for the "azimuth of the sun". The a_M stands for the "altitude of the module" and a_S for the "altitude of the sun". The optimal position of the PV module to get the highest incident direct irradiance, is when the panel faces directly into the Sun.

2.3.2. Diffuse Irradiance

The diffuse irradiance (G_M^{diff}) is the radiation received per unit area by a surface does not arrive on a direct path from the sun, but has been scattered by molecules and particles in the atmosphere [20]. It is the illumination coming from clouds and the blue sky. It is very variable.

Opposite to the (G_M^{dir}), the diffuse irradiance calculation is not a straightforward procedure. Its distribution is unknown and it is very variable. There are three main components used to approach the diffuse irradiance behaviour: isotropic radiation, horizon and circumsolar brightening [21].

To calculate the isotropic component, it is assumed that every part of the sky emits light always at equal magnitude. The horizon brightening is the increase of the diffuse radiation close to the horizon due to the interactions of light happening when that radiation reaches ground-sky boundary [21].

The circumsolar component is composed mainly by the radiation coming from the region of the sky close to the sun. It is due to the scattering caused by particles floating in the atmosphere [22].

Several different models have been created using as a base these three subcomponents. The complexity and accuracy of each of these models vary depending on the location's latitude. Nonetheless, the so-called "Sky View Factor" (SVF) parameter is present in all of them.

Sky View Factor (SVF)

It corresponds to the percentage of sky visible from a surface. The SVF depends on the module's tilt angle (θ_M) in its simplest form. Figure 2.5 depicts the SVF of a PV module. As it will be seen later, it is implemented to calculate the G_M^{diff} and it also is needed to get the G_M^{ground}.

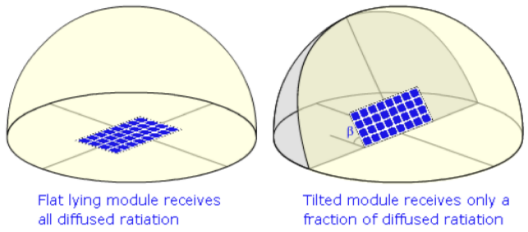

Figure 2.5: The Sky View Factor (SVF) of a flat and a tilted PV Module (in light-yellow colour) [23].

Where β in the figure is the PV module's tilting angle. The SVF is obtained by the following formula:

$$SVF = \frac{1+\cos(\theta_M)}{2} \tag{2.4}$$

Where θ_M stands for the tilting angle of the PV module with respect to the ground.

Isotropic Sky Model

This is the simplest model which only considers the isotropic component for predicting the diffuse irradiance. It is a good approximation for cloudy days, nevertheless, when the sky is clear again, its value is reduced due to the effect of circumsolar and horizon brightening [21]. The next formula is used to calculate the isotropic sky model:

$$G_M^{\text{diff}} = DHI \cdot SVF \tag{2.5}$$

This is a widely used model thanks to its simplicity. It tends to underestimate the diffuse irradiance in surfaces facing the equator though [22].

The Figure 2.6 depicts different models that have been developed in order to determine the diffuse irrandiance incident on a surface.

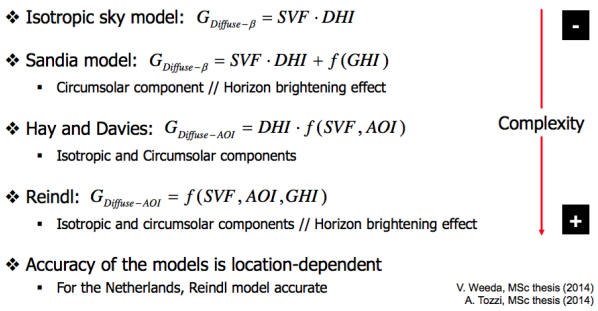

Figure 2.6: The different models to calculate the diffuse irradiance on a surface [23].

Where β in the figure stands for the tilting angle of the PV module. The figure also depicts the level of complexity of each model.

Reindl Model

As the Figure 2.6 states, for the Netherlands, the Reindl model is the most accurate to calculate the diffuse irradiance and its equation is as follows:

$$G_M^{\text{diff}} = DHI \cdot \left[A_i \cdot \cos(AOI) + (1-A_i) \cdot SVF \cdot \left(1 + \sqrt{\frac{DNI \cdot \cos(\theta_z)}{GHI}} \cdot \sin^3\left(\frac{\theta_M}{2}\right) \right) \right] \tag{2.6}$$

Where the first part inside the brackets represents the circumsolar radiation. In it, the anisotropic index (A_i) represents the transmittance through atmosphere of the beam radiation [24]. Its equation would be:

$$A_i = \frac{DNI}{G_0} \tag{2.7}$$

Where G_0 stands for the extraterrestrial irradiance.

Still inside the brackets, the second part includes both the horizon brightening and the isotropic radiation. The first is modelled using a correction factor of the form:

$$\left[1 + \sin^3\left(\frac{\theta_M}{2}\right)\right]$$

This, in conjunction with a modulating function

$$f = \sqrt{\frac{DNI \cdot \cos(\theta_z)}{GHI}}$$

Where θ_z stands for the Sun's zenith angle. When the DNI tends to zero,(for days with poor solar radiation) this model acts as the isotropic sky model. According to several comparisons, this model is one of the most accurate when representing diffuse irradiance [25].

Perez Model

SAM and PVSyst use the Perez model in order to determine G_M^{diff}. According to SAM's help sheet [26]: "The Perez method is the default value and is best for most analysis. It accounts for horizon brightening, circumsolar and isotropic diffuse radiation using a more complex computational method than the Reindl and Hay and Davies methods." The Perez model equation for the diffuse irradiance is as follows [27]:

$$G_M^{diff} = DHI \cdot \left[(1 - F_1) \cdot \left(\frac{1 + cos(\theta_M)}{2} + F_1 \cdot \left(\frac{a}{b}\right) + F_2 \cdot sin(\theta_M)\right)\right] \tag{2.8}$$

Where,F_1 and F_2 stand for the circumsolar and horizon brightness coefficients, respectively. They depend on the sky condition parameters clearness and brightness. The "a" and "b" are terms that take the Sun's incidence angle on the considered slope into account [24]. These terms will not be discussed here since the Perez model will not be used in this Thesis Project. If the reader is interested on how to calculate these terms, please refer to the article written by Loutzenhiser et al [24].

Sandia Model

The formula used to determine the diffuse irradiance in this Project, is the model developed by the Sandia laboratories, who claim that it is the best compared with other models (Hay-Davies, Reindl and Perez models)[28] [29]. This is because the Sandia model's albedo correction applied to the isotropic model, caused to always have a larger POA (Plane-Of-Array) estimated than the isotropic model [29]. The equation of the Sandia model would be:

$$G_M^{diff} = (DHI \cdot SVF) + \left[GHI \cdot \frac{(0.012 \cdot \theta_z - 0.04) \cdot (1 - cos(\theta_M))}{2}\right] \tag{2.9}$$

Where:

- G_M^{diff} = Diffuse irradiance onto the module in W/m^2
- DHI = Diffuse Horizontal Irradiance in W/m^2
- SVF = Sky View Factor
- GHI = Global Horizontal Irradiance in W/m^2
- θ_z = Sun Zenith angle. Seen at 5.1.1
- θ_M = Module's tilting angle

The term to the left is the isotropic sky diffuse model. The term to the right is an empirical correction term accounting for the circumsolar and horizon brightening effects. The angles are in degrees [28].

It has been proofed that the Reindl model performs the best for locations at high latitudes (such as in the Netherlands) according to what was exposed at Figure 2.6. Nevertheless the SANDIA model for diffuse irradiance was used in this project in order to determine the diffuse irradiance incident on a PV module.

The first reason is that the MSc. Engineer N. Narayan had started a Project using this formula and it seemed to be an interesting proposal to work with the Sandia model instead of other tested models.

The second reason is that this is the most recent model from all of the known models (it is from 2015).

The third reason is because the Sandia laboratories claim to perform better than other models.

The fourth and last reason to choose the Sandia model over others, is because several simulations from different parts of the world were performed, not only from the Netherlands, and it would be interesting to see the results from this model in other locations. That's why the Reindl model, for instance, was discarded.

As a final comment for the diffuse irradiance, the best tilting angle for a PV module in order to get the highest incident diffuse irradiance, is when the PV panel is flat (0º tilting). Because the sky view factor is 1 at this tilt. Refer to Figure 2.5 to a clearer example.

2.3.3. Ground or Albedo Irradiance

It corresponds to the radiation reflected by the neighbouring surfaces around the module. The following equation is used to determine it:

$$G_M^{\text{ground}} = GHI \cdot \alpha \cdot (1 - SVF) \tag{2.10}$$

Where the α stands for the reflectivity (or albedo) of the surroundings and its value goes from 0 to 1. There are several values for this variable. For urban zones it goes from 0.14 and 0.22. For grass is between 0.15 and 0.25, whereas for snow it can be 0.82. Depending on the wetness, the asphalt's albedo can be 0.18 and for concrete it varies from 0.25 to 0.35 [30]. For oceans 0.06 or 0.1 can be used [31]. For the calculations in the simulations, the α value will be 0.2 for the tracking and static modules and 0.1 for the floating PV module.

The best tilting angle of a PV module to get the highest incident ground irradiance is 90º (when the PV panel is perpendicular to the ground).

2.3.4. Location Selected for the Simulations: Delft

Even if several locations around the world can be tested using any of the simulation tools used in this project (SAM, PVSyst and MATLAB), the default location used for this Project will be the city of Delft, in the Netherlands, whose coordinates are shown in the Table 2.1.

Latitude	52.01° N
Longitude	4.364° E

Table 2.1: Location of the city of Delft.

The data used to perform the calculations for Delft was extracted from the KNMI, which is the Meteorological Center managed by the Dutch Government. The meteorological data obtained from KNMI corresponds to the years 2010-2014. The 5 years were compared amongst them using SAM in order to see their Global Horizontal Irradiances (GHI) throughout each year. The time format of all the files is given in minutes. Moreover, a file with the meteorological conditions of Delft was also obtained from Meteonorm, but this one uses the year 2005 as reference. Its time format is also in minutes. Figure 2.7 deploys the graphs obtained from SAM, where 2.7a corresponds to the year 2011, 2.7b to the year 2013 and 2.7c to 2014. They were calculated using the information collected from KNMI as input data. The Figure 2.7d used Meteonorm's input-data (year 2005) also in minute-based format. The years 2010 and 2012 are not shown since their shapes are very similar from the other years extracted from KNMI.

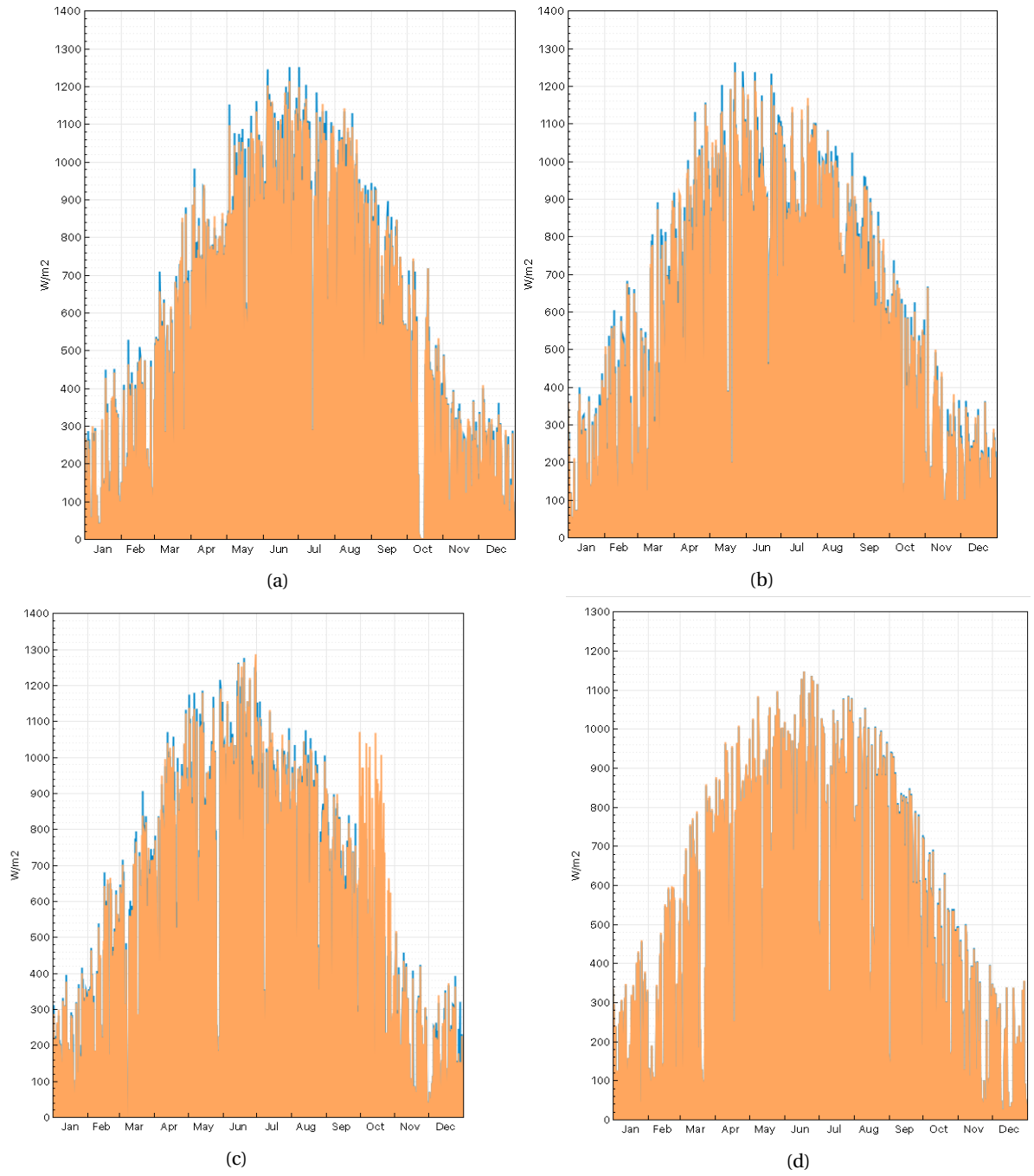

Figure 2.7: (a)2011 GHI for Delft; (b)2013 GHI for Delft; (c)2014 GHI for Delft; (d)2005 GHI for Delft.

As it can be seen from Figure 2.7, the 4 figures have a very similar dromedary-shaped curve where the maximum irradiance is usually reached in June and the minimal is found in December, with slight differences amongst them. For instance, in Figure 2.7c (which corresponds to the GHI from 2014) has an unusual peak in October, probably caused by an abnormal high irradiance condition in that year. Whereas for the same month in Figure 2.7a there is a small blank space. The graphs can be consulted in the results consultation window of SAM, in the "Time Series" tab.

The blue colour in the graph corresponds to the GHI obtained directly from the input data file, SAM does not make any calculations here. Whereas for the orange colour in the graph corresponds to the GHI calculated by SAM. The shapes of these GHI (file vs SAM) are very alike, as it can be observed at the Figures 2.7. The Figure 2.8 depicts the options to select in SAM in order to see the GHI from the weather file (blue lines in graphs) and the GHI calculated by SAM (orange lines) in Figure 2.7. These combo boxes are also found in the

"Time Series" tab in the results window of SAM.

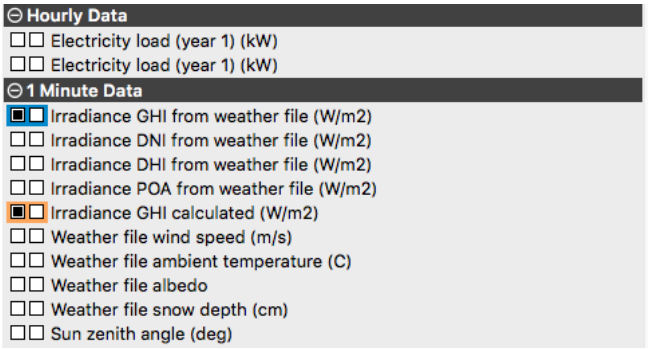

Figure 2.8: GHI from the file and calculated by SAM.

According to SAM's help sheet [26] the formula used for the GHI, where θ_z is the sun zenith angle, is:

$$GHI = DHI + DNI \cdot cos(\theta_z)$$

The year that will be used for the simulations in SAM and MATLAB will be 2013, since it is the closest year to 2016 (year in which this thesis was done) and because it has a standard dromedary-shape without any anomalies in it. A standard dromedary-shaped year was selected since the anomalies from 2014 or 2011 could give wrong results (e.g. the optimal tilting angle for a static PV Module might be altered due to these anomalies). For the SAM vs PVSyst modelling comparison, the hourly-based data from Meteonorm will be used, because it provides all critical information for both softwares and KNMI does not.

2.4. Determination of the PV Module's Optimal Tilting Angle

The module's tilting angle is crucial to get the maximum amount of energy coming from the sun. This solar radiation is best and more effectively absorbed when the sun rays strike the panels at a right angle (90º) [6]. That is why every location needs a specific tilt on the PV module to achieve this.

A rule of thumb is to mount the modules facing the Equator at an angle equal to the location's latitude + 10º. Along the Equator, the Sun varies its position from 23º N to 23º S throughout the year. Thus, the modules are mounted with an extra tilting of 5º-10º facing the Sun during the least sunny months (autumn and winter) [6]. Figure 2.9 shows a tilting estimation according to the latitude.

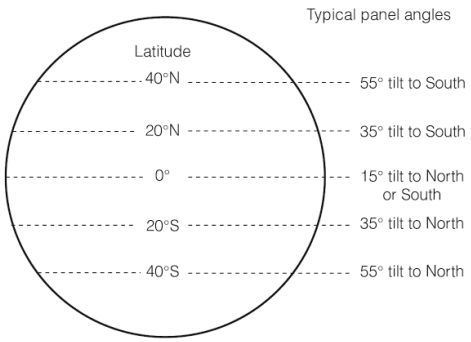

Figure 2.9: PV Module Tilting according of the latitude [6].

Moreover, SAM and PVSyst applications use default PV module's optimal tilting angles of about 30º~35º for high latitudes (such as in the Netherlands). The best performances in energy yield was obtained with a tilting of 37º for Delft using SAM. Nonetheless, SAM also has the option of implementing the "latitude tilting" in its simulations [26].

Boxwell [32] in his solar calculator (which can be consulted at [33]) specifies that the optimal tilting angle for any location was always equal to the latitude of the place itself. Several tests from different cities around the globe were performed using Boxwell's solar calculator and all of them specified that the optimal tilting

angle for a PV module was equal to the latitude of the city consulted. For instance: in Den Haag, the solar calculator indicates that the best yearly average tilting angle for a PV panel is 52º, and the latitude of Den Haag is 52.05º. See Figure 2.10

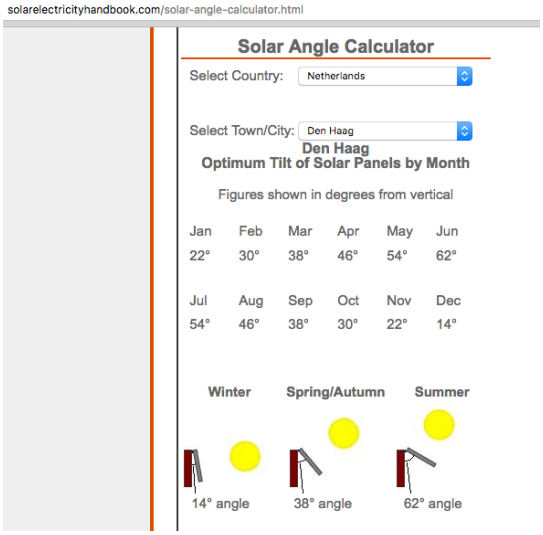

Figure 2.10: PV module optimal tilting angle for Den Haag according to the online solar calculator of M. Boxwell [33].

Note that in Figure 2.10 the PV module's tilt angles are defined in a vertical position; usually the tilting angle for a PV module is defined in terms of horizontal orientation, which will be the only one considered in this project. The vertical angle from Figure 2.10 is one of the very few exceptions in which a vertical angle is used as the tilting angle of a PV module. In the next simple calculations is corroborated that the optimal horizontal tilting angle for a PV module in Den Haag is equal to the city's latitude:

$$\theta_M = 90^o - 38^o = 52^o$$

$$DenHaag_{Latitude} = 52.05^o N$$

Where θ_M stands for the optimal tilting angle of the PV Module.

2.5. Conclusions of this Chapter

In this chapter it was noted that the input data that the different models use in order to perform their simulations is critically important to get accurate results. These software calculate relevant variables (such as the Sun's position) which can be useful when the MATLAB models are developed. The shape of the GHI for the studied location (Delft) tends to be dromedary-shaped. It was decided that the meteorological data of 2013 will be used in this project as input data in order to perform the simulations in the different softwares used in this thesis project.

The formulas to determine the different incident irradiances were also discussed. It was noteworthy that the diffuse irradiance has different models in order to calculate it. The model that will be implemented in this project is the one developed in 2015 by Sandia laboratories.

Finally, it could be observed that different authors propose different methodologies to get the best tilting angle at a determined location. Further in the results it will be corroborated what is the optimal tilting angle that the MATLAB model calculates at a determined location.

3

Software Used in this Project

Different tools were used in order to get the best possible results at the MATLAB model. Some of these softwares were already created and are available for the public to use them. Some are free, some are not. These tools are the following: SAM (System Advisor Model), PVSyst, Meteonorm and MATLAB.

First, there will be a comparison between the SAM and PVSyst models to see if their results are not different from one another when they simulate a scenario using exactly the same devices (such as the models of the PV modules, inverters, cable losses and location). Second, one model will be selected in order to use it as a "calibrator" to reduce the systematic errors found at the MATLAB model, which will be developed from scratch in this project.

The purpose of this task, is to have the maximum reliability in the MATLAB model by using existing tools that might help to design the best model with the minimum of errors.

3.1. Meteonorm

Meteonorm is the first application to be used in this project. The input data needed to perform the simulations in both SAM and PVSyst models is obtained from it. It runs only in Windows and is not free for the public, the buying of a license is required. Information from all over the world can be extracted into files with different format, being the comma separated values (CSV) the most common format for the models used in this project. The information can be exported in hourly or minutely basis. For the comparison between SAM and PVSyst, the hourly format will be used, whilst for the comparison of SAM and the results obtained from MATLAB, the minutely format will be implemented.

As stated in Chapter 2, the file extracted from Meteonorm contains crucial information required for the calculation of the diverse irradiances (direct, diffuse and ground/albedo) that a PV module would receive throughout a year. Figure 3.1 depicts the Meteonorm's main window.

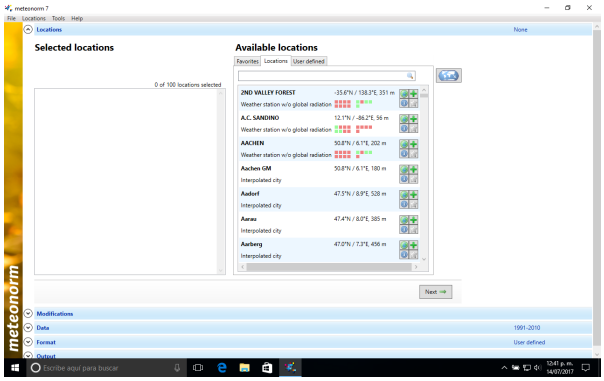

Figure 3.1: The application Meteonorm.

Figure 3.2 shows the window where the .csv file can be exported to any location in the computer.

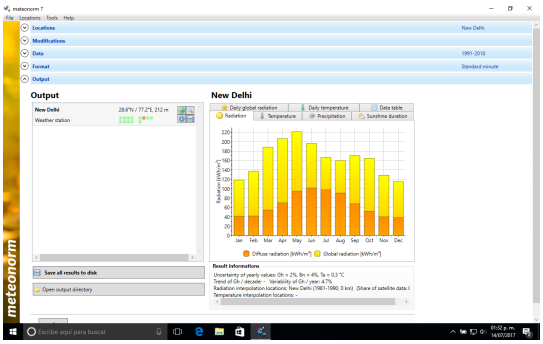

Figure 3.2: The results given by Meteonorm. Export files.

Meteonorm is a very handy and easy-going application whose utilization can be very straightforward. As it was stated before, it is not the scope of this paper to act as a tutorial for the software used here. But the help sheets can be downloaded from its official website.

3.2. System Advisor Model: SAM

SAM is an application created by NREL (National Renewable Energy Laboratory) which can run in several Operative Systems, such as Windows, Mac OS X and Linux. It is a performance and financial model which facilitates the decision making for people involved in the renewable energy industry [34]. It is a free-cost software. Figure 3.3 depicts the work flow window of SAM. It can also work with projects related to wind, geothermal, concentrated solar power (CSP) and biomass combustion. Nonetheless, only the PV solar projects will be considered. It is not possible to get access to the code which determines all the results performed by SAM.

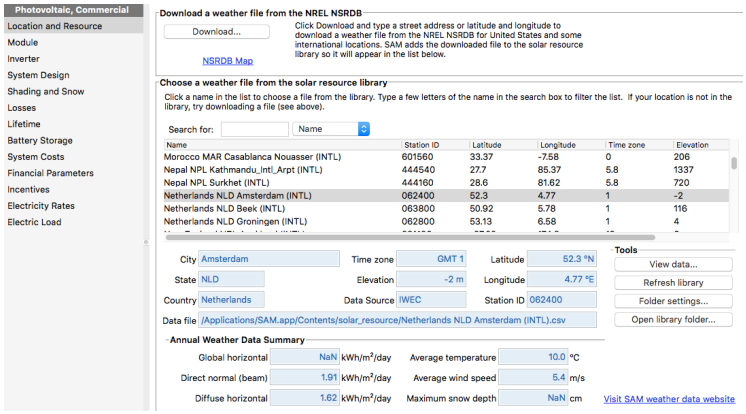

Figure 3.3: SAM Layout.

In the left column, it can be observed several functions, which help to customize and select all the devices described in the previous section. Only those that are relevant for the scope of this project are considered, which would be:

- **Location and resource:** The input data of the desired location to analyse are loaded. An internal database of SAM can be used or an external .csv file with the correct format can also be useful
- **Module:** Select the PV panel to be used in the project. SAM uses a local database with numerous models
- **Inverter:** Select the inverter desired in the project. SAM uses a local database with numerous models
- **System Design:** Configuration of the panels: fixed module, 1 or 2 axis tracker, azimuth tracker, seasonal tilt and tilt = latitude can be chosen here amongst other characteristics. See Figures 3.4a and 3.4b
- **Shading and Snow:** Configuration of the shades affecting the PV module. It offers the possibility of a 3-D analysis of the region in particular. See Figures 3.5

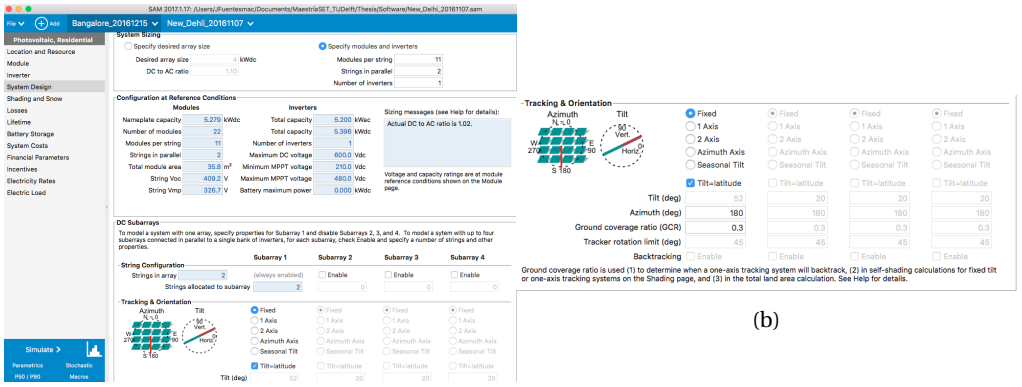

(a) (b)

Figure 3.4: (a)System Sizing and configuration at reference conditions. (b)Tracking and Orientation.

3.2.1. Model Used by SAM for the Diffuse Irradiance

According to the help-sheet of SAM, the model used in order to determine the diffuse irradiance is the Perez model, because they claim it is best for most analysis [26]. It accounts for horizon brightening, circumsolar and isotropic diffuse radiation, which is more complex than the Reindl and Hay/Davis methods.

3.2.2. SAM Useful Tools: Shading

Some of the interesting tools that SAM offers to the user, is the possibility of create a shading scenario based on real locations. SAM connects to a Google Maps satellite in order to recreate the scenario where the PV system will be developed. It counts with 3-D modelling and it calculates the amount of shading incident on the PV array at every hour of the year. The Figure 3.5 describes this tool.

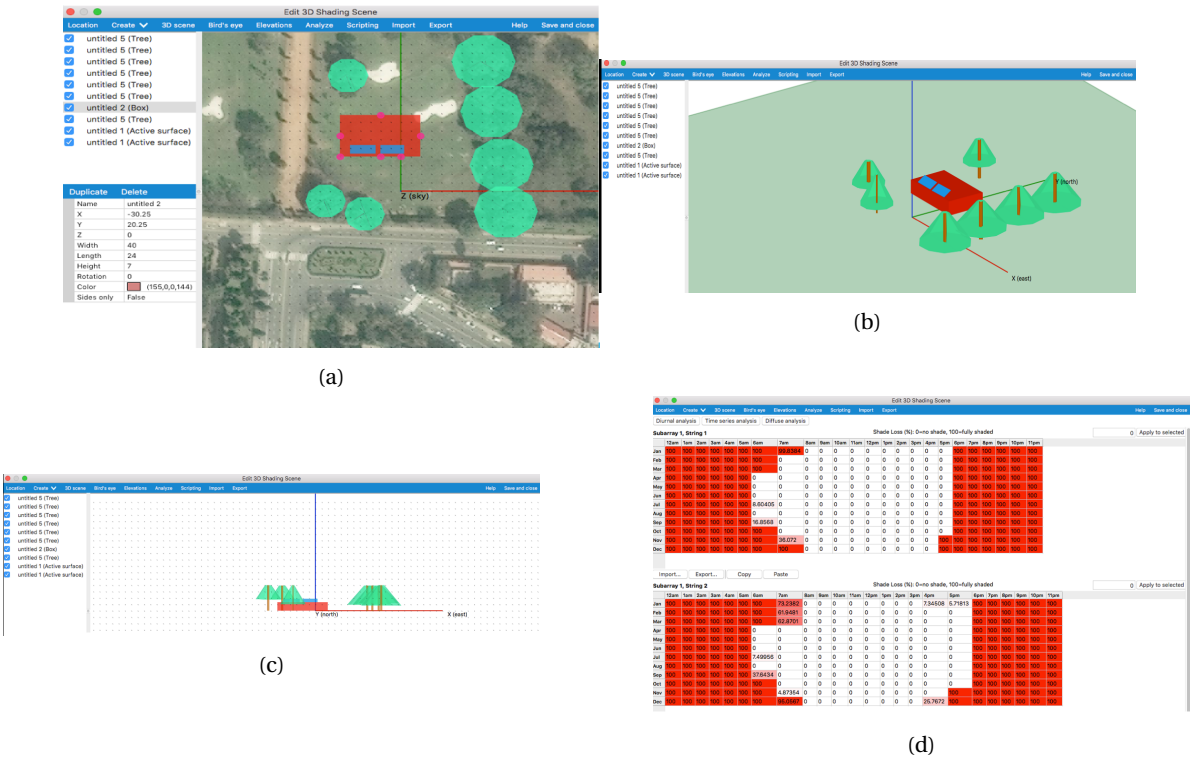

(a) (b) (c) (d)

Figure 3.5: (a)Shading Scene, satellite picture (b)Shading Scene, 3-D (c)Shading Scene, elevations (d)Shading Scene, shade time line and percentage of shades presented onto the PV modules.

SAM offers several tools to work with, nevertheless only some of them are mentioned here in a very summarized way. Those are the ones considered as the most relevant and useful tools for the scope of this project.

The SAM tool regarding the economical analysis is not studied here.

3.2.3. SAM Data Tables

In Figure 3.6 it is appreciated that the user can consult several important final calculations preformed by SAM. In this figure is appreciated the GHI which is the one in the input file, the GHI that was calculated by the SAM model, the solar azimuth and the solar elevation calculated by it.

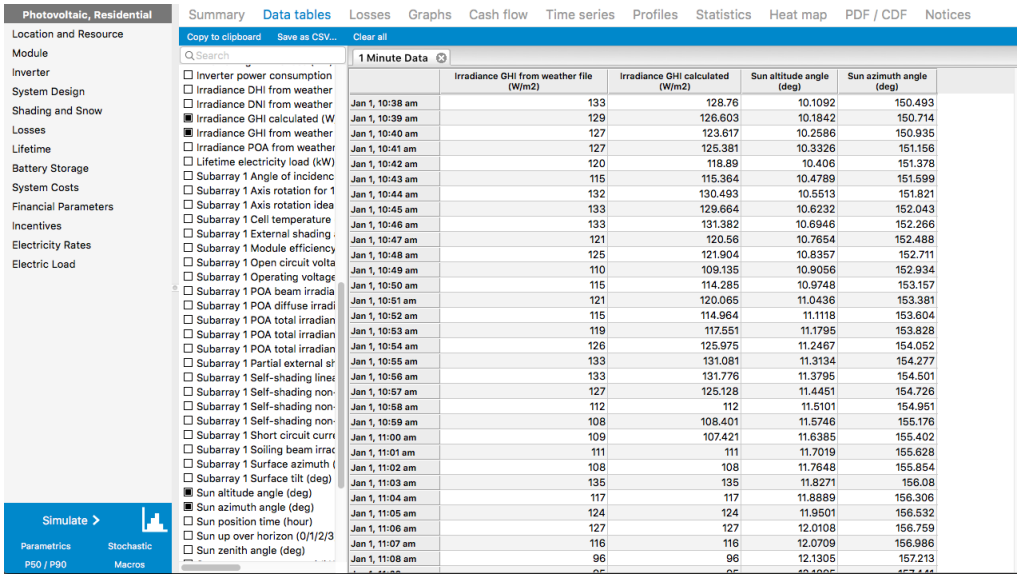

Figure 3.6: System Advisor Model data tables. On the image: GHI from file, GHI calculated by SAM, Solar Altitude calculated by SAM, Solar Azimuth calculated by SAM.

3.2.4. Validation and Reliability of SAM

SAM is an application that has more than 10 years. It has been developed and improved throughout the years and today it has a great acceptance at the renewable energy community. The developers of this software are recognized scientists working for the USA government. For these reasons, SAM was selected to be part of the tools used in this project. More information about the history of SAM can be found here [35].

3.2.5. The Reduction of the Systematic Errors in SAM

In order to prevent mistakes or incoherent results from SAM, a standard scenario will be setted up on the configuration parameters in SAM (such as shading on the PV array, losses in the cables, finding and setting the best tilting angle on the PV array to get the maximum performance on the module, etc.) as close to a realistic scenario as possible. This is because the results from SAM will be compared with those from PVSyst in this first step to determine which software will be used as a base to "calibrate" or correct the systematic errors found at the MATLAB model.

3.3. PVSyst Model

PVSyst is the other software used to measure the results of a determined location and using the devices described at Section 3. This model is only available for Windows operative system and only performs projects related to PV systems. Figure 3.7 shows the selection of the project window. The time step of its input file is in hours, PVSyst does not support minutely-based input files.

Figure 3.7: PVSyst project selection window.

3.3.1. PVSyst Useful Tools: Shading

PVSyst also counts with characteristics similar to the ones found in SAM: the selection of losses in the wiring and other components, a shading-loss analyser, energy yield production, amongst others. Moreover, it also counts with unique characteristics, such as the location's analemma and a scenario which simulates the Sun's path. Figures 3.8 depict the Sun's path and the location's analemma generated by the model and the shading caused by the objects surrounding the PV system.

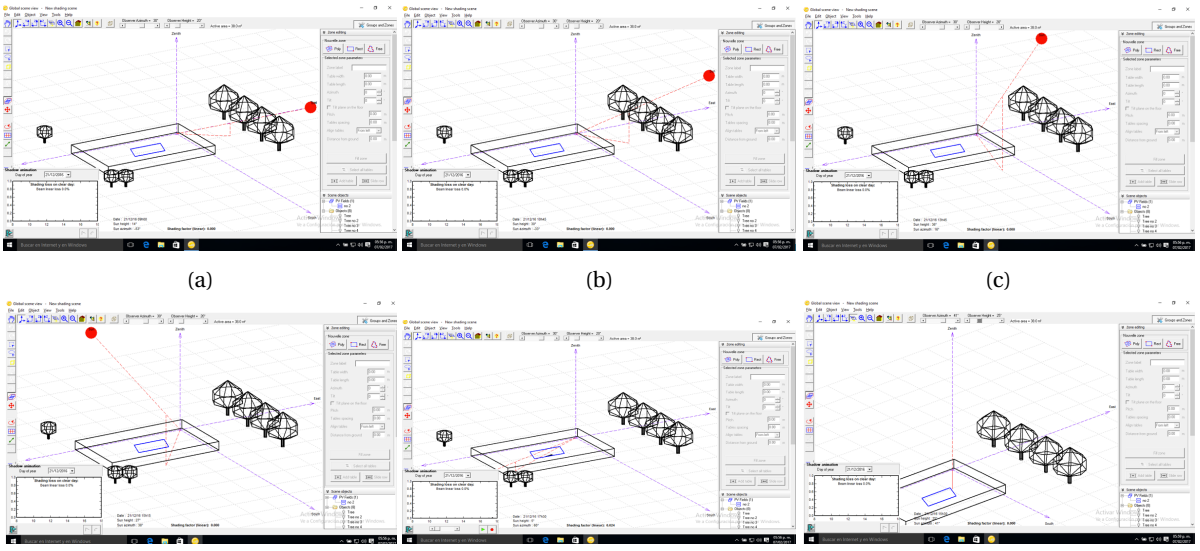

(a) (b) (c)

(d) (e) (f)

Figure 3.8: From (a) up to (e): Simulation of Sun path at a 3^{rd} person view; (f): Camera moves along with the Sun during its path.

The Figure 3.9 shows the analemma of the location and the shadowing occurring at the PV module.

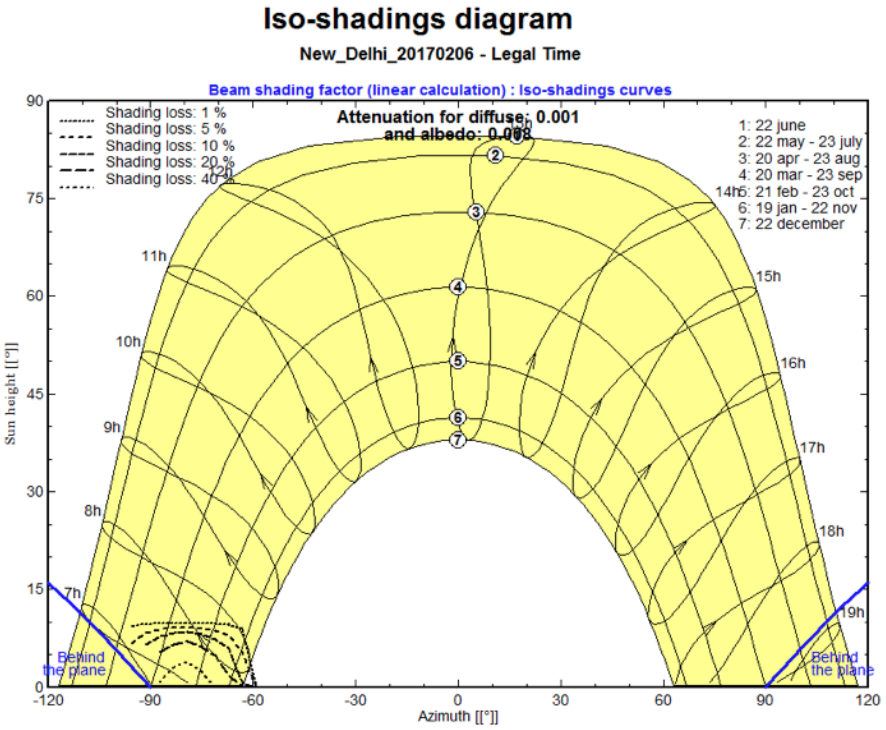

Figure 3.9: Analemma shown by PVSyst and the shading occurring at the module.

3.3.2. Validation and Reliability of PVSyst

PVSyst is a software that has been in the market since 1996 [36], which makes it one of the pioneer softwares in the photovoltaic field. As it was previously seen, PVSyst is only focused on PV technologies, so its set of tools is wider than SAM's in that aspect. Having 20 years in the market makes it a reliable tool to perform simulations regarding PV Systems connected in both on-grid or off-grid scenarios.

3.3.3. The Reduction of the Systematic Errors in PVSyst

Just like SAM, PVSyst also allows to configure several aspects in order to reduce as much as possible the errors performed by the software. It allows to choose the PV modules models, the inverters, batteries and charge controllers (for off-grid projects), the wiring losses, PV module tilt angle ant the location.

The Figures at 3.10 depict the different windows to configure the PVSystem, such as the selection of the PV modules models, inverters and losses in the system.

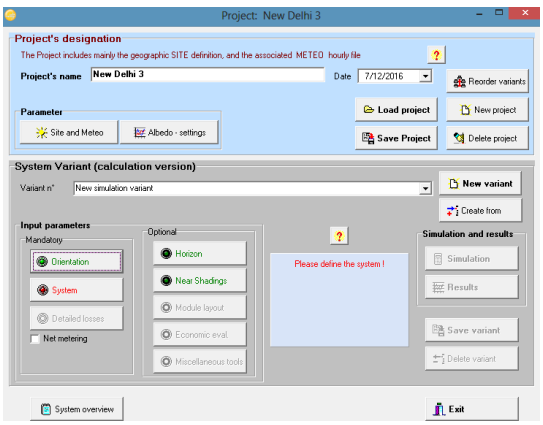

(a)

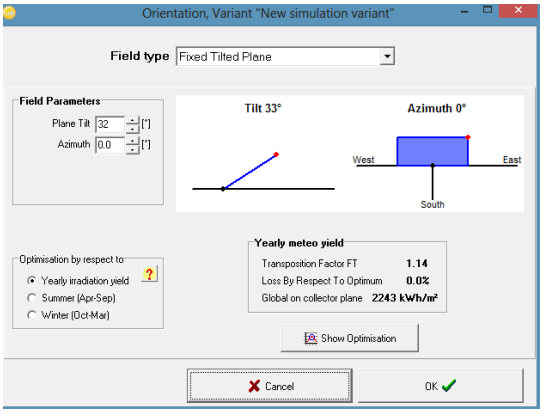

(b)

Figure 3.10: (a)Location selection (b): PV module's orientation and tilting angle.

The Figures 3.11 depict the selection of inverters and charge controllers for on-grid and off-grid projects respectively. The selection of the system losses due to wiring and the efficiency of the devices, helps to have a realistic scenario with the minimal amount of losses.

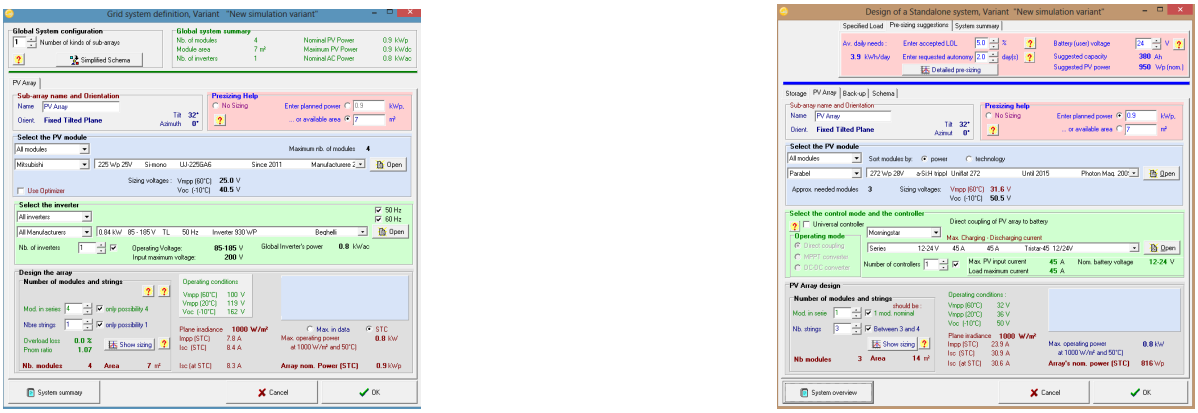

(a) (b)

Figure 3.11: (a) Inverter and PV module selection for an on-grid project (d)Inverter, charge controller and PV module selection for an off-grid project.

As it can be seen, both SAM and PVSyst share many characteristics that will be useful for the first purpose of this project, which is to determine the software that will act as the "guide" for the MATLAB model.

3.4. MATLAB

The name MATLAB is a contraction for "matrix laboratory". It is a high performance programming language for technical computing. Its main uses include [37]:

- Math and computation
- Algorithm development
- Modelling, simulation, and prototyping
- Data analysis, exploration, and visualization
- Scientific and engineering graphics
- Application development, including graphical
- User Interface building

It runs at any Operative System, being Windows the most complete one (for instance, Mac OS X and Linux MATLAB versions can not create Microsoft Excel files with the extension .xlsx). The Figure 3.12 depicts the Mac OS X MATLAB Version R2016b. This is the one used to create the modellings and scripts to get the results later shown in this Thesis Project. The version for Windows 10 was also used.

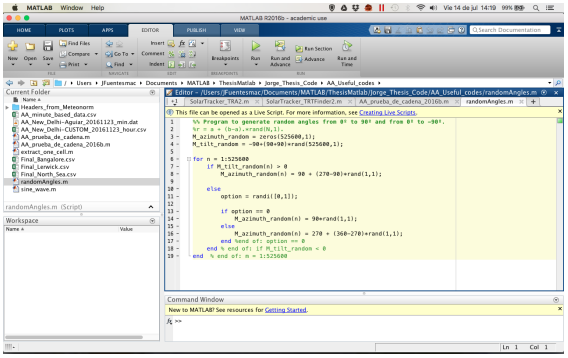

Figure 3.12: MATLAB for Mac OS, version R2016b.

The reason to use MATLAB as the modelling tool for this project, strongly dwells in the fact that many similar projects developed at the TU Delft were written in MATLAB, therefore, more information was available in the repository of the University. Besides, it is a powerful programming tool with several options which help to develop this kind of projects. Another option was the programming language "Python", but it was discarded because it was thought that MATLAB suited best for this project.

The model developed under MATLAB, will be deeply discussed at Chapter 5.

3.5. Conclusions

It can be seen that in these modern days, the use and implementation of available technology or software will be indispensable whether to create, improve or compare results amongst these models. These tools are highly valuable since they help us to make enormous calculations in a relatively fast way than if they were manually calculated.

SAM, PVSyst, Meteonorm and MATLAB will prove themselves later in this work, that they are useful and reliable tools for engineers and researchers. Nevertheless, this project does not focus on the "how to" of their functions and configurations. If there is any further interest on how to use these or other softwares used in this project, the reader can always consult the tutorial included in each software or visit their websites and download the PDF help sheet of any of the software treated in this chapter. Their websites can be found in the reference section, which are:

- SAM: [34]
- PVSyst: [38]
- Meteonorm: [13]
- MATLAB: [39]

Finally, at Chapter 4 will be described the set up scenario in each application for the later comparison between the results from SAM and PVSyst. In Chapter 5 the description of the Matlab model will be explained along with the flowcharts of each topology introduced at Section 1.6.

4

Comparison of Results: SAM vs PVSyst

Now that the characteristics of each tool that will be used for this project have been discussed, validated and their reliability on the market of the photovoltaic industry has been corroborated, the results obtained from them in this chapter will be discussed to later compare them.

The scope of this comparison is to answer the research questions asked in Section 1.7: *Can 2 different softwares calculate the same annual energy yield of a PV System when both use the same setup scenario?* and its sub-question: *Is it possible to use any of these tested softwares as a corrector for systematic errors for the development of the MATLAB model?*. The difference in the results of these applications will be analysed. If the differences amongst these results are high, then other software will be compared, if not, then that will mean that whether SAM or PVSyst models can be used to design and simulate PV systems projects.

In order to answer the research questions, one same scenario was used as the default setup. This means that both SAM and PVSyst must have the same elements in their PV system, which are: the same PV module model, the same inverters, the same input data and the same location, as well as the same losses in the system (DC and AC wiring, module mismatch, soiling, inverters, amongst many others).

As stated before, the results from SAM and PVSyst could be useful to be used as a "calibrator" (correct systematic errors) for when the MATLAB model is developed. Now, an explanation of the scenario used to make the comparison between SAM and PVSyst is introduced.

4.1. Setup Scenario: Input Data and Elements for the Simulations

The next images will show what is the standard scenario considered in order to make the comparison between the results of each software. The Figure 4.1 explains what are the characteristics used in the PV system and that were loaded in both SAM and PVSyst models in their settings.

PV System Characteristics	Quantity-Information
LOCATION	New Delhi
CONFIGURATION	On grid installation
POWER CAPACITY	5.3 kWp
NUMBER OF PANELS	22
PANELS IN SERIES	11
PANELS IN PARALLEL	2
PV MODULE TILT ANGLE	30°

Figure 4.1: System Advisor Model.

The Figure 4.2 depicts the characteristics of the PV module which were loaded in both SAM and PVSyst models. The parameters seen in the figure can not be changed by the user, they are set by default in each simulator. The module is a Suniva PV Panel, MODEL MVX240-60-5-7B1

Module Characteristics	SAM	PVSyst
Area	1.627 m^2	1.63 m^2
Nominal Efficiency	14.75%	14.8%
V_{OC}	37.2 V	37.2 V
I_{SC}	8.6 A	8.64
V_{MPP}	29.7 V	29.6 V
I_{MPP}	8.1 A	8.1 A
Power Temperature Coefficient, P_{MPP}	-0.43%/ºC	-0.45%/ºC
P_{MPP}	239.98 W	240 W

Figure 4.2: Suniva MVX240-60-5-7B1 PV module. Characteristics in SAM and PVSyst models.

Where:

- V_{OC}: Open Circuit Voltage
- I_{SC}: Short Circuit Current
- V_{MPP}: Voltage at Maximum Power Point
- I_{MPP}: Current at Maximum Power Point
- P_{MPP}: Power at Maximum Power Point
- MPPT: Maximum Power Point Tracker

The Figure4.3 depicts the characteristics of the inverter in both models. Once again, the parameters seen in the figure are unchangeable by the user, they are set by default in each model. The inverter model is an SMA Sunnyboy 6000TL-US-22-208V

Inverter INPUT Characteristics	SAM	PVSyst
Minimum MPPT Voltage	210 V	210 V
Maximum MPPT Voltage	480 V	480 V
Maximum AC Power	3.2 kW	3.2 kW
Absolute Maximum PV voltage	480 V	480 V
Inverter OUTPUT Characteristics	--	--
Grid Voltage	208 V	208 V
European Avg. Efficiency	96.16 %	96.5 %
Nominal AC Power	5.2 kWac	5.2 kWac

Figure 4.3: SMA Sunnyboy 6000TL-US-22-208V Inverter. Characteristics in SAM and PVSyst models.

The Figure 4.4 depicts the losses by different factors in the whole PV System. These parameters can be modified by the user in both models (except for the inverter and the module related losses, which are default unchangeable values).

PARAMETER	SAM	PVSyst
AC Wiring	-1 %	-1 %
DC Wiring	-1.1 %	-1.1 %
Inverter	-3.18 %	-3.6 %
Soiling losses	-1.2 %	-1.2 %
Module Mismatch	-0.8 %	-0.8 %
Module related losses	-11.7 %	-14 %

Figure 4.4: Different causes of losses in the PV System.

These characteristics also were considered in order to run the simulation under identical conditions and thus obtain as much similar results as possible when comparing the performance of PVSyst vs SAM:

- The simulations were done only on an on-grid scenario, since SAM can not simulate under off-grid conditions but it does it under on-grid ones.
- The input data was in hourly format, since PVSyst can not simulate under sub-hourly formats and SAM does it even in minutely based format.

Now that the scenario characteristics and the power electronics for each model have been setted-up, the next sections will explain the results that each model prompted to finally perform the comparison between these results and analyse it.

4.2. Results. SAM vs PVSyst

The Figure 4.5 shows the results obtained in both SAM and PVSyst models and compared between them. Two tilting angles were used: the one calculated in the thesis of Bosch [40], which is the optimal tilting angle for New Delhi (23º) and 30º, which is the default optimal tilting angle in SAM and PVSyst for that same location: New Delhi, India.

PARAMETERS	SAM	PVSyst
PERFORMANCE RATIO (PR) [%] Tilt: 23º	0.78	0.7923
ANNUAL ENERGY YIELD	9.086 MWh/yr	9.17 MWh/yr
Difference in perfomance (SAM/PVSyst)	0.92 %	
-----	-----	-----
With a tilt of 30º we have a PR of:	0.78	0.784
Annual Energy Yield	9.163 MWh/yr	9.25 MWh/yr
Difference (SAM/PVSyst)	0.94 %	

Figure 4.5: SAM vs PVSyst results.

Figure 4.6 depicts the results calculated by SAM, whereas the Figure 4.7 shows the calculations performed by the PVSyst model at a tilting angle of 30º. Each software has its own format for their correspondent input datafile, they are not the same. Inside the red squares the produced energy and the performance ratio compared at Figure 4.5 are referenced. Also the tilting angle and the PV module's model are shown in PVSyst.

Metric	Value
Annual energy (year 1)	9,163 kWh
Capacity factor (year 1)	19.8%
Energy yield (year 1)	1,736 kWh/kW
Performance ratio (year 1)	0.78
Battery efficiency	0.00%
Levelized COE (nominal)	5.68 ¢/kWh
Levelized COE (real)	4.49 ¢/kWh
Electricity bill without system (year 1)	$826,030
Electricity bill with system (year 1)	$825,069
Net savings with system (year 1)	$961
Net present value	$2,543
Payback period	10.7 years
Discounted payback period	21.8 years
Net capital cost	$11,231
Equity	$0
Debt	$11,231

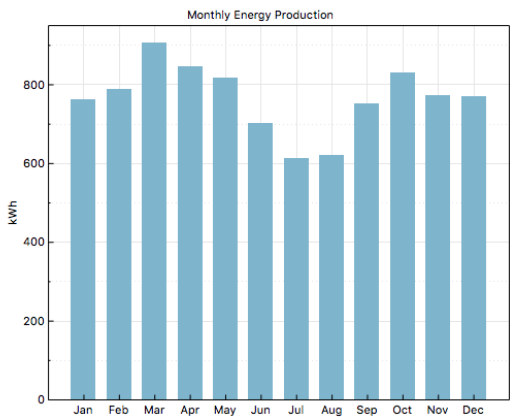

Figure 4.6: SAM results.

The economical analysis for the Figure 4.6 can be ignored since they are outside of the scope of this project. Those are default values calculated by SAM and have no value for this project.

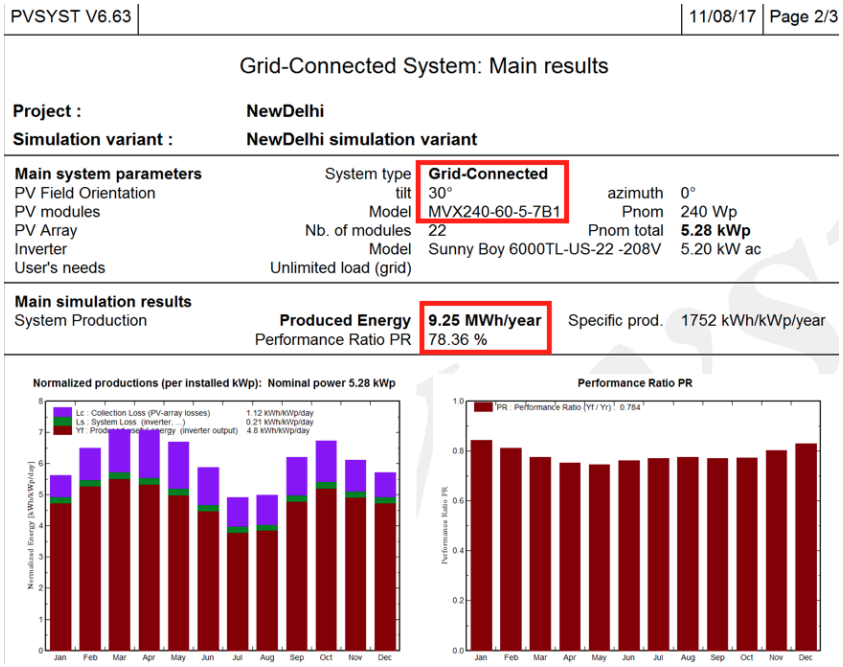

Figure 4.7: PVSyst results.

4.3. Simulator Chosen to be the Reference Model For the MATLAB Model

Since the sources obtained from KNMI and Meteonorm can be exported in minute based format, SAM was the selected model to be the base in order to correct the potential systematic errors in MATLAB. Besides, SAM allows to see the calculations for the position of the Sun, which will be useful for when these calculations are performed in MATLAB, since the results (of the solar position) obtained from the MATLAB model will be compared with those calculated by SAM and make the necessary corrections if needed.

4.4. SAM Simulations: Minute Based Data Vs. Hourly Based Data

Now that SAM has been selected to be the reference software for the model developed in MATLAB, the next step in the simulations using SAM was to compare the energy yield generated by using the same scenario described at 4.1 in both hourly and minutely time steps. The Figure 4.8 depicts the results obtained by SAM under the same scenario and using the hourly and minutely based formats in the file. The economical analysis shown in the figures can be ignored.

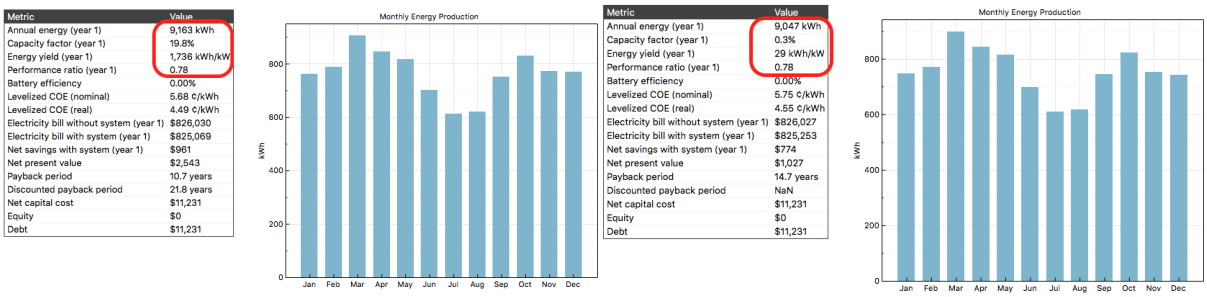

(a) (b)

Figure 4.8: Results calculated by SAM (a)Input file in hourly format (b)Input file in minutely format.

Please note that inside the red squares in the figure, can be seen the most important parameters for this analysis: the annual energy yield, the capacity factor, the energy yield and the performance ratio. These 4 parameters are known as the "Performance Metrics". They are "values that SAM calculates from the hourly performance model results and, for some variables such as capacity factor, the system specifications" [26].

According to the SAM's help sheet, these are the definitions of each parameter.

Annual Energy

SAM reports the total quantity of electricity generated by the system in Year one of the project cash flow and reports it in the Metrics table. Where:

Annual Energy = Sum of Hourly Energy Delivered

Capacity Factor

Is the ratio of the system's predicted electrical output in the first year of operation to the nameplate output, which is equivalent to the quantity of energy the system would generate if it operated at its nameplate capacity for every hour of the year. For PV systems, the capacity factor is an AC-to-DC value.

Performance Ratio (PR)

It is a measure of a photovoltaic system's annual electric generation output in AC kWh compared to its nameplate rated capacity in DC kW, taking into account the solar resource at the system's location, and shading and soiling of the array. Its equation is:

$$PR = \frac{AE[kWh]}{POA(nominal)[kWh] \cdot \eta[\%]}$$

Where AE stands for "annual energy", POA for the "annual Plane Of Array of the nominal total radiation" and η is the module's efficiency.

The Figure 4.9 pinpoints the most noteworthy differences between the simulation performed with an hourly and minutely input data. The PV system and its components were the same for these 2 example cities (Delft, in the Netherlands and New Delhi, in India).

PARAMETERS	SAM Hours	SAM Minutes
DELFT	-----	-----
PERFORMANCE RATIO (PR) [%] Tilt: 37º	0.78	0.78
ANNUAL ENERGY YIELD	5.42 MWh/yr	5.46 MWh/yr
Difference in perfomance (hr/min)	+0.73 %	
New Delhi	-----	-----
PERFORMANCE RATIO (PR) [%] Tilt: 30º	0.78	0.77
ANNUAL ENERGY YIELD	9.16 MWh/yr	9.04 MWh/yr
Difference in perfomance (hr/min)	-1.31 %	

Figure 4.9: SAM results.

It is seen that depending of the location, different tilting angles are used. For both cities, SAM used as a default value a PV module's tilting angle of 30º. It was found after some tests that their real optimal tilt angles were 37º and 30º; for Delft New Delhi respectively. The tilt angle of Delft will be used for the further simulations performed by SAM and it will also be used in the MATLAB simulations.

Another important observation is how variable the results can be when the input data is at hourly or minutely format. These changes can be whether for a positive or negative performance. The explanation for this could be that since the minutely based input file is has 60 times more data than the hourly based format, a more accurate result could be approached. In places such as the Netherlands, in a period of 1 hour can be observed several climate conditions (sunny-cloudy-rainy-cloudy-sunny), whereas in the hourly format all these details could be neglected, affecting the final results.

As an extra note, the results shown in Figure 4.9 were performed using the latest version of SAM at that moment (v. 2017.1.17). Previous simulations were also performed with oldest versions of SAM, where exactly the same scenario and devices were used as setup. The results obtained from these old versions when the comparison of performance between the minute and the hourly input data, showed a difference of performance of ±6% and not <±2% as shown in Figure 4.9.

The only explanation for this reduction of differences, is that the developers team of NREL improved the code in their programming in order to reduce the difference gap between hourly and minutely based simulations. Since the code of SAM is private and the public can not access to it, is impossible to completely confirm this. The difference reduction thanks to an update seems to be the most logical scenario.

4.5. Observations

In this section, the observations between the comparative amongst the 2 softwares will be explained, as well as their strong and weak points.

4.5.1. Pros of using SAM

+ It is free software
+ Can work with one minute time scales
+ Shows very close results when the same components (PV Modules, inverters, losses, etc.) are used in the PVSyst software
+ AEY is variable when working with minutely measurements (<±2%). The reason is that the minute-based input files have more detailed information than the hour-based ones
+ "Help forum" from NREL's website is fast and very helpful
+ The hourly and/or minutely time series can be consulted in the results (generation of graphics throughout the year)
+ Fast simulations (in 6 seconds for minute based input and 2 seconds for the hourly ones)

4.5.2. Cons of using SAM

- Performs only on-grid configurations
- In order to make the minutely measurement, it is necessary to manually create a new file, which is time consuming (this can be overcome if a script is made at any programming language. In this case, MATLAB was used to create such script)
- Not all the required data to do this file is available in Meteonorm in minutes, only in hours, which has to be converted into minutely format (if working with minutes)
- This might prompt information not 100 % accurate

4.5.3. Pros of using PVSyst

• Designed exclusively and solely for PV System projects
+ It is flexible to work in both off-grid and on-grid configurations
+ Fast simulations (in 5 seconds)
+ It shows the Sun path,the solar analemma and the shading on the PV modules dynamically of the region in which it is being working
+ Its results are similar to the ones shown by SAM when the same components and scenario are present (only for on-grid connections and using an hourly-based input file)
+ This makes it reliable for hourly based simulations

4.5.4. Cons of using PVSyst

- Not free, only a 30 days free-trial is available
- Sub-hourly simulations are difficult to perform
- This avoids to make a deeper analysis for a different time scale (sub-hourly analysis)
- Therefore, the information might not be 100 % accurate or the AEY could be lesser compared to a minute based analysis

4.6. Conclusions

After several tests on both models (SAM and PVSyst), it is observed that the gap between the results of these softwares is not significant (less than 2%) from one another. This small difference indicates that it is possible to trust either software if someone needs a tool to simulate the performance of a PV system project connected to the grid (for off-grid projects, PVSyst would be needed) without having to worry about having big differences on the results. The following are the reasons that answer the research questions from Section 1.7.

Can 2 different softwares calculate the same annual energy yield of a PV System when both use the same set up scenario?

The short answer is "yes". In general, these are the conclusions regarding the results obtained from each software and the most relevant observations of them that helped to answer this first research question:

- Both applications have similar annual energy yield, but PVSyst showed a slightly higher performance when using the same scenario and devices
- There was in average about 1 % difference from one software result to another
- Both models demonstrated to be reliable and with no significant differences when each one uses their default losses/characteristics + the setup configured by the user
- Both have higher energy yield when using their default tilting angle value (around 30º)
- When using the tilting found in the literature (23º) the performance decreased by about 1 % in both models (see results in Figure 4.5)
- For both models: the source code, the algorithms or the calculation variables used by them, are unavailable to the public
- SAM has a difference of ±2% in its AEY in a minutely based measurement, depending of the location and the input data content. Refer to Figure 4.9
- Both applications have good characteristics and of course, they have limitations
- This comparison demonstrated that any of these softwares is reliable to make a simulation in an hourly based analysis (only for on-grid projects)

Is it possible to use any of these tested softwares as a corrector for systematic errors for the development of the MATLAB model?

The following answers the sub-question from Section 1.7. After the analysis of both models (SAM and PVSyst), it has been decided that SAM will be the "guide" to correct the systematic errors found during the development of the MATLAB model. Especially when it comes of the solar position calculation. In Figure 3.6, the last 2 columns on the right (the "sun altitude angle" and the "sun azimuth angle" columns) will be extremely useful in the MATLAB model. This systematic error correction will help to get a more accurate model in MATLAB.

Another reason to pick SAM over PVSyst is that it performs minute based simulations, and the MATLAB model is also thought to perform them with that same minute format. Moreover, SAM is free.

The next sections will explain the methodology used in order to make the MATLAB models for the static, floating and tracking systems explained in Section 1.4.

5

MATLAB Models

Once that the analysis performed in Chapter 2 were finished, (the characteristics needed to determine the solar path and the elements and formulas that compose the Global Irradiance on the Module (G_M), the optimal tilting angle of a PV panel in order to receive the highest energy yield during the year and the software available in Chapter 3 to "calibrate" the models of this thesis) the next and final step is to create them in MATLAB. These models will determine the highest energy yield [kWh/m^2] incident on a PV module, to finally compare some of its results with those from SAM. In this chapter, the research questions addressed in Section 1.7 will be answered. The first question would be:

Why are these models created and what is the novelty in it that other models do not have?

The models created in MATLAB will measure the incident irradiance on a PV module during one year, in a minute-based time step, it will create at least 2 .csv files (depending on the topology of the MATLAB model) and it will plot the annual energy yield and the irradiances incident on a PV module in detailed graphs. SAM and PVSyst perform and show the final performance of the whole PV system (including its power electronics components, such as inverters). Therefore: they show the final output, but not the input of the system (the incident annual energy yield onto a PV panel). Moreover, the MATLAB model will give detailed information about the contribution on the incident energy yield from the direct, diffuse and ground irradiances. Thus, it will be capable to measure these irradiances and energy yields from any location in the world.

Research Questions Related to the Energy Yield and the Irradiance Incident on the PV Module

The next research questions will be answered at the section of "results" from each topology. The research questions and sub-questions are:

1. What is the energy yield that a PV module can receive on each Static and Tracking system technologies?

   (a) How much direct, diffuse and ground irradiance the module receives under each configuration, what is the relevance of each one of them at a certain location and what is the main radiative contributor under each topology?

   (b) Are the suggested tilting angles found in literature the same as the ones obtained in this MATLAB model?

   (c) What is the influence of the diffuse irradiance on a PV module on a tracking system?

5.0.1. General Flowchart of the MATLAB Model

At Chapter 1, the 7 models were introduced with their respective flowcharts. The Figure 5.1 describes a general overview of how the models work. Every model has its unique way of work and they will be explained one-by-one later in this chapter.

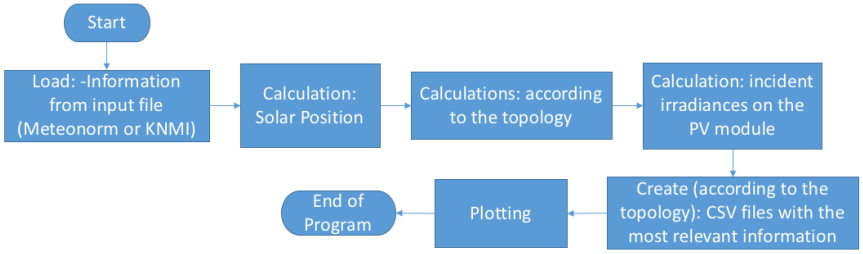

Figure 5.1: General flowchart of the MATLAB models.

In the next sections of this chapter, the equations implemented to perform all the relevant calculations for all the topologies (such as the solar position) will be explained. Naturally, the formulas from Chapter 2 to determine the incident irradiance onto the PV modules (global, direct, diffuse and ground irradiances) and the annual energy yield incident on a PV module will be implemented in these models.

Case of Study: Delft

Delft will be the location where the models of the topologies will be tested. For this reason, the meteorological data from Delft was extracted from KNMI [12] and not Meteonorm. This is because more years were available using KNMI and with Meteonorm only 2005 is given as a reference and the model of MATLAB wanted to be tested by using updated data. The year chosen to perform the simulations on the MATLAB model is 2013. An explanation about why 2013 was chosen is given at Section 2.3.4. The Table 5.1 gives the geographical location of Delft.

Latitude	52.01° N
Longitude	4.364° E

Table 5.1: Location of the city of Delft.

Tilting Angles Used as Reference

For the topologies that need a fixed tilting angle on their PV modules (PV static and Azimuth-tracker) there will be 3 tilting angles which will be compared in these models:

- **Flat tilting angle (0º):** To determine the annual incident energy yield when a PV module lays flat on the ground. The MATLAB model should show a graph similar to the GHI calculated by SAM. Refer to Figures 2.7
- **Optimal tilting angle found using SAM:** For Delft, it will be 37º
- **Optimal tilting angle found with the MATLAB model:** for the PV Static and azimuth tracking system

At the end, the results of the incident annual energy yields on the PV panel at these 3 different tilting angles, will be compared and discussed.

5.1. Solar position in the sky: Solar Altitude and Solar Azimuth

The first important calculation and which will be present in all the PV topologies (static, tracking and floating), is the Solar azimuth and the Solar altitude. According to the dictionary, the azimuth is the direction of a celestial object from the observer, expressed as the angular distance from the north or south point of the horizon to the point at which a vertical circle passing through the object intersects the horizon. The altitude is defined as the apparent height of a celestial object above the horizon, measured in angular distance. Figure 5.2 depicts these definitions.

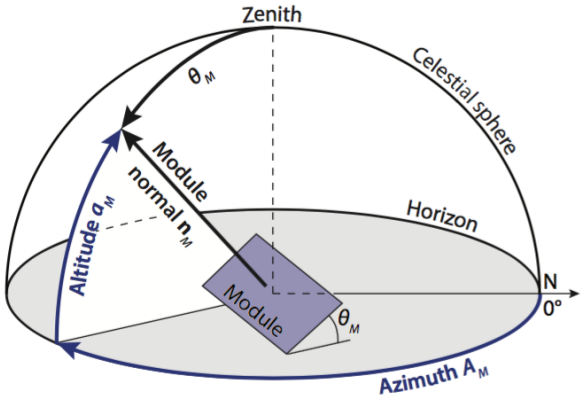

Figure 5.2: Altitude and azimuth of a celestial object [2].

Where θ_M is the PV module's optimal tilting angle, a_M stands for the PV module's altitude and A_M for the PV panel's azimuth. Moreover, as it was already stated in 2.2.1, the azimuth and altitude of the Sun will be determinant to know what is the PV module's optimal tilting angle at a certain location for every topology.

5.1.1. ASHRAE Model to Calculate the Solar Altitude and Azimuth

Back in 2.2 it was stated that the formula presented at [16] will be the one used to get the Sun's position due to its flexibility (it proofed to work at any location on Earth) and simplicity, since the summer saving time is not considered (and this characteristic was present in other consulted models).

Algorithm to calculate the solar altitude and azimuth

The important first variable to calculate is the PV module's azimuth (A_M), which will be facing True North or True South depending on the latitude: if the PV module is located at the northern hemisphere, then it will face south, hence, $A_M = 180^o$, else (if the PV module is at the southern hemisphere) it will face north, hence, $A_M = 0^o$. The procedure and formulas to build this algorithm were based on the material found at [16] unless it is specified otherwise.

The local longitude of standard time meridian (LSTM), is the next variable to obtain. This is calculated only once in the algorithm by using the longitude of the location where the PV module will be placed. It is represented by the following equation [41]:

$$LSTM = 15^o \cdot \left(\frac{Longitude}{15}\right)_{RoundToInteger} \tag{5.1}$$

All the following variables henceforth could be calculated whether at every minute, or at each hour, or at each day of the year. The next variable to calculate is the declination angle (δ) which is represented by the following formula:

$$\delta = 23.45^o \cdot sin\left(\frac{N+284}{365} \cdot 360^o\right) \tag{5.2}$$

Where N stands for the number of days passed in the year, with January 1 equal to 1.

The next element to calculate is the Apparent Solar Time (AST). But in order to calculate it, the next variables must be calculated first, starting with the difference among the true solar time (TST) and the mean solar time (MST), which changes continuously day-to-day with an annual cycle [41]. This is represented by "D" and its equation is the following:

$$D = 360^o \cdot \left(\frac{N-81}{365}\right) \tag{5.3}$$

Again, N stands for the number of days passed in the year.

Once the day-to-day change was obtained, the equation of time (ET) [41] is the next to be calculated with:

$$ET = 9.87 \cdot sin(2 \cdot D) - 7.53 \cdot cos(D) - 1.5 \cdot sin(D) \tag{5.4}$$

Then the AST is calculated by:

$$AST = LST + 4_{mins} \cdot (LSTM - |Longitude|) + ET \tag{5.5}$$

Where LST is the Local Standard Time, given in minutes. For instance: if LST = 14h41, in minutes it would be LST = (14·60) + 41 = 881 minutes. |Longitude| stands for the absolute value of the location's longitude, so it does not matter if the location is at the western hemisphere (which value is negative) or at the eastern hemisphere (which is positive).

The next variable to get before calculating the altitude and finally the azimuth of the Sun, is the hour angle (H). The following equation is then used:

$$H = \frac{MPM - 720}{4 min/deg} \tag{5.6}$$

Where MPM stands for the "number of minutes past midnight at the AST", not at the LST.

The solar altitude (β_1) is then calculated by using the following equation:

$$sin(\beta_1) = cos(Longitude) \cdot cos(\delta) \cdot cos(H) + sin(Longitude) \cdot sin(\delta) \tag{5.7}$$

$$\beta_1 = \arcsin(cos(Longitude) \cdot cos(\delta) \cdot cos(H) + sin(Longitude) \cdot sin(\delta)) \tag{5.8}$$

Finally, the solar azimuth (α_1) is calculated by using the next formula:

$$\alpha_1 = \arccos\left[\frac{sin(\beta_1) \cdot sin(Longitude) - sin(\delta)}{cos(\beta_1) \cdot cos(Longitude)}\right] \cdot (sgn(H)) \tag{5.9}$$

Where sgn(H) represents the final sign (positive or negative) obtained from the hour angle calculation.

Moreover, another important variable will be calculated: the Solar Zenith Angle (θ_z) by using the latitude of the location, whose sign does not affect the calculation (it can be negative or positive, depending of the location's latitude). θ_z will be later used to calculate the diffuse irradiance reaching the PV module G_M^{diff}. The following equations determine the solar zenith angle [42]:

$$cos(\theta_z) = sin(Latitude) \cdot cos(\delta) + cos(Latitude) \cdot cos(\delta) \cdot cos(H) \tag{5.10}$$

$$\theta_z = arccos(sin(Latitude) \cdot cos(\delta) + cos(Latitude) \cdot cos(\delta) \cdot cos(H)) \tag{5.11}$$

The solar zenith angle is a complementary angle of the solar azimuth, so it also can be calculated as:

$$\theta_z = 90^o - \beta_1 \tag{5.12}$$

5.2. Annual Energy Yield Incident onto the PV Module [kWh/m^2]

Once the solar altitude (β_1), azimuth (α_1) and zenith angle (θ_z) have been determined, all the formulas from Chapter 2 are applied in order to calculate the direct, diffuse and ground irradiances incident on the PV module in order to calculate the total irradiance falling onto the module (G_M). Now, to obtain the annual energy yield (AEY) incident onto the module, the following equation is applied:

$$AEY[kWh/m^2] = \frac{\sum_{t=1}^{525600} G_m(t)\left[\frac{J}{(s \cdot m^2)}\right] \cdot 60[s]}{3.6 \cdot 10^6 \left[\frac{J}{kWh}\right]}$$

$$AEY[kWh/m^2] = \frac{\sum_{t=1}^{525600} G_m(t)}{6 \cdot 10^4} \left[\frac{kWh}{m^2}\right] \tag{5.13}$$

Now that the algorithm to determine the solar position, the incident irradiances onto the PV module and the AEY has been explained, the next sections will explain all and each of the models used to calculate the incident energy yield on the PV panel for each topology (PV static, tracking systems and floating PV modules).

First, the static topologies will be analysed. Starting with the PV Static Finder topology, which acts more as a calibrator than as a definitive modelling topology. The second model to be used will be the PV Static one.

5.3. PV Static Finder

This is the simplest and the first topology of all that will be used. It determines the optimal tilting angle for a static PV module in which the PV panel will receive the highest incident annual energy yield. The figure 5.3 depicts how this model works.

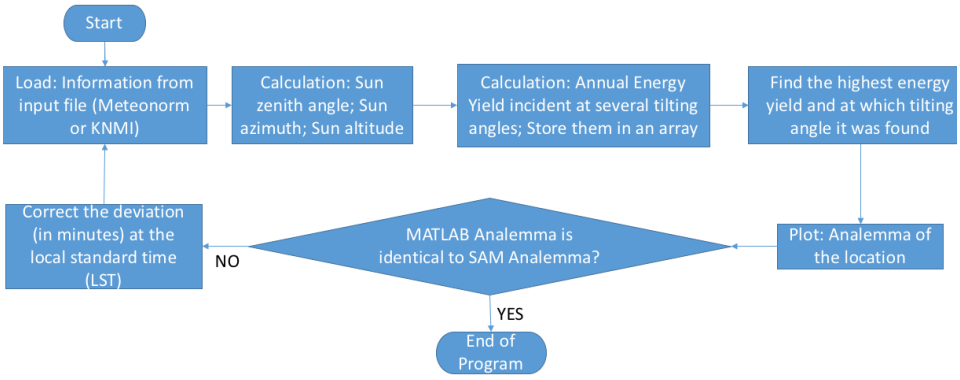

Figure 5.3: Flowchart of the PV Static Finder model.

With this simple MATLAB model, the optimal tilting angle for a static PV model is obtained and it will be used as the optimal tilting angle for the PV Static topology and it will be one of the reference tilting angles for other topologies using a fixed tilting angle in the PV module. These topologies would be: the azimuth tracker (TRA) and the floating PV module models. As it can be seen in the if-statement in the figure, the azimuth and altitude of the Sun calculated by SAM are compared with the azimuth and altitude of the PV Static Finder MATLAB model. If the results of both models are similar, then the program ends, if not, a small correction in the MATLAB model is performed and the model is executed again. This is repeated until both azimuths and altitudes have a minimal difference between them.

Optimal Tilting Angle For Delft According to the PV Static Finder Model

For Delft, the PV Static finder MATLAB model (refer to Section 5.3) determined that the optimal θ_M where the annual incident energy yield on a PV module was the highest, was of 52°. Therefore, the tilting angles used to compare the incident annual energy yield (refer to Section 5.0.1) will be **0° (flat), 37° (obtained from SAM) and 52° (calculated from the PV Static Finder MATLAB model)**. The comparison of these results will be analysed further in this chapter.

5.4. PV Static Topology

This is the first topology to be studied. It is important to remember that this is the most commonly used topology for PV systems. Hence, the incident energy yield on a PV module using a PV Static topology will be the reference point when it is compared against the incident energy yield of all the other topologies.

Let us remind that there are two subcategories for the PV static topology: one in which the PV module's tilting angle is completely fixed and can not be changed during the year (fixed tilting angle); and the other one denominated "semi-static", which allows to change the PV panel's tilting angle at least once per month, season or semester, according to the needs of the user. The changing of the angles in a semi-static topology usually is performed manually.

5.5. PV Static, Fixed Module's Tilting Angle and Fixed Module's Azimuth

Once that the optimal tilting angle for a static PV array has been determined by using 5.3, the analysis of the results will be discussed in this section. As described previously at 1.4, the modules are fixed onto a surface

in only one position throughout the year. The PV array is usually tilted at its optimal angle according to its location; it faces the true South or true North in order to maximize its performance and in consequence, it gets the maximum energy yield throughout the year. The Figure 5.4 depicts a static photovoltaic system. This topology usually has the lowest performance from all the standard static and tracking topologies.

Figure 5.4: PV module with fixed Azimuth and Tilting angles [9].

5.5.1. PV Static Topology

As introduced at Section 1.6.2, this topology will calculate the total amount of incident annual energy yield on a PV module at a determined fixed tilting angle. The Figure 5.5 depicts the flowchart to be followed in the MATLAB model.

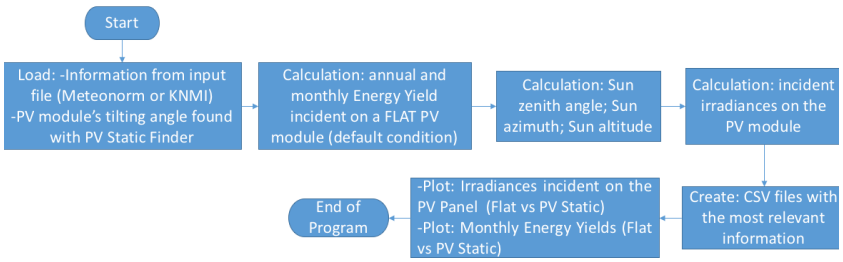

Figure 5.5: Flowchart of the PV Static model.

5.5.2. PV Static. Results

In this section the results from this topology will be discussed. Three different tilting scenarios described at 5.0.1 (0º, 37º and tilt found with MATLAB) will be analysed. The tilting angles will also be compared with those found using the solar calculator [33] of Boxwell [32].

PV Static. Results at θ_M=0°

The first point to analyse under this scenario will be the time series irradiance in [W/m^2] throughout the year in minutes. The Figure 5.6 shows all the irradiances incident on a flat PV panel during one year. Figure 5.7 compares the global irradiance incident onto the flat PV module (G_M) vs the GHI in the KNMI file. The data corresponds to the year 2013 taken from the KNMI source, the city is Delft, the Netherlands. The tilting angle of the PV module (θ_M) is 0º and its azimuth (Az) is 180º (facing South).

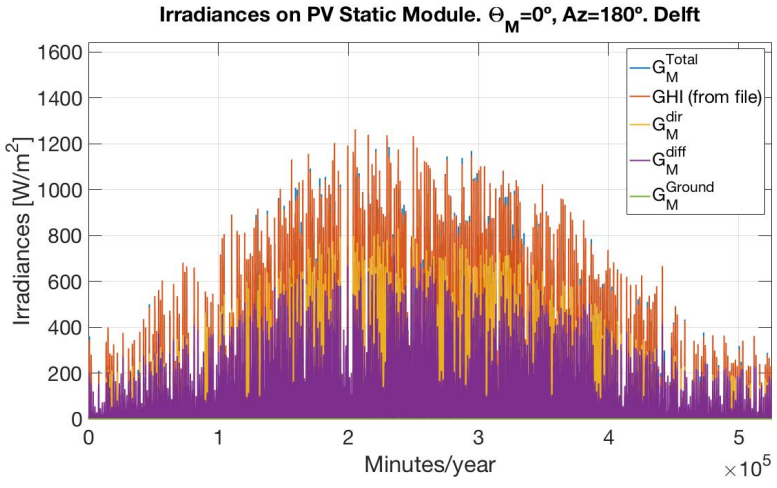

Figure 5.6: Irradiances incident on a flat PV module.

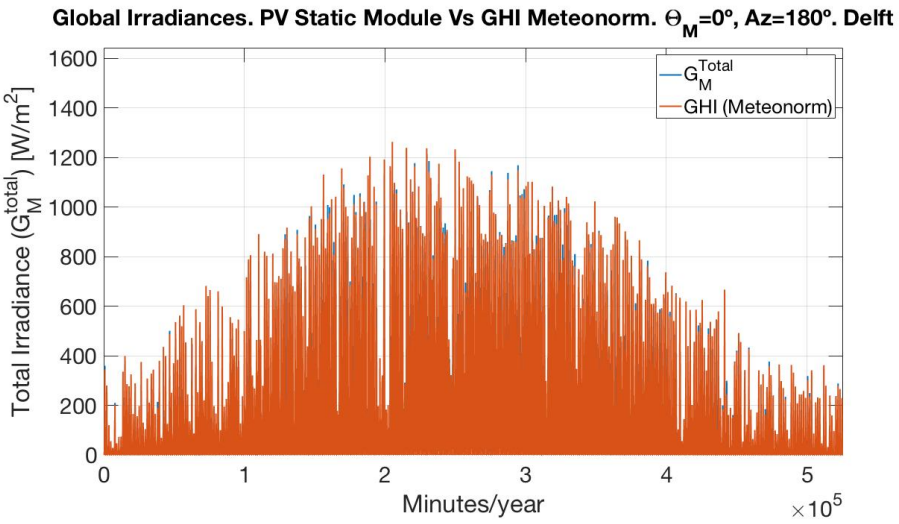

Figure 5.7: Global irradiance falling on the PV module vs GHI from KNMI file.

In the previous figure there are two results: the total irradiance calculated by the MATLAB model (in blue) and the GHI from the input file (in red). Both variables have almost the same dromedary-shape form because both results have almost the same values. It may seem that the GHI is the only graph shown, but the reason is that the GHI almost overlaps G_M^{Total} because they both share a very similar shape. Nevertheless there are blue lines in the graph (at the top of the lines) where both colours can be appreciated.

The Figure 5.8 describes the names and colours of the lines in Figure 5.6.

Figure 5.8: Irradiances incident on the PV module.

Where:

- G_M^{Total}**:** Stands for the total irradiance incident on the PV module (in blue)
- GHI (from file): Stands for the global horizontal irradiance incident on the PV module from the input data file (in red). No calculations are performed here, it is just a direct plot from the file
- G_M^{dir}**:** Stands for the direct irradiance incident on the PV module (in yellow)
- G_M^{diff}**:** Stands for the diffuse irradiance incident on the PV module (in purple)
- G_M^{ground}**:** Stands for the ground irradiance (caused by the albedo) incident on the PV module (in green)

It can be observed that the irradiance calculated by MATLAB is almost identical to the one obtained by SAM when θ_M=0º. This means that so far at this point, the MATLAB model works properly and its results are strongly alike to those from SAM's when they are compared. Further in this chapter, when the PV module is tilted at its optimal tilting angle, a closer look to the equivalent of Figure 5.6 is analysed, by zooming-in for the period of one week and also one day of that week. Then all the irradiances and colours will be visible when the panel is tilted.

The Figure 5.9 depicts the monthly energy yield incident onto the PV module with a flat tilting and Figure 5.10 the individual contribution to the annual energy yield that each one of the irradiances provides.

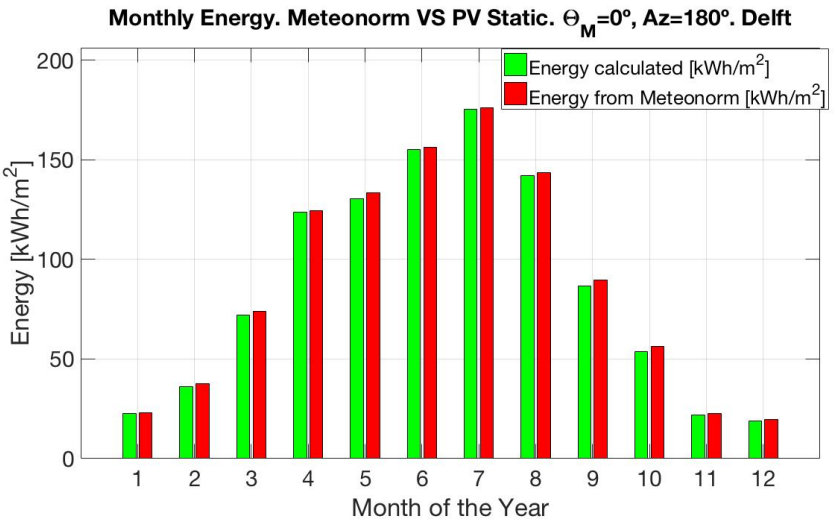

Figure 5.9: Monthly energy yield incident on the PV module, in [kWh/m^2].

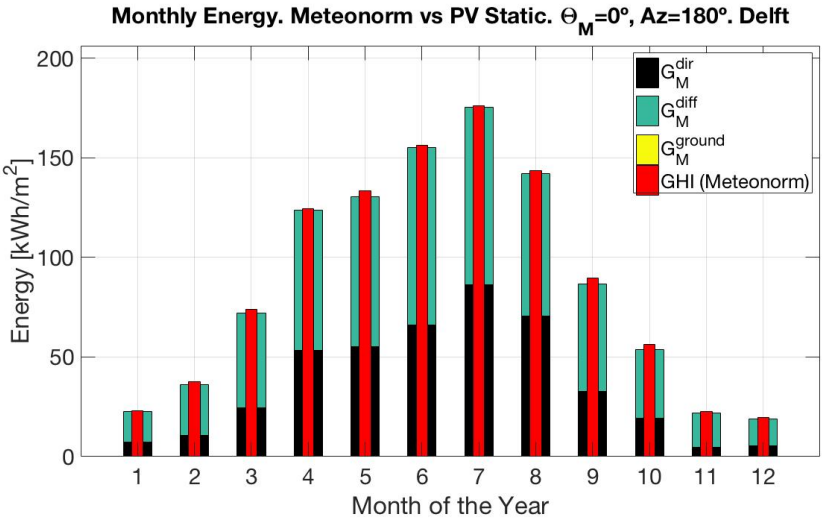

Figure 5.10: Individual energy yield provided by the direct, diffuse and ground irradiances in [kWh/m^2].

Where:

- G_M^{dir}**:** Stands for the annual energy yield contribution by the direct irradiance incident on the PV module (in black)
- G_M^{diff}**:** Stands for the annual energy yield contribution by the diffuse irradiance incident on the PV module (in turquoise)
- G_M^{ground}**:** Stands for the annual energy yield contribution by the ground irradiance incident on the PV module (in yellow)
- GHI (from file): Stands for the global annual energy yield extracted from the input file (in red), which can be from Meteonorm, KNMI or any other source consulted by the user

From the previous graphics, it is clear that the only irradiances that contribute with the energy yield are the diffuse and the direct ones. There is a small difference between the total energy yield calculated by MATLAB and the one from the KNMI file. Table 5.2 shows what is the energy yield of each irradiance and the total energy yield calculated from both MATLAB and the KNMI input data file.

Source	G_M [kWh/m^2]	G_M^{dir} [kWh/m^2]	G_M^{diff} [kWh/m^2]	G_M^{ground} [kWh/m^2]
KNMI	**1058**	880	602	N/A
MATLAB	**1039**	437	602	0
Difference [kWh/m^2]	**-19**	-420	0	N/A
Difference in [%]	**-1.8 %**	N/A	0.0 %	N/A

Table 5.2: Individual Energy Yield. Contribution by irradiance. PV Static system. θ_M=0º.

From the previous table is observed that the only results to consider for a comparison are: the diffuse and total irradiances incident on the PV module. It could not be determined how the direct irradiance is calculated by KNMI or Meteonorm, since the sum of the diffuse and direct irradiances is 1,482 W/m^2 and not 1,058 W/m^2 as the file indicates. Therefore, the only similar results are the diffuse and the total irradiances and only they will be analysed. It can be seen a deficit of 19 [kWh/m^2] for the global irradiance and no difference at all in the diffuse irradiance. The difference between the global irradiances (KNMI vs SAM) is less than 1.8 %, this insignificant difference can be considered acceptable and therefore, it will not have an important impact on further results.

It is noteworthy that for this location, the diffuse irradiance calculated by the MATLAB model plays an important role for the energy generation, since it is higher than the calculated direct irradiance. This can be explained by the fact that the module is not facing the Sun, therefore, the direct irradiance incident on the PV module is reduced. The next case to analyse is the same PV Static module, but this time the θ_M will be of 37º, which is the optimal tilting angle found in SAM.

PV Static. Results at θ_M=37°

The second case to analyse will be the one when the PV module has a tilting angle of 37º. As mentioned before, in SAM, this was the optimal tilt angle where the highest performance on the PV System was found for Delft. The time series irradiance in [W/m^2] throughout the year in minutes can be seen in the Figure 5.11b, with the annual incident irradiance onto the PV panel.

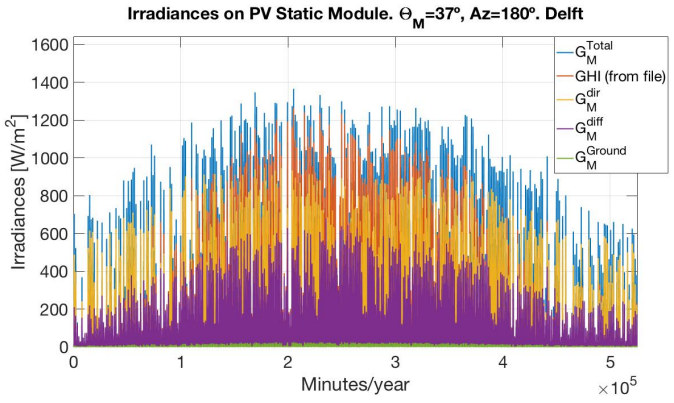

(a)

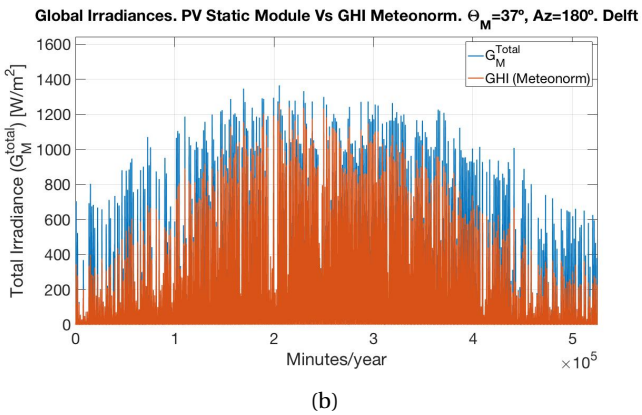

(b)

Figure 5.11: For both figures: θ_M=37º (a)Total, direct, diffuse and ground irradiances calculated vs GHI from Meteonorm. (b)Total irradiance falling onto the module vs GHI from KNMI file.

It can be observed that the irradiance increased if compared with Figure 5.6. Now there are 3 irradiances (direct, diffuse and albedo) in the graph instead of the 2 when the PV module was flat.

The Figure 5.12 depicts the monthly energy yield incident onto the PV module with tilting angle of 37º.

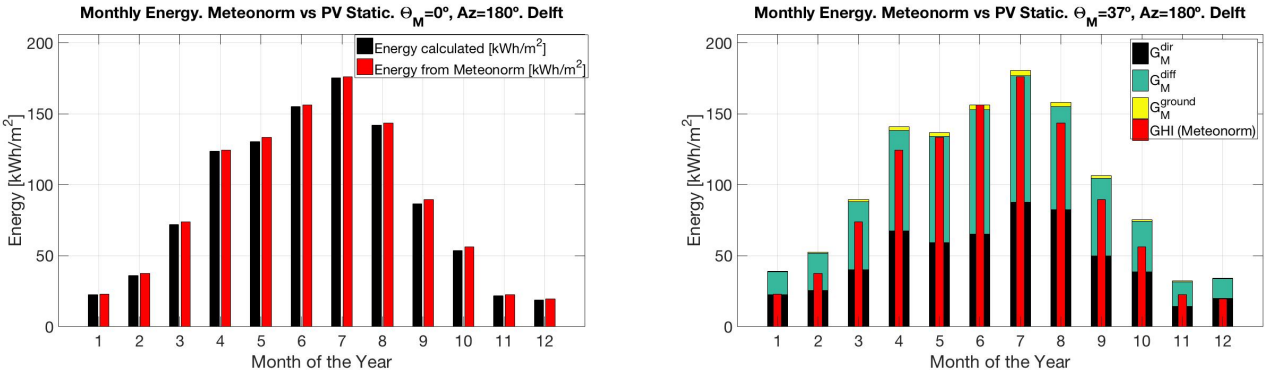

(a) (b)

Figure 5.12: θ_M=37º (a)Monthly energy yield incident on the PV module in [kWh/m^2] (b)Individual energy yield provided by the direct, diffuse and ground irradiances in [kWh/m^2].

Now the 3 irradiances clearly appear in the graph: the diffuse, the direct and ground irradiances are present. The tilt on the module significantly increased their values if compared to the flat panel (0º). The table 5.3 shows the numeric details of the energy yield of each irradiance and the total energy yield calculated from MATLAB at 0º and 37º tilt angles.

θ_M [^{o}]	$\mathbf{G}_M$ [kWh/m^2]	$\mathbf{G}_M^{dir}$ [kWh/m^2]	$\mathbf{G}_M^{diff}$ [kWh/m^2]	$\mathbf{G}_M^{ground}$ [kWh/m^2]
0	**1039**	437	602	0
37	**1203**	574	607	22
Difference [kWh/m^2]	**+165**	+137	+5	+22
Difference in [%]	**+16 %**	+35 %	+0.8 %	N/A

Table 5.3: Individual Energy Yield. Contribution by irradiance. PV Static system. θ_M=0º vs θ_M=37º.

The table above makes it obvious that the big "winners" thanks to the tilting of 37º are the direct and the ground irradiances. The reason is because the tilting angle improves the PV module's position and it now "is looking" more into the Sun, which explains the gaining in the direct irradiance. Curiously, the diffuse irradiance also got a marginal increase. It was expected a slight reduction in this variable due to the tilting angle, since the SVF is no longer 1 (see formula at Section 2.3.2).

The increase is caused because the Sandia model takes into consideration the solar zenith angle and because θ_M>0º. The right side of the equation is added to the isotropic sky diffuse model. This can be seen at the Formula 2.9 from the Section 2.3.2. The Sandia model for the diffuse irradiance is again shown here:

$$G_M^{diff} = (DHI \cdot SVF) + \left[GHI \cdot \frac{(0.012 \cdot \theta_z - 0.04) \cdot (1 - cos(\theta_M))}{2} \right]$$

When θ_M=0º, the term to the right becomes zero and only the isotropic sky diffuse model to the left (DHI·SVF) is present. When θ_M>0º, this is no longer the case and the G_M^{diff} increases.

Moreover, the tilting now makes that the module receive irradiance coming from the light reflected on the ground. Even if it is small compared to the direct or diffuse irradances, it now contributes on the final energy yield production.

Hence, it is evident that all the irradiances increased their contribution to the overall energy yield, which is the desired outcome on a PV system: to produce as much energy as possible. In the next subsection, the θ_M will be of 52º, which is the optimal tilting angle obtained by the MATLAB model PV Static Finder.

PV Static. Results at θ_M=52º

The final scenario to analyse will be the one with a tilting angle of 52º, which was found using the PV Static Finder MATLAB model previously explained at the beginning of this chapter. Figures 5.13b depict the time series irradiances (in [W/m^2]) throughout the year in minutes. Where θ_M=52º.

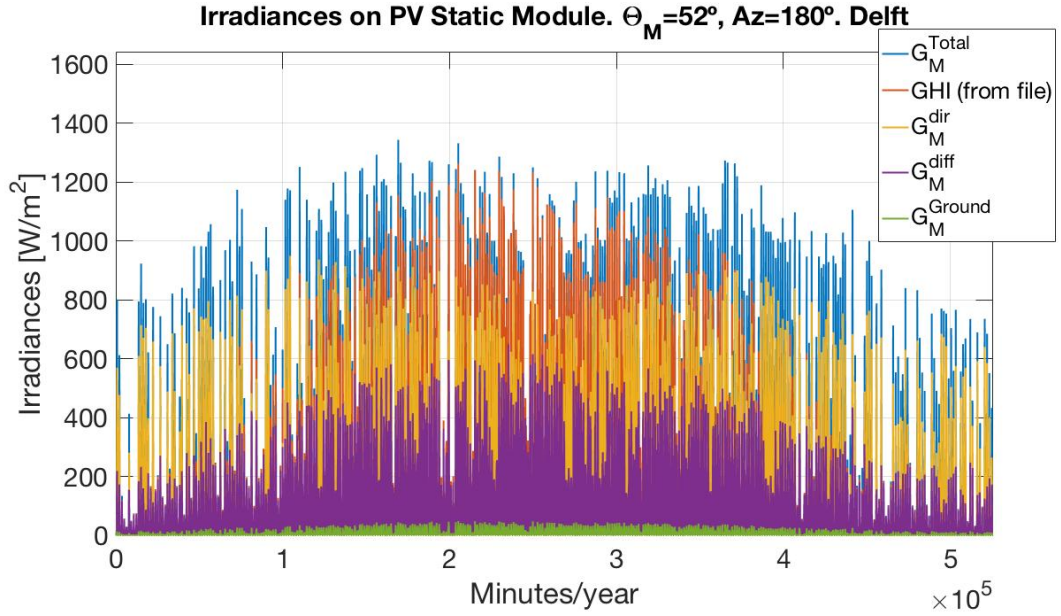

(a)

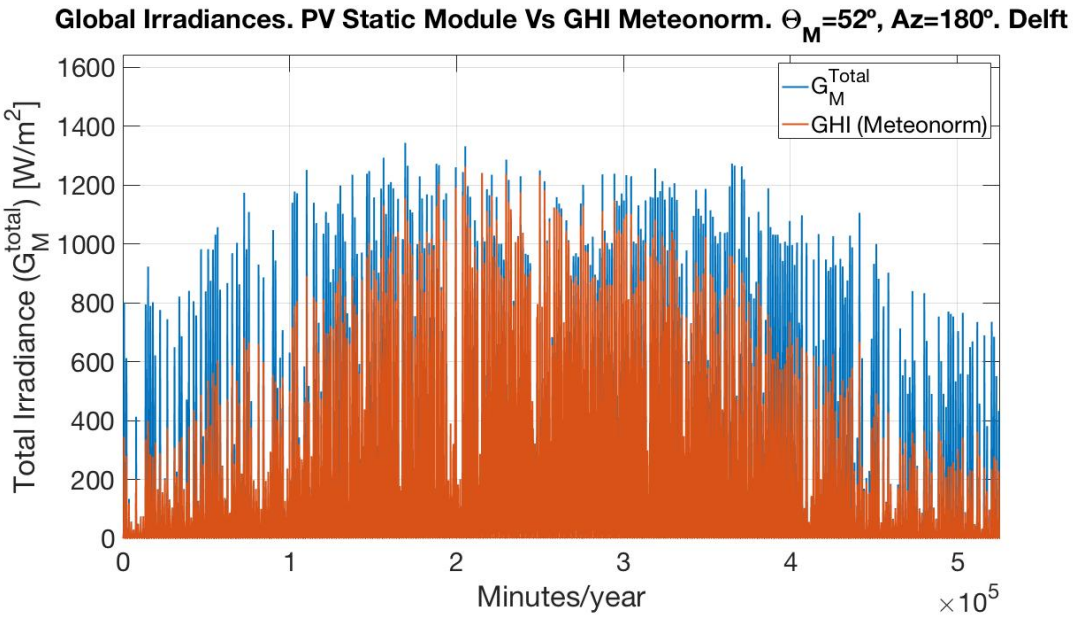

(b)

Figure 5.13: For both figures: θ_M=52º (a)Total, direct, diffuse and ground irradiances calculated vs GHI from Meteonorm/KNMI. (b)Total irradiance falling onto the module vs GHI from Meteonorm/KNMI file.

When these images are compared with the ones shown when the PV module was flat (θ_M=0º vs θ_M=37º), it is appreciated that the Figures 5.13a and 5.13b are denser and slightly higher than 5.11a and 5.11b. This might not be perceived at a simple glance, but taking a closer look to the numeric values will corroborate this. In 5.13a it is also much more remarkable the ground irradiance at the bottom (green lines).

It can be observed that the irradiance increased if compared with Figure 5.16. Now there are 3 irradiances (direct, diffuse and albedo) in the graph instead of the 2 when θ_M=0º.

Zoom-in to the Time Series Irradiances

Now let us take a closer look to one sample week (from 24^{th} up to the 30^{th} of April of 2013) and one sample day (the 26-04-2013) at 10h04. The Figures 5.14 depict these samples.

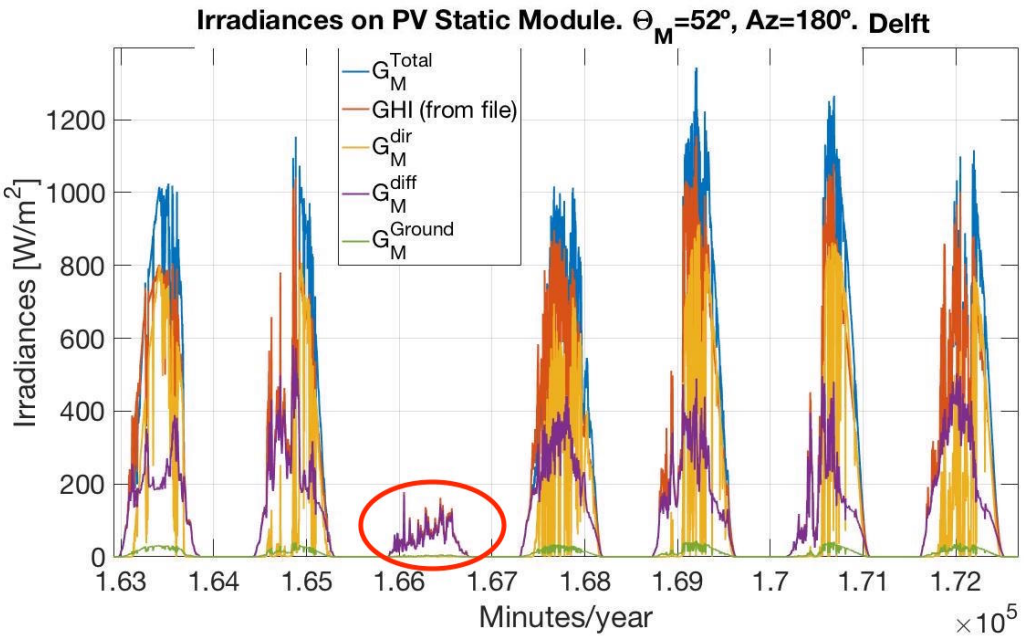

(a)

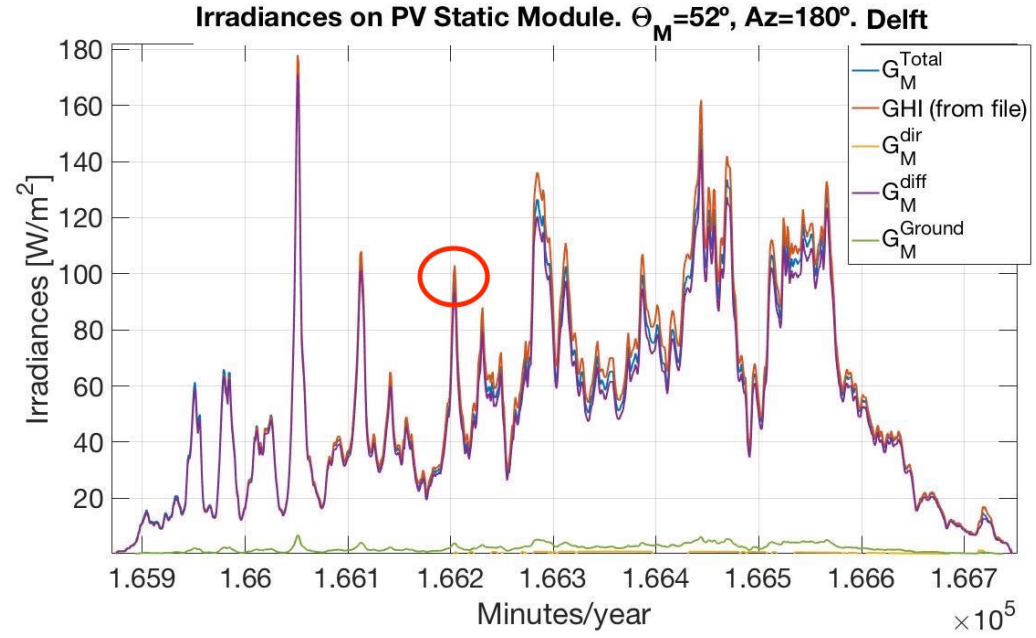

(b)

Figure 5.14: Zoom-in to the 26/04/2013 (a)The week of 24^{th} of April up to the 30^{th} of April. In the red circle: the 26/04/2013 (b)Zoom-in to the 26/04/2013. In the red circle: the sample hour (10h04).

In the Figure 5.14a all the irradiances can be appreciated. It is noteworthy that in that week, there was one day with low solar irradiance (in the red circle), which corresponds to the 26-04-2013. Figure 5.14b corresponds to the zoom-in of that same day. Note that in this day of poor sunlight, the predominant irradiance is the diffuse one (the purple line). The GHI from the file (the red line) almost overlaps the G_M^{Total} (the blue line). It is observed that the G_M^{Ground} (green line) has a moderate contribution to the energy yield. The direct irradiance G_M^{dir} (yellow line) does not contribute to the energy yield production.

The Figures 5.15 depict another zoom-in (which is the red circle from Figure 5.14b), this time corresponding to the time at 10h04 (or 10:04 am) of the day 26-04-2013.

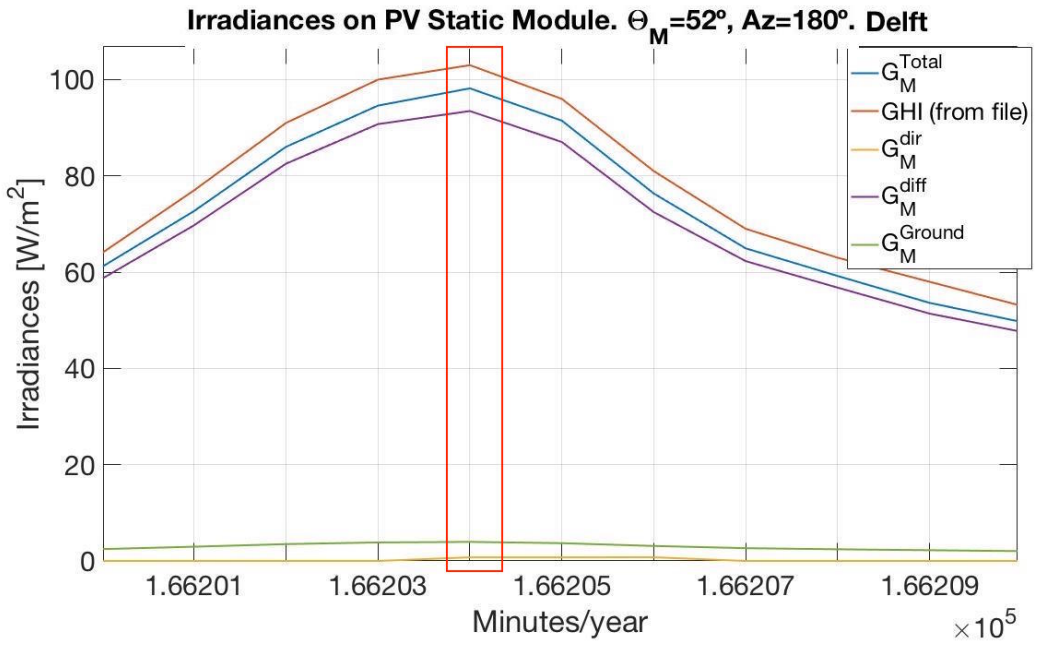

(a)

	A	B	C	D	E	F	G	H	I	J	K	L	M	N	O
1	Month	Day	Hour	Minute	DHI (from fil	G_diff	DNI (from fil	G_dir	G_ground	GHI (from fil	G_module (R	Sun_Altitude	Sun_Azimuth	Module_tilt	Module_azimuth
166196	4	26	9	55	45	41.418	0	0	1.768	46	43.186	38.909	123.61	52	180
166197	4	26	9	56	49	45.076	0	0	1.9217	50	46.997	39.037	123.88	52	180
166198	4	26	9	57	53	48.73	0	0	2.0754	54	50.806	39.164	124.14	52	180
166199	4	26	9	58	53	48.714	0	0	2.0754	54	50.79	39.291	124.41	52	180
166200	4	26	9	59	56	51.34	0	0	2.1523	56	53.492	39.418	124.68	52	180
166201	4	26	10	0	64	58.656	0	0	2.4598	64	61.116	39.544	124.95	52	180
166202	4	26	10	1	76	69.74	0	0	2.9594	77	72.699	39.67	125.22	52	180
166203	4	26	10	2	90	82.541	0	0	3.4975	91	86.038	39.796	125.49	52	180
166204	4	26	10	3	99	90.755	0	0	3.8434	100	94.598	39.921	125.76	52	180
166205	4	26	10	4	102	93.472	1	0.751	3.9587	103	98.182	40.046	126.04	52	180
166206	4	26	10	5	95	87.037	1	0.7537	3.6896	96	91.481	40.17	126.31	52	180
166207	4	26	10	6	79	72.481	1	0.75638	3.1131	81	76.35	40.294	126.58	52	180
166208	4	26	10	7	68	62.292	0	0	2.6519	69	64.944	40.417	126.86	52	180

(b)

Figure 5.15: Zoom-in to the 26/04/2013 (a)26/04/2013, 10h04 (b) Highlighted in green, the characteristics of the day sample (26/04/2013 at 10h04) irradiances, taken from the CSV created by the PV Static model.

Figure 5.15a is the zoom-in made to the red circle in Figure 5.14b. Figure 5.15b is an extract of the CSV file created by the PV Static MATLAB model. Highlighted in green is the day 26-04-2013 at 10h04, and the coloured columns represent each irradiance calculated by the MATLAB PV Static model (blue for G_M^{Total}, red for GHI, yellow for G_M^{dir}, purple for G_M^{diff} and green for G_M^{ground}). Please note that the red vertical rectangle in Figure 5.15a is the peak corresponding to the green horizontal rectangle at Figure 5.15b.

It can be seen that the GHI has a slightly higher value than the G_M^{Total} (103 vs 98.2) [W/m^2]. This is because the θ_M causes losses in the G_M^{diff}, according to the formula to determine the diffuse irradiance incident on a PV Module 2.9.

Now that the analysis of a sample-week and a sample-day has been studied, the calculation of the monthly incident energy yield will be performed. The Figure 5.16 depicts the monthly energy yield incident onto the PV module with a tilting angle of 52º.

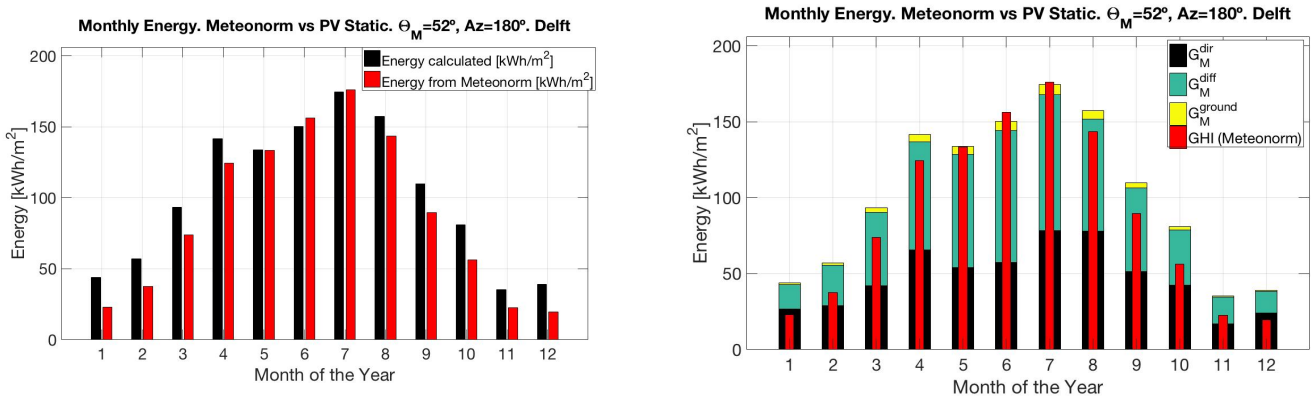

Figure 5.16: θ_M=52º (a)Monthly energy yield incident on the PV module in [kWh/m^2] (b)Individual energy yield provided by the direct, diffuse and ground irradiances in [kWh/m^2].

Now it is noted that the 3 irradiances: the diffuse, the direct and ground irradiances are present. The tilting applied on the module significantly increased. The table 5.4 shows the numeric details of the energy yield of each irradiance and the total energy yield calculated from MATLAB at 0º, 37º and 52º degrees applied on the PV module. Where "Dif." stands for "difference".

θ_M [^{o}]	$\mathbf{G}_M$ [kWh/m^2]	$\mathbf{G}_M^{dir}$ [kWh/m^2]	$\mathbf{G}_M^{diff}$ [kWh/m^2]	$\mathbf{G}_M^{ground}$ [kWh/m^2]
0	**1039**	437	602	0
37	**1203**	574	607	22
52	**1218**	567	611	40
Dif.(52vs0) [kWh/m^2]	**+179**	+130	+9	+40
Dif.(52vs0) in [%]	**+17.23** [%]	+29.75 [%]	+1.5 [%]	N/A
Dif.(52vs37) [kWh/m^2]	**+15**	-7	+4	+18
Dif.(52vs37) in [%]	**+1.25** [%]	-1.22 [%]	+0.66 [%]	+81.82[%]

Table 5.4: Individual Energy Yield. Contribution by irradiance. PV Static system. Comparison between PV module's tilting angles (θ_M): 0º vs 52º and 37º vs 52º.

In general, the three irradiances increase their performance when the PV module is tilted. Let us analyse first the case of the 52º vs 0º tilting angles: when the PV panel's tilting angle was of 52º, the direct irradiance improved by +17.23 % and the diffuse gained a marginal +1.5 %, whereas the ground incident irradiance passed from 0 [kWh/m^2] to 40 [kWh/m^2], making it the biggest "winner" in this comparison.

For the case of the 52º vs 37º tilting angles (also known as: the optimal tilting angle found in the optimal tilting angle found in the PV Static Finder MATLAB model vs SAM): the direct irradiance had a marginal loss of -1.22 %, whereas the diffuse one gained a marginal +0.66 %; once more, the ground incident irradiance had a massive gain of almost 82 %, making it again the greatest "winner" in this tilting comparison.

It is the reflected irradiance from the ground who got the most relevant gaining at a tilting of 52º. The explanation to this is since the module is more steep, it receives more irradiance from the ground. Especially during spring and summer time. This is observed at Figure 5.16b, where the yellow colour corresponds to the ground irradiance incident on the PV module.

The G_M^{dir} is higher at a tilt of 37º than in 52º because more sunlight falls directly on the PV module during summer, where the days are longer. Nevertheless, the Sandia model to determine the G_M^{diff} improves the diffuse irradiance at a 52º tilting angle and the G_M^{ground} has a higher performance.

In overall, 52º is the optimal tilting angle to get a proper balance and the best overall performance in one year for a PV module in a static topology in this MATLAB model.

Figure 5.16b indicates that in the autumn and winter seasons, the PV module strongly increases its energy

yield, whilst in spring and summer (May, June and July) it does not even reach the energy yield as if it were flat. This is understandable because the Sun is at a very high altitude during summer and since the PV module has a very steep angle, it does not receive enough direct irradiance from the Sun as if it did at a flatter tilting.

Moreover, the table of results compares the 3 tilting positions and the conclusion is clear: the most optimal tilting angle on a PV module, is the same as the one of the location's latitude (around 52º), as Boxwell [32] suggests in his online solar calculator [33].

5.5.3. PV Static. Fixed Tilting. Conclusions

Finally, it can be stated as a first conclusion, that for this latitude, the PV Static model designed in MATLAB and using the Sandia model to determine the diffuse irradiance incident on a PV module, determined that the best optimal tilting angle for Delft, is the city's own latitude. At this tilt, the diffuse irradiance was the main contributor for the overall annual energy yield, followed by the direct irradiance and lastly, the ground one. Thus, for latitudes around 50º, it is an accurate assumption to use the θ_M = Latitude, in order to have the highest yearly performance from a PV module.

The previous paragraph leads us to answer the following research question:

Are the suggested tilting angles found in literature the same as the ones obtained in this MATLAB model?

According to the MATLAB model results: the optimal tilting angle for a PV Static topology calculated in the MATLAB model is not the same as the one from SAM. The reason for this might be related to the formula used to calculate the G_M^{diff}, which was the Sandia model, whilst SAM uses the Perez model. Since SAM does not show individual results for the G_M^{diff} (or any other irradiance) calculated by it, is impossible to compare individual results from the direct, diffuse and/or ground irradiances between SAM and the MATLAB model developed in this project.

In appendix A it can be noted that the assumption latitude = PV tilting angle is only valid for locations at very high latitudes (>40º). For places closer to the Equator, this is no longer an accurate assumption. Even though it is a good approximation, there can be a difference of 10º, which is a significant variation and it is more recommendable to recalculate the optimal angle for the PV module in this situation.

5.6. PV Static. Semi-static Tilting

As it was mentioned at 1.4, the semi-static configuration is applicable for those PV modules whose tilting angle changes at least twice per year and these changes are done manually by a simple mechanical structure. Figure 5.17 depicts this kind of system.

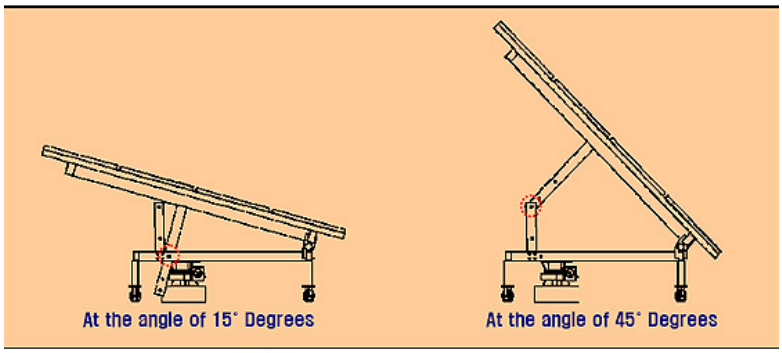

Figure 5.17: PV module with fixed Azimuth and semi-static Tilting [9].

This section did not have a monthly study for an optimal tilting angle, because at the beginning, it was thought to obtain these tilt angles from the "tilting tracking topology", but these results did not correspond to the "optimal tilting angles" of the PV module, but to an "average tilting angle" per season, which was going to be a "false-positive" result. Unfortunately this observation was discovered almost at the end of this research and there was not time to perform the correct approach.

Nevertheless, since for Delft the assumption of θ_M = Latitude is used, it might be implemented as a "rule of thumb" the horizontal tilting angles proposed by Boxwell [32] in his solar calculator shown at Figure 5.18. The image shows the calculations for Den Haag but they could also be implemented in Delft, since they are close cities from one another. In other words: use the tilting angles per month shown at Figure 5.18.

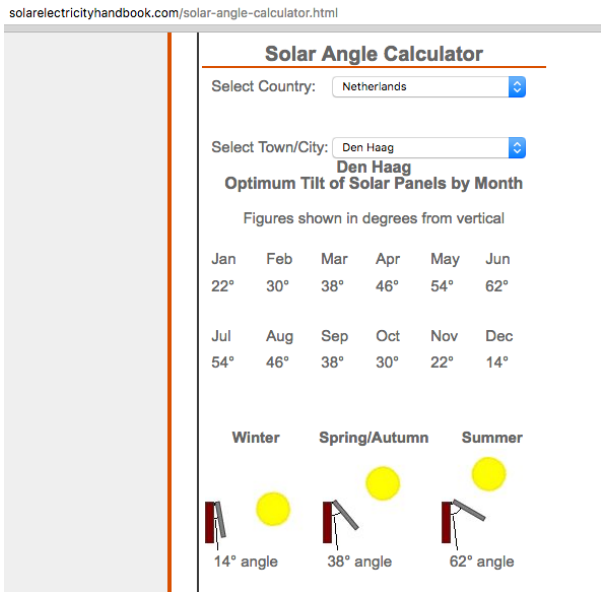

Figure 5.18: PV module optimal tilting angle for Den Haag [33].

5.6.1. Semi-static Tilting. Conclusions

From the previous analysis and for what could be seen for the PV Static topology, a higher incident energy yield is expected thanks to these periodical changes in the PV module's tilting angle.

Moreover, it is well known that this periodical change at the tilting angle of the PV module would mean that the semi-static topology will definitely have a higher performance ratio compared to the PV Static one, making it a better option with a possibly small increase in the installation investment costs.

As previously said, for unexpected reasons it was not possible to create in time a model to determine a monthly, seasonal and semester optimal tilting angle.

In the Section 5.11.1, is given an explanation about the relation that it was primarily thought between the PV Semi-static and the TRT (Tilting Tracking) topologies and that turned out to be different.

5.7. Solar Tracking Systems

The static and semi-static topologies have already been analysed and discussed. Now the tracking system topologies will be approached in this chapter. At the end of it, a comparison between the results so far seen here will be compared and commented. Let us remember that a tracking systems tries to "follow" the Sun in order to extract as much energy as possible from its solar rays.

There are two categories of tracking systems: the 2-axis system, whose follows the sun in both horizontal and vertical directions acting as a sunflower; and two versions of 1-axis system: the azimuth tracker the PV module has a static tilting angle and follows the Sun from East to West during the day; and the tilting tracker which changes the PV module's tilt angle during the day.

In the next sections these tracking topologies will be thoroughly analysed and discussed, where the incident irradiance and annual energy yield of each case will be explained.

5.8. TRAT: the Azimuth and Tilting Tracker with Diffuse Enhancement

The first topology to analyse will be the 2-axis tracker: the "tracker of azimuth and tilt" angles, known as "TRAT" in this project. This kind of trackers work as a sunflower following the Sun at every minute or at any assigned time-scale in order to receive the maximum amount of direct radiation (this is, the system tries to make that the PV module is always facing the Sun). The Figure 5.19 depicts an azimuth-tilting tracking system. In theory and in practice, this is the topology that has the best performance from all the topologies.

Figure 5.19: Azimuth-Tilting tracking system [9].

Usually these trackers on days with low solar radiation are programmed to use the location's optimal tilting angle facing the true South/North. Nevertheless, the version proposed here sets the PV module at a tilting angle of 0º (flat). This is because the diffuse irradiance is the dominant during cloudy days, hence, if the module is flat, there will be a better benefit from the diffuse radiation in the atmosphere. The Figure 5.20 describes the algorithm used for this azimuth-tilting tracking system.

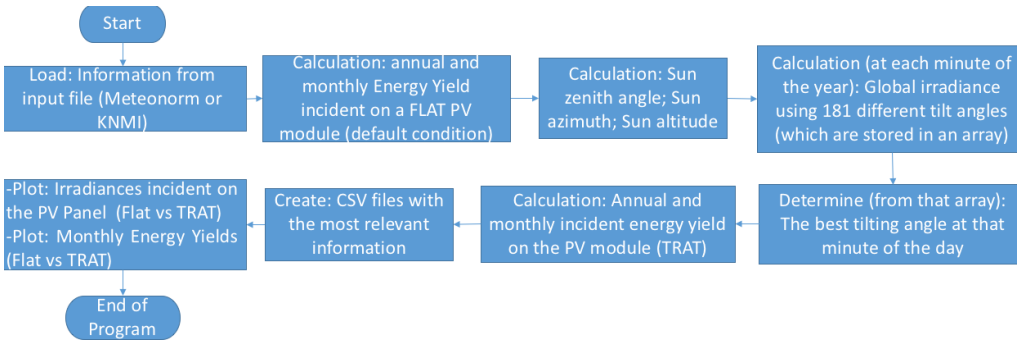

Figure 5.20: Flowchart of the azimuth-tilting tracking model.

Remembering the formula to determine the diffuse irradiance incident on a PV module, it is appreciated that at 2.4 the SVF will become 1 if the module is flat ($\theta_M = 0º$):

$$SVF = \frac{1+\cos(0)}{2} = 1$$

Hence, when SVF = 1, the θ_M =0º and from 2.9, the diffuse irradiance incident on the panel would become:

$$G_M^{diff} = (DHI \cdot 1) + \left[GHI \cdot \frac{(0.012 \cdot \theta_z - 0.04) \cdot (1 - cos(0))}{2} \right] = DHI$$

This is because the operation inside the brackets becomes 0, because (1-cos(0) = 0). This scenario demonstrates that if the tracker is setted at the optimal tilting angle according to its latitude, the diffuse irradiance incident on the PV module would decrease.

What the model does, is to simultaneously calculate 2 options at that same time of the day: one using the PV module's optimal tilting angle calculated and another one using a 0º tilt angle. Once these values are performed, the model compares which has the highest incident energy yield onto the module, to finally choose the angle where the highest AEY is found, which could be 0º (flat module) or whichever optimal tilting angle at that minute of the year. This is done because you might have a day where DHI>DNI, but this does not necessarily mean that the optimal angle should be 0º.

Therefore, the TRAT model determines what is the best tilting angle for the tracking system at every minute of the year, achieving thus the maximum possible performance.

5.8.1. TRAT Results

In this subsection all the results from this model will be analysed. To begin with, the first calculation made in the model is the one of the solar position.

The Figures 5.21 depict the amount of irradiance falling onto the module throughout the year. These graphs can also be called the "time series irradiances", which are in minutely format and represent the irradiances incident onto the PV module at each minute of the year.

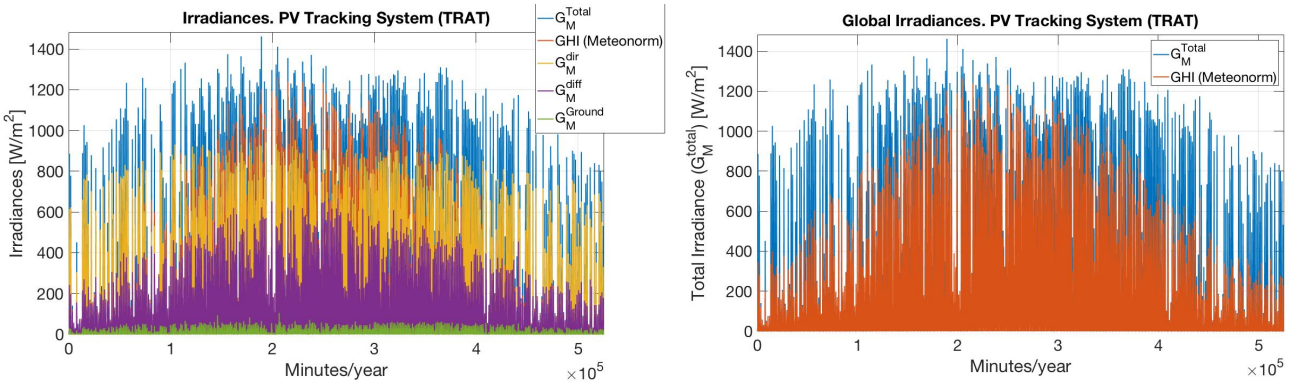

(a) (b)

Figure 5.21: (a)Total, direct, diffuse and ground irradiances calculated vs GHI from Meteonorm. (b)Total irradiance falling onto the module vs GHI from Meteonorm file.

Figure 5.22a depicts the amount of incident energy yield per month in [kWh/m^2] throughout the year and Figure 5.22b what is the contribution of each irradiance (direct, diffuse and ground) in the total incident monthly energy yield.

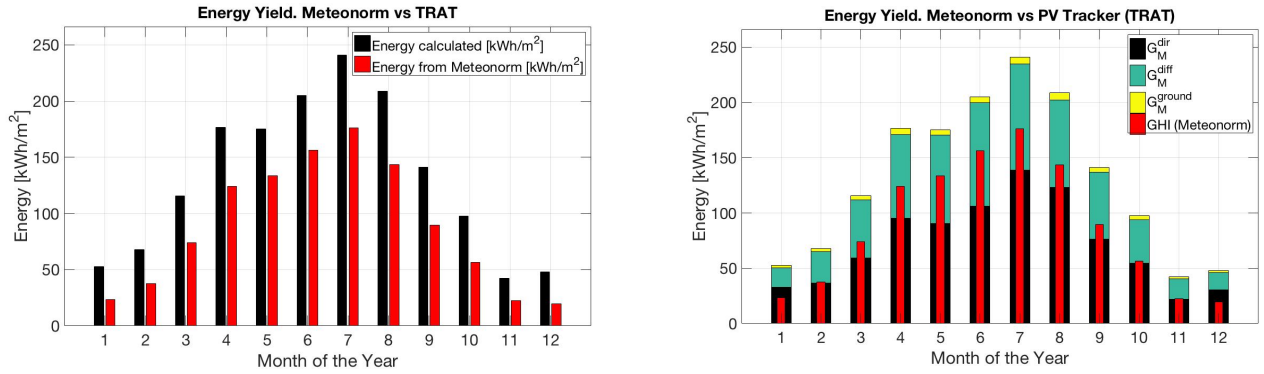

(a) (b)

Figure 5.22: (a)Monthly energy yield incident on the PV module in [kWh/m^2] (b)Individual energy yield provided by the direct, diffuse and ground irradiances in [kWh/m^2].

The Table 5.5 depicts the contribution in [kWh/m^2] of each of the irradiances and the comparison with the flat module (0º tilting) is performed.

θ_M [º] **or Topology**	$\mathbf{G}_M$ [kWh/m^2]	$\mathbf{G}_M^{dir}$ [kWh/m^2]	$\mathbf{G}_M^{diff}$ [kWh/m^2]	$\mathbf{G}_M^{ground}$ [kWh/m^2]
PV Static (0º)	**1039**	437	602	0
TRAT	**1573**	867	657	49
Difference [kWh/m^2]	**+534**	+430	+55	+49
Difference in [%]	**+51.4 %**	+98.4 %	+9.14 %	N/A

Table 5.5: Individual Energy Yield. Contribution by irradiance. TRAT vs PV Static Flat (0º).

As it can be seen, the direct irradiance plays the most significant role in the incident annual energy yield. This is an expected behaviour since the tracker tends to face directly into the Sun as much as possible, except in the cases where the PV module is flat so that it can get more diffuse irradiance.

It is outstandingly noticeable that the energy yield of the direct irradiance almost doubled its value compared with the flat PV module. The diffuse irradiance annual energy yield gained 9 % in its performance and finally, the ground irradiance also had an important gaining. The total incident energy yield increased from 0 [kWh/m^2] to almost 50 [kWh/m^2].

5.8.2. TRAT conclusions

The numbers found in the MATLAB corroborated what the literature and the practice had already demonstrated: the TRAT had the highest energy yield per square meter. The MATLAB model searches, finds and uses the best tilting angle on the PV panel so that it receives the highest possible amount of irradiance. This includes to set the PV panel flat (0º tilting) if the diffuse irradiance is the best at that time of the day, even if in practice the standard tilting angle at that moment is commonly implemented.

In other words: this is a smart tracking system which optimises at its maximum the irradiance incident onto the PV panel. This was demonstrated at the Section 5.8, where if the angle in which the PV module receives the highest direct irradiance is not the best, and a 0º angle is the optimal one (to increase the diffuse irradiance contribution), then the diffuse irradiance will have a higher priority since it would be the main provider of irradiance incident onto the PV panel and the tilting angle is set to 0º.

As for the distribution of the contribution of energy yield by the irradiances, the direct irradiance had the highest contribution to the overall energy. The diffuse irradiance was the second best contributor. This is because during the year the PV tracking system "follows" the Sun in order to get more direct irradiance.

5.9. TRA: Azimuth Tracker with fixed PV Module's Tilting Angle

TRA stands for "Tracker of Azimuth" in this thesis project. This is the second tracking topology whose results will be analysed: the 1-axis azimuth-tracker system also known as azimuth tracker. This tracking configuration moves horizontally following the Sun's azimuth (from East to West) and the PV panel/array is tilted to its optimal tilting angle according to its latitude. The Figure 5.23 depicts an azimuth tracking system. In theory and in practice, this is the tracking topology that has the second best performance.

Figure 5.23: Azimuth tracking system [9].

Three different angles will be tested in this model: 37º (corresponding to the tilting angle of SAM); 52º (found in the PV Static Finder model) and 67º, which is the optimal tilting angle found for this azimuth-tracker topology. The Figure 5.24 describes the flowchart used to develop the TRA model in MATLAB.

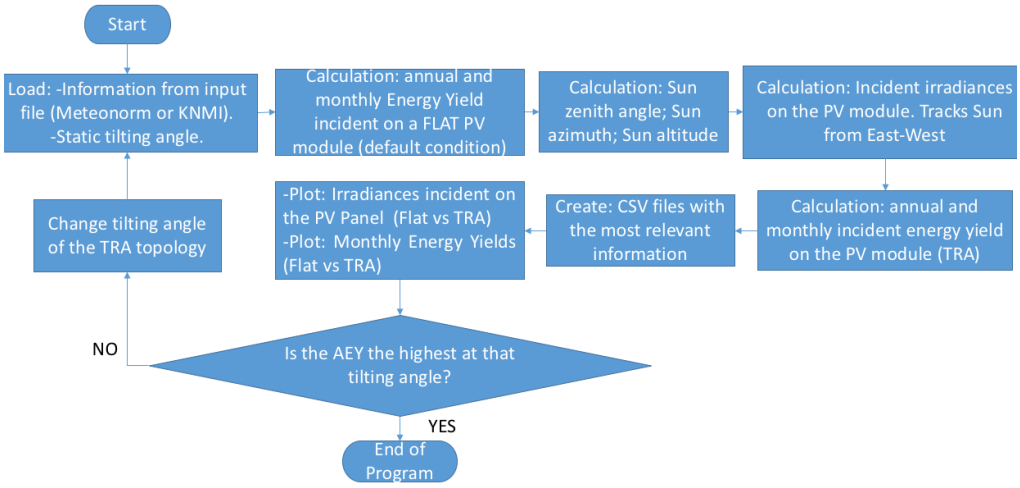

Figure 5.24: Flowchart of the azimuth tracking model.

NOTE: the optimal tilting angle has to be done manually. In other words: the user has to manually test different angles and compare the results at each angle. A "TRA Tilt Angle Finder" (similar to the PV Static Finder model) is being developed.

5.9.1. TRA Results

In this sub-section the most important results and observations regarding the 1-axis azimuth tracking system (TRA) will be discussed. Again, it is important to state that 3 module tilting angles are analysed in this topology: one at 37º (SAM's optimal tilting angle), at 52º (PV Static Finder Model) and 67º (which is the optimal tilt angle for the TRA topology).

TRA Results at 37°

The time series irradiance graphs are shown at Figure 5.25 at a tilting angle of 37º

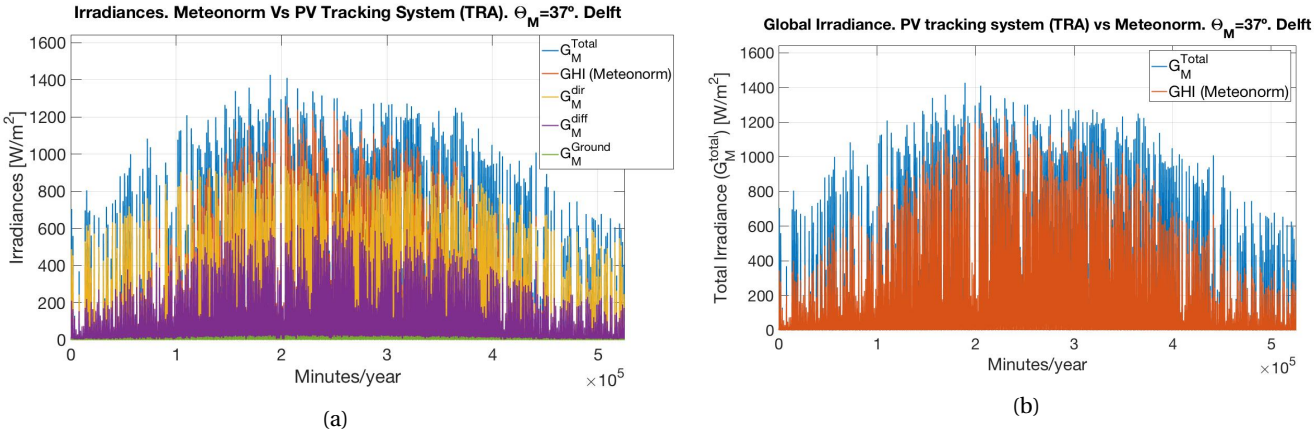

Figure 5.25: (a)Total, direct, diffuse and ground irradiances calculated vs GHI from KNMI. (b)Total irradiance falling onto the module vs GHI from KNMI file. At θ_M=37º.

Again it can be seen that the PV module's tilting and the azimuth tracker give a higher irradiance if compared with a flat surface (compare it with Figure 5.6).

The Figure 5.26 depicts the monthly energy yield incident onto the PV module.

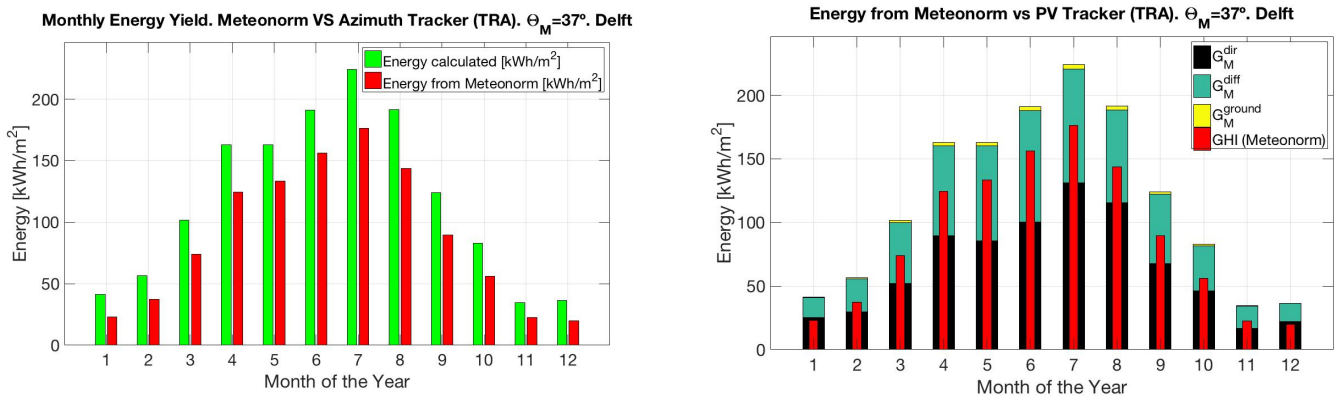

(a) (b)

Figure 5.26: θ_M=37°(a)Monthly energy yield incident on the PV module in [kWh/m^2] (b)Individual energy yield in [kWh/m^2] provided by the direct, diffuse and ground irradiances.

At Figure 5.26b it is seen that all the irradiances contribute for the generation of the annual energy yield incident on the PV module. The contribution of the ground irradiance is minimal though.

TRA Results at 52°

The results of the optimal tilting angle found using the Tilting Finder model are now analysed. 52° is the found optimal tilting angle for a PV Static topology. The reason to use the same tilting angle is to see if it is also the optimal tilting angle for a TRA topology. The time series irradiances graphs are shown at Figure 5.27:

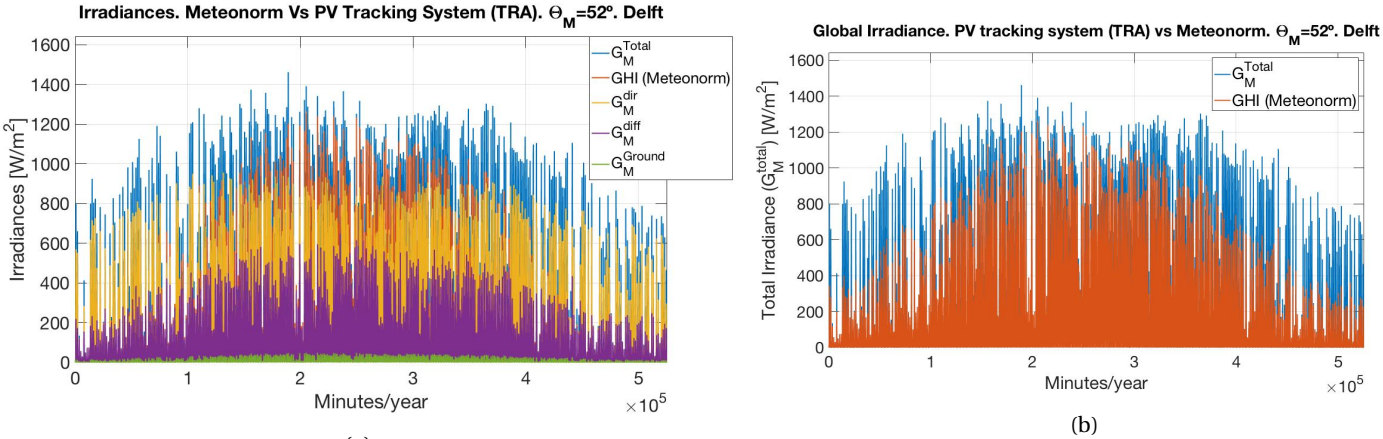

(a) (b)

Figure 5.27: (a)Total, direct, diffuse and ground irradiances calculated vs GHI from KNMI. (b)Total irradiance falling onto the module vs GHI from the KNMI file. At θ_M=52°

Again, it can be seen that the PV module's tilting angle and the azimuth tracker give a higher irradiance if compared with a flat surface. This is because more sun rays reach the PV module's surface for longer periods. The Figure 5.28 depicts the monthly energy yield incident onto the PV module.

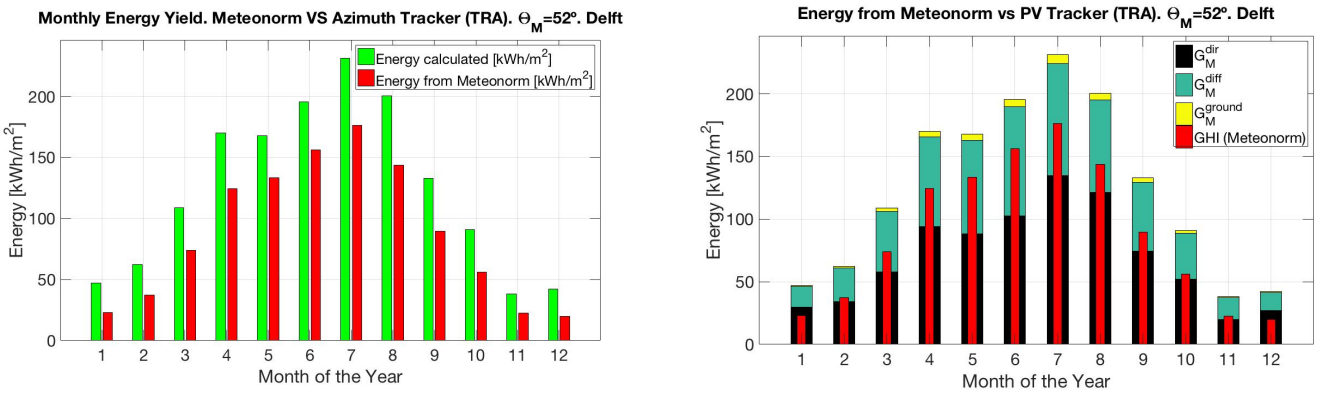

(a) (b)

Figure 5.28: θ_M=52º (a)Monthly energy yield incident on the PV module in [kWh/m^2] (b)Individual energy yield provided by the direct, diffuse and ground irradiances in [kWh/m^2].

TRA Results at 67°

Now the results of the optimal tilting angle found for the TRA topology (67º in this case) are analysed. The Figure 5.29 depicts the incident irradiances on the PV module using a TRA topology.

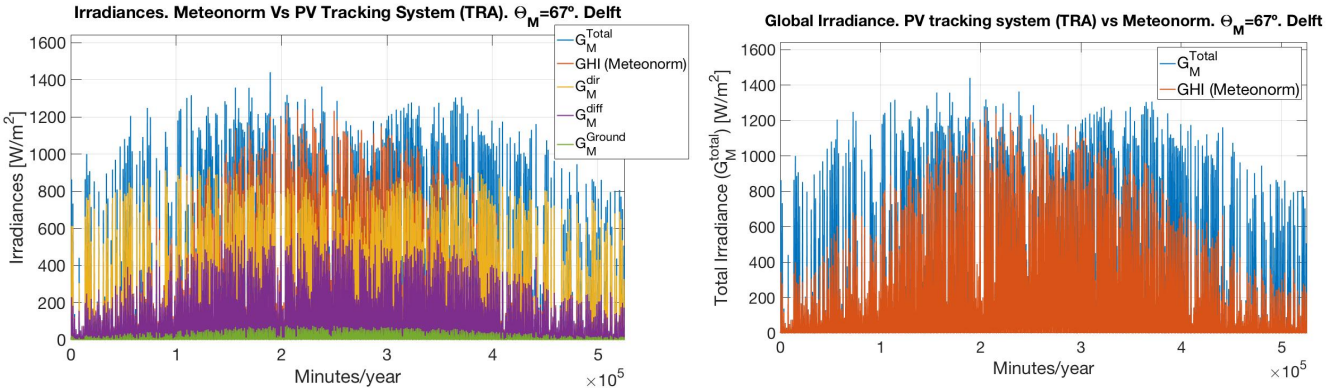

(a) (b)

Figure 5.29: (a)Total, direct, diffuse and ground irradiances calculated vs GHI from KNMI. (b)Total irradiance falling onto the module vs GHI from the KNMI file. At θ_M=67º

Now, the Figure 5.30 depicts the monthly energy yield incident onto the PV module in a TRA topology.

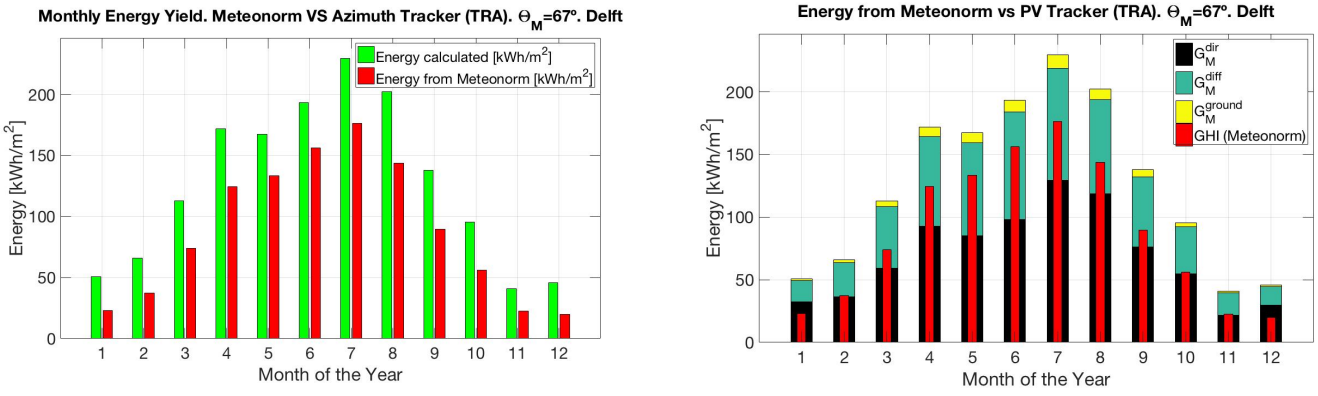

(a) (b)

Figure 5.30: θ_M=67º (a)Monthly energy yield incident on the PV module in [kWh/m^2] (b)Individual energy yield provided by the direct, diffuse and ground irradiances in [kWh/m^2].

In this case (when the TRA has a tilting angle of 67º) it is noted that the ground irradiance has the highest contribution when compared vs the other two tilts tested here (37º and 52º). In the next section, the results of each angle will be compared and discussed.

5.9.2. Comparison Between the TRA Topology vs the PV Static Module at 0º

Table 5.6 depicts the contribution in [kWh/m^2] of each irradiance for the Azimuth Tracking system at the different tilting angles tested. Only the comparison between the optimal tilt angle of the topology and the flat PV module (which is the reference point) are shown in the table.

θ_M [º] **or Topology**	G_M [kWh/m^2]	G_M^{dir} [kWh/m^2]	G_M^{diff} [kWh/m^2]	G_M^{ground} [kWh/m^2]
PV Static (0º)	**1039**	437	602	0
TRA (37º)	**1410**	782	607	21
TRA (52º)	**1488**	837	611	40
TRA (67º)	**1515**	835	615	65
Dif.(67º vs 0º) [kWh/m^2]	**+476**	+398	+13	+65
Dif.(67º vs 0º) in [%]	**+45.8 %**	+91 %	+2.16 %	N/A

Table 5.6: Individual Energy Yield. Contribution by irradiance. TRA vs PV Static Flat (0º). Comparison TRA(67º) vs PV Static Flat (0º).

Where "Dif." stands for "difference". The TRA topology tilted at its optimal angle (67º) shows a surplus in its performance when compared to the flat scenario. This gaining is of almost 46 %. All the irradiances improved its incident energy yield, but the G_M^{dir} and the G_M^{ground} had the highest improvement. As it was previously discussed at 5.5.2, the Sandia model for the G_M^{diff} improves the diffuse irradiance when the θ_M>0º, that's why it is observed a small gaining in the G_M^{diff} (of about 2 %) when TRA(67º) and TRA(0º) are compared.

The energy yield from the ground is the highest at this tilt angle. This is a expected outcome since the reflected light on the ground is higher at steeper tilting angles, as mentioned at Section 2.3.3.

Determine the Optimal Tilt Angle for the TRA Topology

At the moment of comparing the 67º vs 52º tilt angles, it is noteworthy that the optimal tilt angle for a PV Static topology definitely is not the same as for an azimuth tracking topology and other approach has to be taken in order to determine it.

By using the results of the solar calculator shown at Figure 5.18, it is possible to calculate a close approximation to determine the optimal tilting angle for an azimuth tracking system. This rule-of-thumb calculates the average tilting angle for a module during winter (January, February, March and December). So from Figure 5.18 is obtained:

$$\theta_M = \frac{68^o + 60^o + 52^o + 76^o}{4} = 64^o$$

Even if 64º is not the same tilting angle as the one found in the MATLAB TRA model (67º), this is nevertheless a good approximation to the real optimal tilt angle for the PV panel. As a result, using the average tilting angle for a PV module in winter is an acceptable assumption and it could be used as a rule of thumb. This still has to be tested in other latitudes closer to the Equator though.

5.9.3. TRA Conclusions and Observations

As expected, the energy yield perceived by the azimuth tracker was slightly lesser than the TRAT one. The interesting point here is that there was the opportunity to compare 3 different tilting angles on the PV module: 37º, 52º and 67º.

The table 5.6 indicates that for an azimuth tracker with a fixed module's tilting angle, the most significant surpluses in the irradiances at these angles were present at the direct and ground irradiances. The diffuse irradiance incident onto the PV module had a slight increase. The overall gaining between the tilting angles was close to 480 [kWh/m^2], which is almost 46 % when the 67º and 0º angles are compared. In other words: the steeper the PV module's optimal tilting angle, the more the available area to reach for the ground irradiance, thus, the higher the energy yield produced by it.

A recommendation for further research, is to improve the current TRA model or create a new one so that it can also find the optimal tilting angle for a PV module mounted on an azimuth tracking system (like it is performed in the PV Static Finder model).

5.10. TRT: Tilting Tracker with fixed PV Module's azimuth

TRT stands for "tracker of tilting angle" in this thesis project. It is the third tracking topology to be analysed, it is another 1-axis tracking system. It tracks the PV panel's best optimal tilting angle. This tracking configuration only moves vertically and it faces to the true South or true North depending of its location. The Figure 5.31 depicts a tilting tracking system. In theory and in practice, this is the topology that has the least performance of the existent tracking topologies.

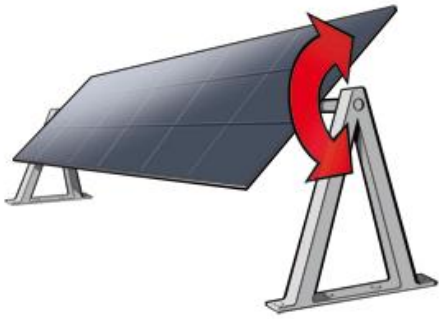

Figure 5.31: Tilting tracking system [9].

The MATLAB model also is optimised to take into consideration a flat tilting angle, for days where the diffuse irradiance is significantly higher than the direct one. In other words: the module will choose a 0º tilting angle instead of the standard one at a determined location and at a certain time of the day if the climate conditions to do this are satisfactorily met (poor sunlight). The Figure 5.32 depicts the flowchart used for this TRT MATLAB model.

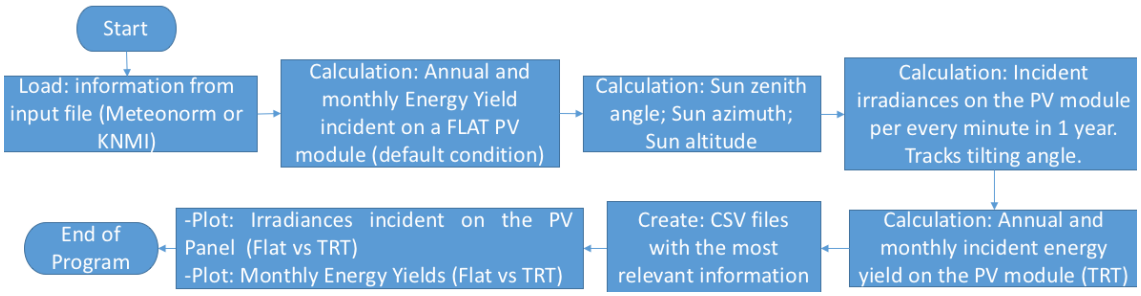

Figure 5.32: Flowchart of the tilting tracking model.

5.11. TRT Results

The Figure 5.33 depicts the irradiance time series for this topology. Let us remind that the function of the time series is to indicate how much irradiance in [W/m^2] does the surface receive at every minute of the year.

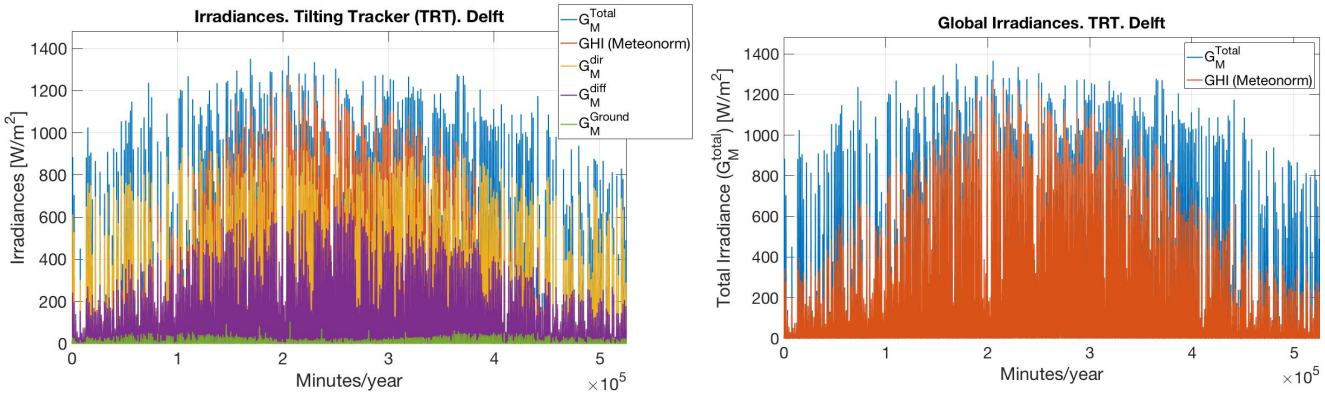

(a) (b)

Figure 5.33: (a)Total, direct, diffuse and ground irradiances calculated vs GHI from Meteonorm. (b)Total irradiance falling onto the module vs GHI from KNMI file.

The Figure 5.34 depicts the monthly energy yield incident onto the PV module.

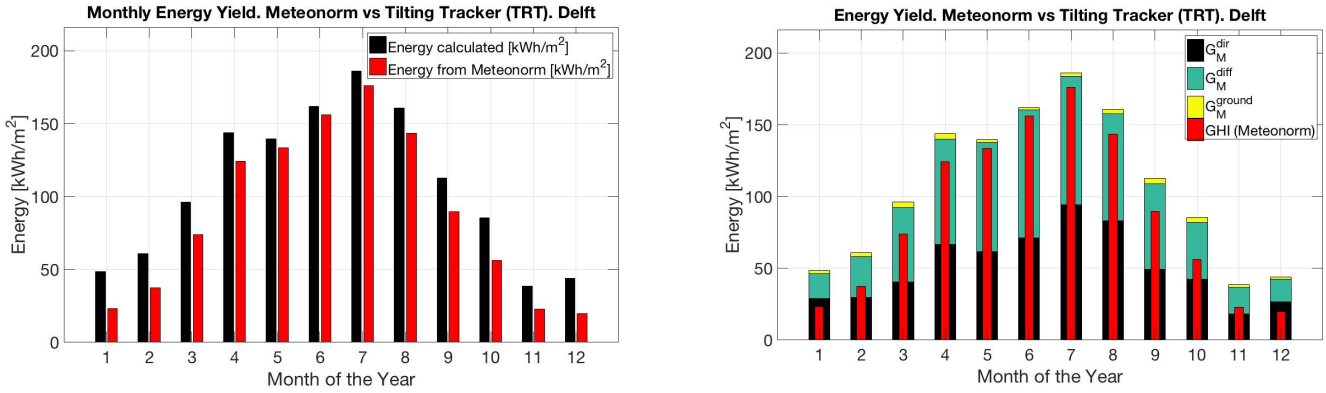

(a) (b)

Figure 5.34: (a)Monthly energy yield incident on the PV module in [kWh/m^2] (b)Individual energy yield provided by the direct, diffuse and ground irradiances in [kWh/m^2].

It is observed in Figure 5.34b that the energy yield produced by the TRT topology is still higher than the one calculated from the KNMI file, nevertheless, it is also noticeable that the difference from one to another is not as big as in the TRAT or TRA topologies. In order to have a better understanding of these graphs, the Table 5.7 explains the contribution in [kWh/m^2] of each irradiance for the Tilting Tracking system. The comparison with the PV Static at 0º tilting is also shown.

θ_M [^{o}] **or Topology**	$\mathbf{G}_M$ [kWh/m^2]	$\mathbf{G}_M^{dir}$ [kWh/m^2]	$\mathbf{G}_M^{diff}$ [kWh/m^2]	$\mathbf{G}_M^{ground}$ [kWh/m^2]
PV Static (0º)	**1039**	437	602	0
TRT	**1280**	613	634	33
Difference [kWh/m^2]	**+241**	+176	+32	+33
Difference in [%]	**+23.2 %**	+40.3 %	+5.32 %	N/A

Table 5.7: Individual Energy Yield. Contribution by irradiance. TRT vs PV Static Flat (0º).

For the first time in the tracking topologies, it is observed that the diffuse irradiance incident on a PV module is the main contributor for the annual energy yield and not the direct irradiance. Again, all the irradiances improved their performance when compared with the PV Static topology at 0º. There was an overall increase

of 23 %. The G_M^{dir} and the G_M^{ground} had the highest improvements, with 40 % and 33 kWh/m^2 respectively. The G_M^{diff} had a moderate improvement; this is due to the "smart" configuration on the TRT MATLAB model of prioritizing the 0º tilt over the location tilting on days with poor insolation, optimizing thus the incident diffuse irradiance.

5.11.1. TRT Conclusions and Observations

The results from Table 5.7, corroborated that even if the TRT model was enhanced to receive more diffuse irradiance for cloudy days, it still had a lower performance than the TRAT and TRA tracking topologies also studied previously here.

Surprisingly, also in the same table, is observed that for the first time amongst the tracking topologies, it is the diffuse irradiance incident on the PV panel that had the highest energy contribution, leaving the direct irradiance on second place. Since the data file was too big how to make an analysis element-by-element, it could be deduced that the reason of this is that there was several occasions where the module had to be tilted at 0º instead of using the standard optimal tilting angle at that specific time. Besides, it could be noted that the tilting change by itself is insufficient to increase the direct incident irradiance.

This might rise the question of why this (diffuse irradiance > direct irradiance) was not present during the TRAT system. One answer could be that the TRAT system is a dual axis tracker, the TRT only tracks the tilting angle and not the azimuth. This leads to a logical conclusion where the azimuth tracking topology has more relevance in terms of incident irradiance than the tilting trackers.

TRT - PV Semi-static relation

As mentioned in the Section 5.6.1, it was thought that the average tilting angles calculated by the TRT MATLAB model and the optimal tilting angles of a Static or Semi-static topology would be the same. Nevertheless, this was not the case.

The TRT MATLAB model calculates the monthly (which was going to be used for the PV semi-static MATLAB model) and annual average tilting angles for a determined location. The annual average calculated by the TRT MATLAB model (36.7º) matched with the optimal tilting angle (37º) in which SAM has its best performance for a PV system project in the same location (Delft). Nevertheless, the optimal angle for a PV Static topology in Delft was of 52º according to the PV Static Finder MATLAB model (please refer to Section 5.3).

After comparing the results of the PV Static topology in the Section 5.5.2 in the Table 5.4, the conclusion was clear: for the TRT MATLAB model, the average tilting angle is not the same as the optimal angle for the PV Static MATLAB model. Unfortunately this observation was discovered when there was no more time to create a "optimal tilting angle finder" for a semi-static topology.

5.12. Conclusions on Tracking System Topologies

Table 5.8 depicts in descending order the total annual energy yields incident on a PV module that each tracking topology has to offer. The TRA topology only shows its optimal tilting angle (67º), the other angles (37º and 52º) are not included, in order to compare the maximum yields only. Also the PV Static model at its optimal tilting angle (52º) is shown to demonstrate the differences between the tracking topologies vs the optimal tilting of a static one.

Topology	$\mathbf{G_M}$ [kWh/m^2]	$\mathbf{G_M^{dir}}$ [kWh/m^2]	$\mathbf{G_M^{diff}}$ [kWh/m^2]	$\mathbf{G_M^{ground}}$ [kWh/m^2]
PV Static (0º)	**1039**	437	602	0
PV Static (52º)	**1218**	567	611	40
TRAT	**1573**	867	657	49
TRA (67º)	**1515**	835	615	65
TRT	**1280**	613	634	33
Dif.(TRAT vs PV Static 0º)[%]	**+51.4**	+98.4	+9.14	N/A
Dif.(TRA (67º) vs PV Static 0º)[%]	**+45.8**	+91	+2.16	N/A
Dif.(TRT vs PV Static 0º)[%]	**+23.2**	+40.3	+5.32	N/A

Table 5.8: Tracking topologies comparison vs PV Static (0º).

Where "Dif." stands for "difference". It is clear that the 2-axis tracking system (TRAT) has the best performance of all the tracking topologies, it performs up to 4.5 % better than the azimuth tracker (TRA) and up to 22.56 % more than the tilt tracker (TRT), whilst the TRA performed 17.3 % better than the TRT.

Another conclusion is that for the tracking topologies, the direct irradiance was the dominant one, except for the TRT topology. It was notable that with the diffuse irradiance enhancement, the tracking systems were "smarter" and they determined that the optimal angle was 0^o for the cases where the diffuse irradiance was significantly higher than the direct one.

A detail which was surprising, is the fact that the TRA finds its PV module's optimal angle at a highly steeped inclination (67^o). This leads to the conclusion that one optimal tilting angle found in one topology (PV Static) does not mean that it also is the optimal one for the TRA topology.

6

Floating PV Module

The concept of a photovoltaic system floating on the water is not a new concept, nowadays is implemented. Nevertheless, the existent projects take place on dams, artificial and natural lakes of relatively small size. This might be for two reasons: there are no significant waves on the lake's surface and that the fresh water is not as corrosive as the sea salty water for the materials and the PV modules themselves in which the PV system is built. Figure 6.1 depicts one example of a floating PV plant in a Japanese artificial lake.

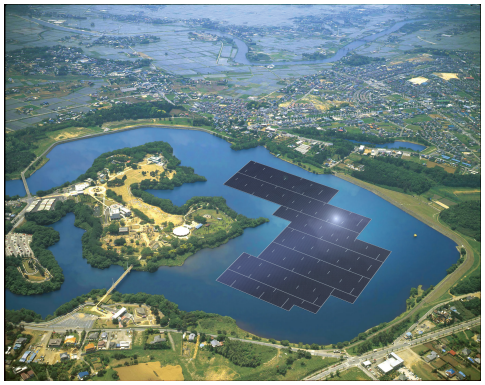

Figure 6.1: Floating PV Plant in a in the Yamakura Dam reservoir, Japan. [43].

It is well known that the salt water has a different effect of corrosion on the materials. This can be one obstacle to try to build a high scale PV plant offshore. The current PV technology is fabricated to endure different climate conditions and the salty sea water is not one of them. Thus, the warranty of a proper performance of a PV module on the sea could not be assured since it is not used under standard conditions.

Nevertheless, it is interesting to know the amount of irradiance that a floating PV module would receive if it is offshore. That is one of the reasons to perform this study. In the next sections different scenarios will be covered regarding this.

In this chapter, the floating PV module (located offshore) and the energy yield incident on it will be analysed in order to answer the research questions approached in Section 1.7. The first one would be:

What is the irradiance incident on a PV module located offshore under a controlled wave scenario and under a random wave scenario?
This will be addressed in the section of results of each case and in the final conclusions in this chapter.

What is the optimal tilting angle under each scenario (controlled and random waving) and why?
This sub-question will be as well addressed in the section of results of each case and in the final conclusions in this chapter.

Before starting the detailed analysis of this MATLAB model, it is necessary to clarify which were the assumptions considered to perform these calculations, even if some of them are impossible to happen for real:

- For sake of simplicity, it will be assumed that wave components such as wavelength, valleys and crests in the wave do not have an impact on the PV panel's tilting angle and thus, its performance. These elements probably have some impact, but that is out of the scope of this project
- There will be 2 scenarios: In the first one, it is assumed that the location has a constant wave movement that goes from a negative tilting angle to a positive one, in steps of 0.5 degrees per minute throughout the year. Figure 6.2 gives a small example of a wave tilting going from +2º to -2º and going back to +2º at 0.5º steps. Where a positive number indicates that the wave is facing the Sun and a negative one the opposite case
- The second scenario: one with a completely random wave movement, in which the PV module's position varies at every minute
- The location of the simulation takes part in the Northern hemisphere
- The PV module is assumed to stay at that angle for one minute, then it changes its tilting angle by increasing/decreasing it by 0.5º
- This behaviour is assumed to happen during the whole year, even if in real life this is impossible
- The albedo for the sea water used here has a value of 0.1 [31]
- The location is still Delft, even if it is not underwater, it is assumed that the coordinates given are meant to be at the open sea
- The PV module has a static tilting angle, is not semi-static and it has no tracking system. The floating PV plants on artificial lakes have this static configuration, so it is assumed that on offshore conditions they will have this same static topology
- The decision to perform the simulation with very slow waves, is because the movement of the waves offshore are usually quiet. Nevertheless, the Floating PV MATLAB model allows to perform simulations at different wave-tilting angles

Minute	1	2	3	4	5	6	7	8	9	10	11	12	13	14	15	16	17
Wave Tilt	2	1.5	1	0.5	0	-0.5	-1	-1.5	-2	-1.5	-1	-0.5	0	0.5	1	1.5	2

Figure 6.2: Wave tilting from +2º to -2º and going back to +2º.

It is known that the waves offshore presented in the assumptions are not realistic. Nevertheless, later in this chapter it will be demonstrated that the "speed" of the waves tilting is irrelevant when the incident annual energy yields and irradiances are calculated.

Controlled Wave Movement

In this scenario, the waves move at a single and constant rate. Figure 6.3 refers to the controlled waving scenario flowchart.

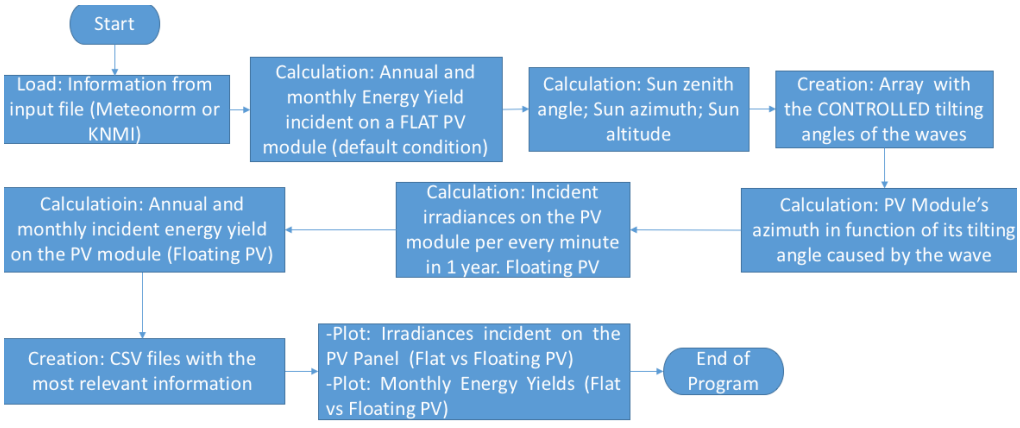

Figure 6.3: Flowchart of the Floating PV model with CONTROLLED waving.

Random Wave Movement

In this scenario, the waves have a completely unpredictable movement, making that the PV module has different tilt angles and azimuth positions the whole time. Figure 6.4 depicts this case scenario.

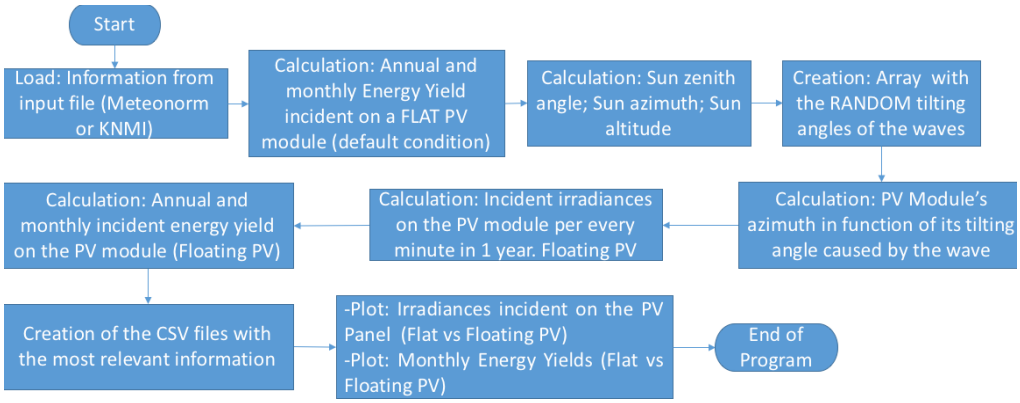

Figure 6.4: Flowchart of the Floating PV model with RANDOM waving.

6.1. Controlled Wave. Reference PV Module Tilting Angle: 0º

The first reference point in this topology, is to measure the amount of energy yield incident on a floating PV module which is moving along with the waves that have a controlled tilting angle (refer to Section 6 for details). The assumption in this scenario is that the module lays flat onto a floating frame on the sea, making it to have the same tilting angle as the wave. This means that the 3 possible positions of the PV panel with respect to the Sun will be: facing the Sun, horizontal (0º tilting) and not facing the Sun. Figure 6.5 depicts this.

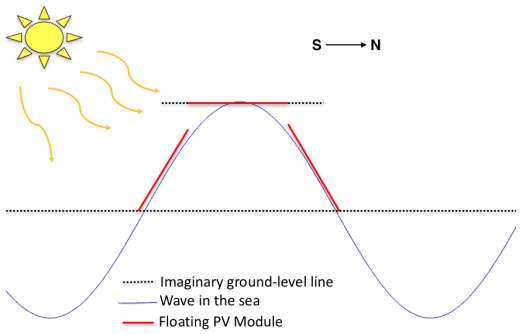

Figure 6.5: Floating PV panel with 0º Tilting angle. Three possible scenarios

Figure 6.6 depicts a possible scenario for a controlled wave movement sequence with more detail.

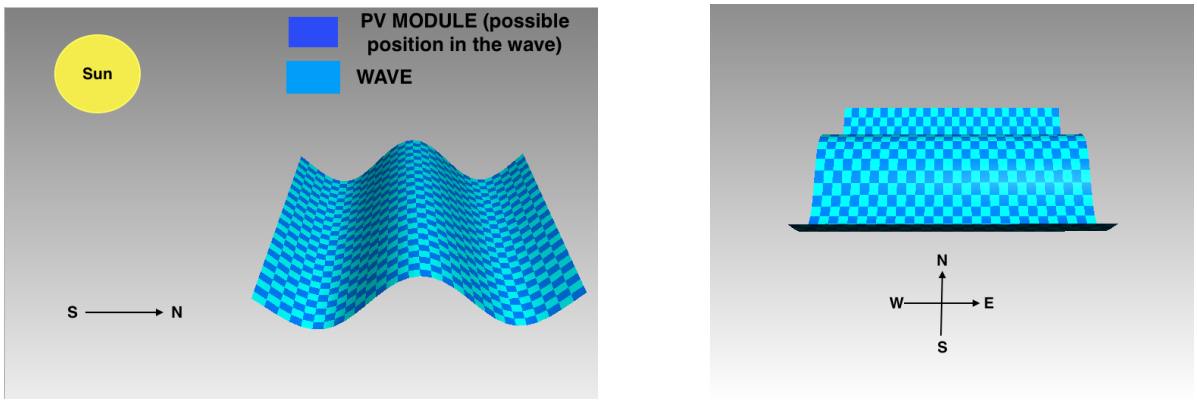

(a) (b)

Figure 6.6: (a) 3-D perspective for the wave controlled scenario with a floating PV module with θ_M=0º (b) View on the wave from the Sun's perspective.

From Figure 6.6 it is clearly appreciable that the PV module's azimuth (Az) will only have 2 directions throughout the year when its tilting angle is 0º: Az=180º when it's facing South and Az=0º when it faces North. When Az=0º, it is perfectly foreseen that the main contributors for the annual energy yield will be the diffuse and albedo irradiances, since at that moment there is no direct irradiance incident on the floating PV.

The next point to discuss, is the total amount of incident energy yield of this floating PV panel with 0º tilting. Figure 6.7 explains which were the angles caused by the movement of the waves.

WAVE/MODULE TILTING	ANNUAL ENERGY YIELD ON THE MODULE [kWh/m²]
PV Static 0º	1039
15º	1083
30º	1117
45º	1143
60º	1156
69º	1160
80º	1157

Figure 6.7: Flat floating PV module at different wave angles (Θ) and their corresponding maximum incident AEY.

Figure 6.7 shows an imaginary scenario in which the calculation of the wave tilt is performed and the purpose of this is to find the "optimal wave tilting angle" where the PV module receives the highest incident annual energy yield when the PV panel lays flat onto the wave. The scenarios went from a slight steeping on the wave/module up to a severe one. The wave tilting in which the module received the maximum incident annual energy yield was found manually, by testing different angles and comparing them until the optimal angle in which the highest incident annual energy yield was found. In this case: when the wave tilt is 69º.

If it is compared with the PV Static model at a θ_M=0º (1039 [kWh/m^2]), this floating PV model has a slightly higher performance than the PV static one at θ_M=0º thanks to the tilting caused by the waves. The moderate surplus is of 4.14 %.

Figure 6.8 shows the incident annual yield on a floating PV when Θ=69º and θ_M=0º.

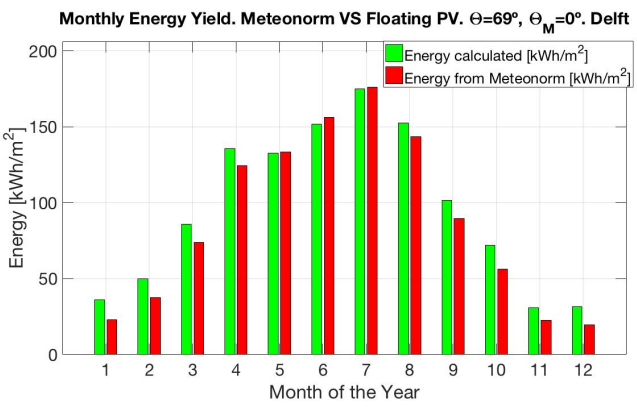

(a)

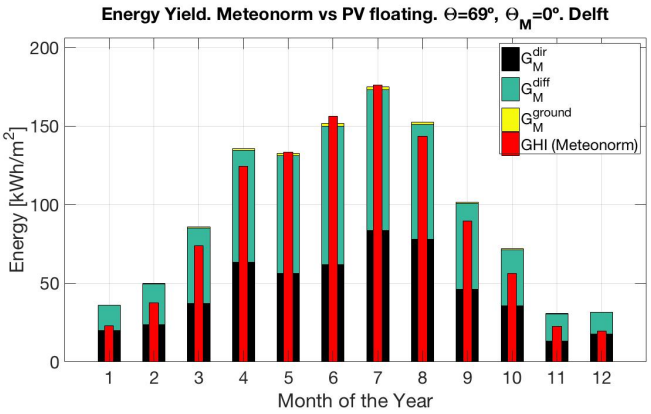

(b)

Figure 6.8: (a)Monthly energy yield incident on the PV module in [kWh/m^2] (b)Individual energy yield provided by the direct, diffuse and ground irradiances in [kWh/m^2].

At a first glance, the ground irradiance has a poor performance, followed by the direct irradiance. The main contributor for the annual energy yield is the diffuse incident irradiance. Table 6.1 describes the contribution of each irradiance to the annual incident energy yield.

Topology	$\mathbf{G}_M$ [kWh/m^2]	$\mathbf{G}_M^{dir}$ [kWh/m^2]	$\mathbf{G}_M^{diff}$ [kWh/m^2]	$\mathbf{G}_M^{ground}$ [kWh/m^2]
PV Static (0°)	**1039**	437	602	0
Float PV, Θ=69°;θ_M=0°	**1160**	540	608	12
Difference [kWh/m^2]	**+121**	+103	+6	+13
Difference in [%]	**+11.6 %**	+23.6 %	+1 %	N/A

Table 6.1: Individual Energy Yield. Contribution by irradiance. TRT vs PV Static Flat (0°).

The previous table demonstrates that the diffuse irradiance is the main contributor and that the direct irradiance improved significantly with a surplus of 23.6 %. In this case, the irradiance produced by the water reflection poorly contributes with the annual incident enery yield since its albedo is barely 0.1.

In the next subsection it is explained how to determine the optimal tilting angle for a floating PV module when the wave has a determined tilting angle. Also the wave position with respect to the Sun and how it affects the incident energy on a PV module is explained.

6.1.1. Floating PV. Optimal θ_M at a Determined Wave Tilting Angle Θ

For the development of this model, two variables were considered: the tilting caused by the wave and the optimal tilt angle assigned to the module according to the location. The wave tilt will go from a starting positive angle (for instance, 20°) and it will end at its negative angle (-20°). Where the positive sign will mean that the wave is tilted towards the Sun and the negative the opposite case. Refer to Figure 6.9.

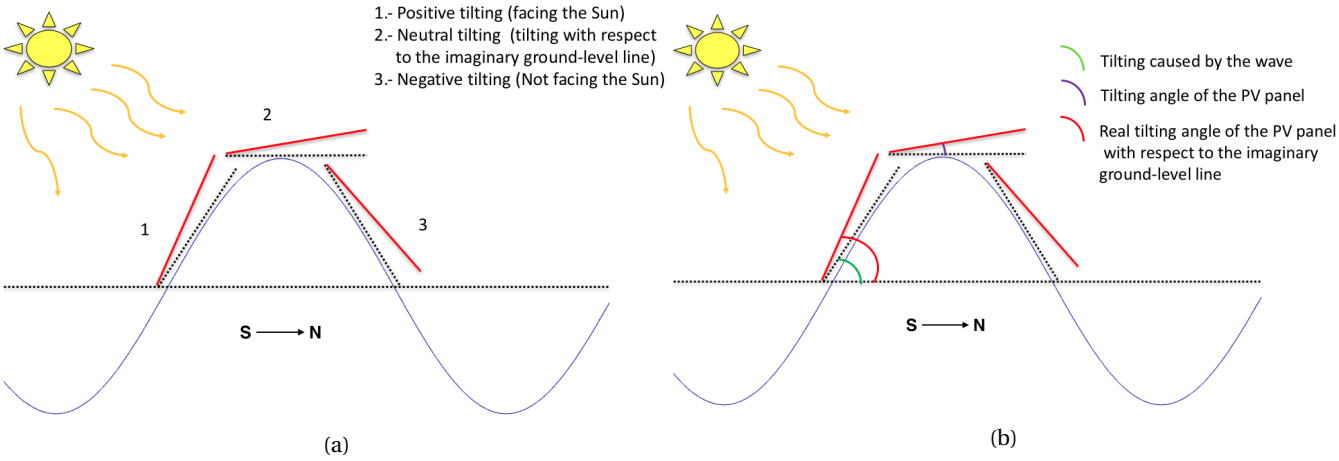

Figure 6.9: (a)Positive, neutral and negative wave tilting scenarios (b)Wave tilting, PV module tilting and real/final module's tilting angle.

The positive, neutral and negative tilting angles are always in reference between the wave inclination and the imaginary ground-level line. Figure 6.10 describes how each case must be referred.

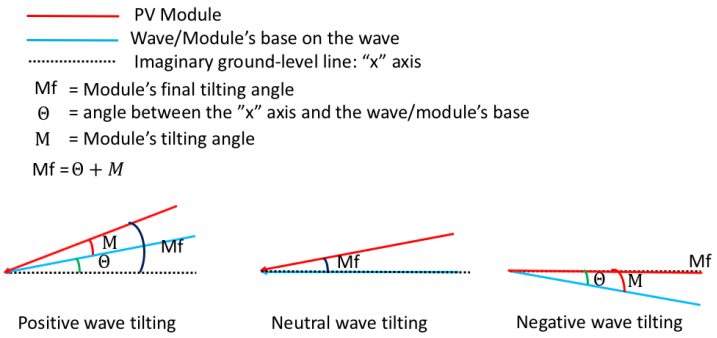

Figure 6.10: Different tilting angles on a floating PV module depending on the wave position.

In order to understand a bit better how these results were obtained, in the next sub-sections an example will be explained. The analysis of the scenario with a tilting angle of 15º caused by the wave and a PV optimal tilt of 47º will be disclosed.

PV Module's Real Tilting Angle When the Wave Has a Positive Tilting

The "positive tilting" of Figure 6.10 is explained here. Figure 6.11 depicts the elements considered to determine the PV panel's final tilting angle.

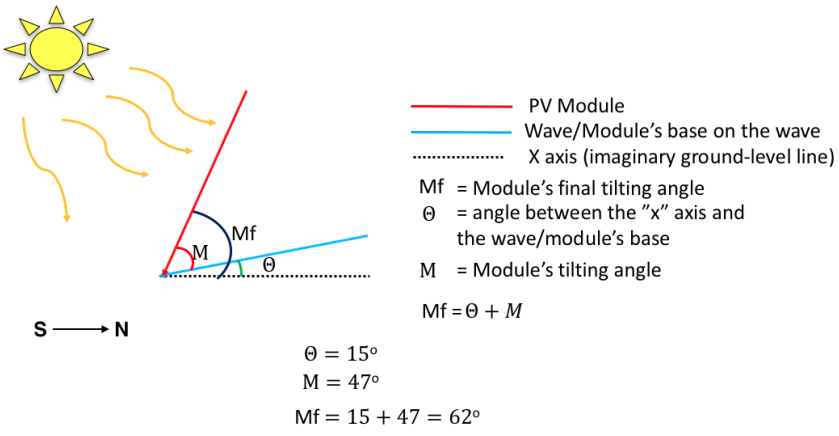

Figure 6.11: PV module's final tilt angle when the wave is at positive tilting (facing the Sun).

It is observed how the final tilting angle of the PV module is the angle formed between the imaginary ground-level line and the module itself. The panel's final angle is a simple addition between the angle between the imaginary ground-level line and the angle between the module's base (which is at sea level) and the module.

PV Module's Real Tilting Angle When the Wave Has a Neutral Tilting

The "neutral tilting" from Figure 6.10 is explained next. Figure 6.12 depicts the elements considered to determine the PV panel's final tilting angle.

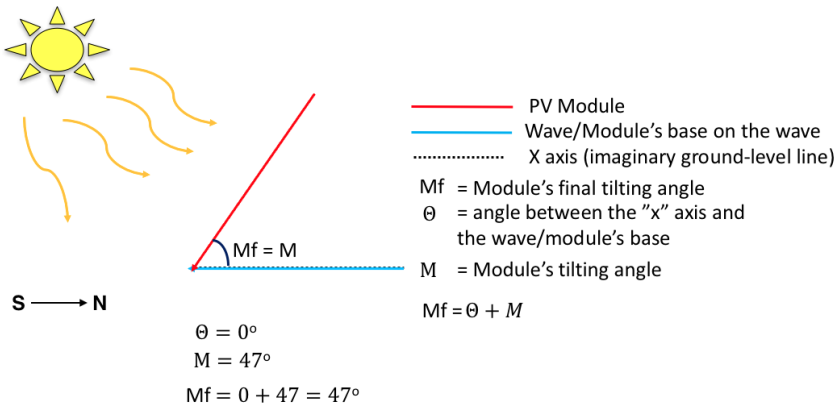

Figure 6.12: PV module's final tilt angle when the wave is at neutral tilting (the wave is horizontal to the imaginary ground-level line).

In this case, the final angle of the module is the same as the module's tilting angle found in the MATLAB model. Here, the PV panel's base is horizontal to the imaginary ground-level line.

PV Module's Real Tilting Angle When the Wave Has a Negative Tilting

The "neutral tilting" from Figure 6.10 is lastly explained. Figure 6.13 depicts the elements considered to determine the PV panel's final tilting angle. Note that the wave is not facing the Sun in this case.

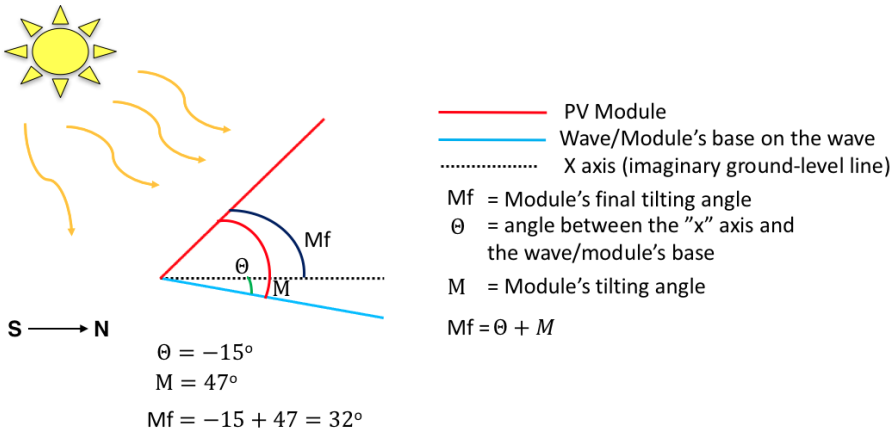

Figure 6.13: PV module's final tilt angle when the wave is at negative tilting (the wave does not face the Sun).

Here it is noticeable that the PV module is still facing the Sun, even if the wave is not. This helps to get more irradiance from the sun even if the wave is continuously moving.

Now that the explanation of the possible positions of a floating PV module has been given, the analysis of an example for the controlled waving scenario will be performed.

6.2. Scenario for Controlled Wave Movement. Determine Optimal θ_M at a Determined Θ (Wave Tilting)

These are the assumptions taken for a scenario with a wave which tilting angle (Θ) is 45°:

- The location has a constant wave movement that goes from a negative tilting angle to a positive one, in steps of 0.5º/minute throughout the year. Where a positive number indicates that the wave is facing the Sun and a negative one the opposite case
- The maximum tilting angle for the wave is 45º (when the wave is at +45º, it faces the Sun, -45º is the opposite case)
- The PV module's static tilting angle (θ_M) is 49º, which is the optimal tilt when the wave tilting is 45º (Θ=45º). As for the reference scenario (Θ=69º and θ_M=0º, refer to Figure 6.7), this angle was also found manually

6.3. Floating PV Results. Controlled Wave Case. Θ=45º, θ_M=49º

Before starting with this case scenario, a brief analysis of several tilting angles (on both the PV modules and the waves) is treated first. The Table 6.2 discloses some optimal tilting angles found on a floating PV panel (assuming that the waves have a constant movement at the place). All the optimal θ_M were manually found using the Float PV MATLAB model.

Table 6.2 discloses an example for the tilting caused by the waves. The PV Module's optimal tilting angle found at that wave movement and the annual energy yield incident on the panel at those tilts are also shown in the table. Only results from the floating topology are shown. Further in this chapter the comparison of these results with the ones obtained from the other topologies will be analysed. The table also shows the point of reference: the incident energy yield of the PV Static MATLAB model at θ_M=0º

Wave Tilt (Θ) [º]	**Module's Optimal Tilt Angle Found [º]**	**Annual Incident Energy Yield [kWh/m^2]**
Reference: PV Static (0º)	0º	1039
69º	0º	1159
15	47	1194
25	47	1184
30	46	1175
45	49	1147.5

Table 6.2: Different annual energy yields incident on a floating PV module depending on the wave tilting.

It is important to note that different changes in the tilt steps were tested (the wave's tilt steps were of 4.5º and 5º, not 0.5º) for the case where Θ=45º and θ_M=49º and the difference in the annual incident energy yield was not significantly different from one tilt-step to another. When these tilt-steps had a value of 0.5º, the AEY was 1,147.51[Wh/m^2], 1,148.7[Wh/m^2] for a tilt step of 4.5º/min and 1,146.8[Wh/m^2] for a tilt step rate of 15º/min. Hence, the simulation of this model will be performed with a 0.5º tilt-step rate.

It is possible to observe from Table 6.2 that the PV Static model with a θ_M=0º has the lowest value of all, even if θ_M is also 0º in the floating PV model. This is understandable since in the floating model, the tilting caused by the waves temporarily improves the incident energy yield on the floating PV module, whereas the PV Static does not do this. The float PV model with a Θ=69º has an improvement of +11.55 % with respect to the PV Static at θ_M=0º.

Also from Table 6.2, when the PV module is flat onto the sea surface, it is necessary that the wave has a very steeped tilting angle in order to achieve the highest incident irradiance. One interesting observation, is that the steeper the wave, the lesser the incident energy yield on the module. Another interesting observation, is that the PV module's optimal tilting angle barely changes even if the wave tilt drastically does it. This could indicate as a first conclusion that: an ideal wave behaviour would be the one where the waves barely have movement (that they are as flat as possible). Also, this topology has the lowest incident energy yield if compared to any of the other topologies previously treated.

Now that the clarification about the cases at different tilting angles is done, it is continued the studied case of this section (which is Θ=45º and θ_M=49º). Figure 6.14 depicts the irradiance time series when Θ=45º (wave tilting) and θ_M=49º (PV module's tilt angle).

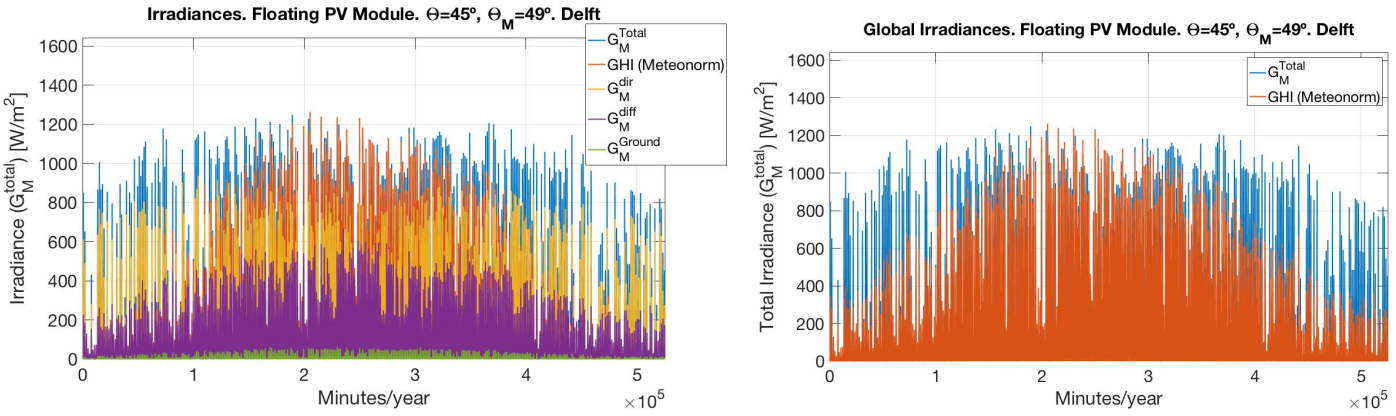

(a) (b)

Figure 6.14: (a)Total, direct, diffuse and ground irradiances calculated vs GHI from KNMI. (b)Total irradiance falling onto the module vs GHI from KNMI file.

Figure 6.15 depicts the annual energy yield incident on the floating PV module.

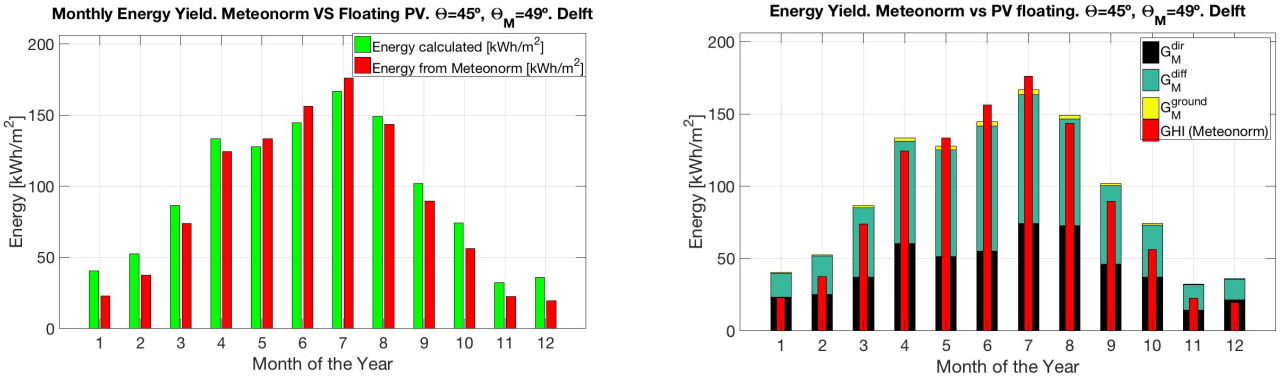

(a) (b)

Figure 6.15: θ_M=52º (a)Monthly energy yield incident on the PV module in [kWh/m^2] (b)Individual energy yield provided by the direct, diffuse and ground irradiances in [kWh/m^2].

It is seen at Figure 6.15b that there is a surplus of energy during the winter period, in which the final tilting angle of the PV module takes advantage of the movement caused by the wave. The G_M^{ground} has a poor contribution and the G_M^{diff} is the main contributor. Table 6.3 describes the contribution of 3 scenarios: PV Static model at 0º tilting angle, floating PV panel with a flat tilt and Θ=45º and θ_M=49º. Where "Dif." stands for "difference".

Topology	G_M [kWh/m^2]	G_M^{dir} [kWh/m^2]	G_M^{diff} [kWh/m^2]	G_M^{ground} [kWh/m^2]
PV Static (0º)	**1039**	437	602	0
Float PV, Θ=69º;θ_M=0º	**1160**	540	608	12
Float PV, Θ=45º;θ_M=49º	**1147.5**	519	607	21
Dif.(Θ=69º vs PV Static) [kWh/m^2]	**+121**	+103	+6	+13
Dif.(Θ=69º vs PV Static)[%]	**+11.6 %**	+23.6 %	+1 %	N/A
Dif.(Θ=45º vs PV Static)[kWh/m^2]	**+108.5**	+82	+5	+21
Dif.(Θ=45º vs PV Static)[%]	**+10.4 %**	+18.8 %	+0.83 %	N/A

Table 6.3: Individual Energy Yield. Contribution by irradiance. Floating PV Model vs PV Static at θ_M=0º.

6.3.1. Other Cases at Different Θ and Different PV Module's Tilting Angle

In this subsection other different tilting angles for the same location will be analysed. The formulas developed at 6.1.1 to determine the optimal tilting angle for a floating PV module at a determined wave tilting (Θ) are shown at Figure 6.16.

Wave Tilt (Θ) [°]	Optimal Module Tilt Found (M) [°]	Mf when Θ (Positive) [°]	Mf when Θ (Neutral) [°]	Mf when Θ (Negative) [°]	Energy Yield [kWh/m²]
69	0	69	0	-69	1157
15	47	10+47 = 57	0+47 = 47	-15+47 = 32	1194
25	47	15+47 = 62	0+47 = 47	-25+47 = 22	1184
30	46	30+46 = 79	0+46 = 46	-30+46 = 16	1175
45	49	45+49 = 94	0+49 = 49	-45+49 = 4	1147.5

$$Mf = \Theta + M$$

Mf = Module's final tilting angle
Θ = angle between the "x" axis (imaginary ground-level line)and the wave/module's base
M = Module's tilting angle

Figure 6.16: Different Annual Energy Yields (AEY) at different wave tilting angles. Optimal PV module's tilting angle at that wave tilt-angle. Final tilting angle of the PV panel.

If the AEY from Figure 6.16 are compared with the AEY of PV Static MATLAB model at 0º tilt angle (1039 [kWh/m^2]), it is seen that all the AEY of the floating PV have a higher value where the lowest difference was seen at Θ=49º and module's tilt of 45º (with a surplus of +10.45 %) and the highest is found at Θ=15º and M=47º (where "M" stands for the optimal tilting angle corresponding at a determined Θ) with a surplus of 14.92 %.

Probably the most relevant detail from Figure 6.16 is that M (optimal Module Tilt Found) barely changes even if Θ does it. Evidently M tries to find a balance to get the highest diffuse irradiance as possible without losing the direct one. In the next section more details are given about this situation.

6.3.2. Conclusions Float PV Model, Controlled Wave Scenario

There are several interesting observations that can be extracted from the previous cases which provide relevant information to be a step closer of a better understanding of how the behaviour of a floating PV module offshore could be.

The first observation is that for a PV panel with a 0º tilting angle it is necessary that the wave has a very steeped wave movement in order to find the tilting angle that has the highest incident energy yield on the PV module. This case is considered as the reference point of the incident energy yield for a floating PV module offshore. As expected, the oscillations of the waves caused a slight surplus on the annual energy yield if compared with a PV module laying on a flat surface on the ground.

The second observation is that the steeper the wave, the lower the incident energy yield onto the PV module even if it is at its optimal tilting angle (θ_M). It also can be observed that the panel's optimal tilting angle for that wave tilt angle barely changes when the wave tilt does it. This has a direct and remarkable impact in the annual energy yield.

The third observation is that the optimal tilting angle of the PV panel will always be higher than the tilting angle of the wave. This is because when the wave tilting is negative (not facing the Sun), the module has to keep facing the Sun in order to get the highest possible incident energy yield. That is why the module's tilting angle has to be bigger than the one of the wave.

The fourth and final observation is from Section 6.3.1, where it is observed that even if a steep angle on the PV module allows to have the maximum amount of energy from the Sun when the wave is negatively tilted (not facing the Sun), this also is a problem when the wave is in a positive tilting angle (facing the Sun). For instance, this can be easily observed in Figure 6.16, when the tilting angle on the wave is at 45º and the PV module's tilting angle is 49º, the final inclination of the PV panel is 94º when the wave is facing the Sun. This is according to the formulas developed at Section 6.1.1 regarding the final tilt angle of a PV module at a determined wave tiling. This indicates that there is a reduction of the direct irradiance incident on the module in this case. Whilst when the wave is negatively tilted (not facing the Sun), the module's final tilting angle is barely of 4º; it still is looking at the Sun's direction, but the inclination is too poor to get a better energy yield. There are, thus, more losses on the direct irradiance.

With these results, is can be concluded that for a floating PV panel on a controlled wave scenario, the

highest amount of incident energy yield on the module, will come from the diffuse irradiance, followed by the direct irradiance and it is expected that the albedo/ground irradiance contribution is despicable in comparison to the module on a solid surface due to its low albedo (0.1). Therefore, the expected performance of a floating panel offshore is similar as the PV static topology in a flat position, but with a lower incident AEY.

6.4. Random Wave. Reference Case: θ_M=0º

This scenario is similar to the one previously analysed, the difference now is that the wave has a complete random tilting angle. Therefore, the PV module's θ_M and azimuth will have a different unpredictable position all the time. The assumption in this scenario is that the module lays flat on the wave (θ_M=0º) and it will have the same tilting angle as the wave. Figure 6.17 depicts a possible scenario for a random wave movement sequence with more detail.

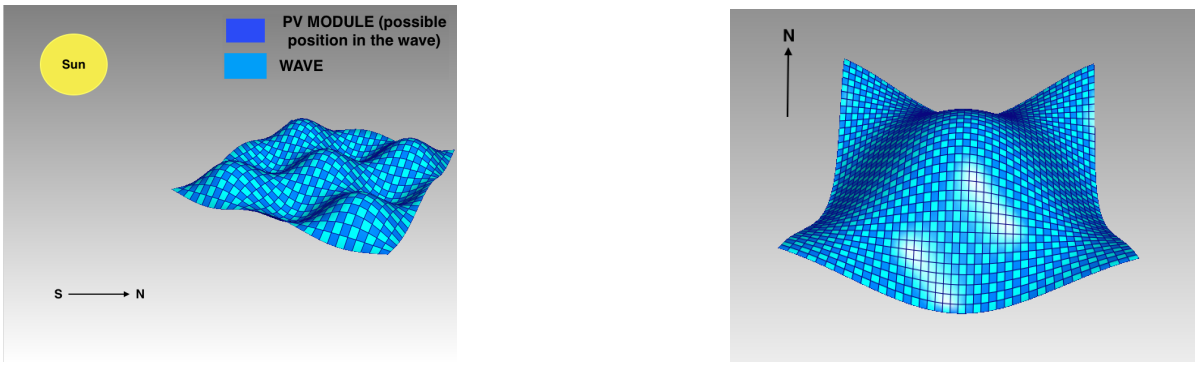

(a) (b)

Figure 6.17: (a) 3-D perspective for the random wave tilting scenario with a floating PV module with θ_M=0º(b) View on the wave from the Sun's perspective.

It is observed at Figure 6.17 that the floating PV module can be at any position on the wave at every minute. Therefore, its orientation and tilting angle will never be predicted. This is more appreciated at Figure 6.17b.

Figure 6.18 depicts the irradiance time series for a random wave tilting and a θ_M=0º.

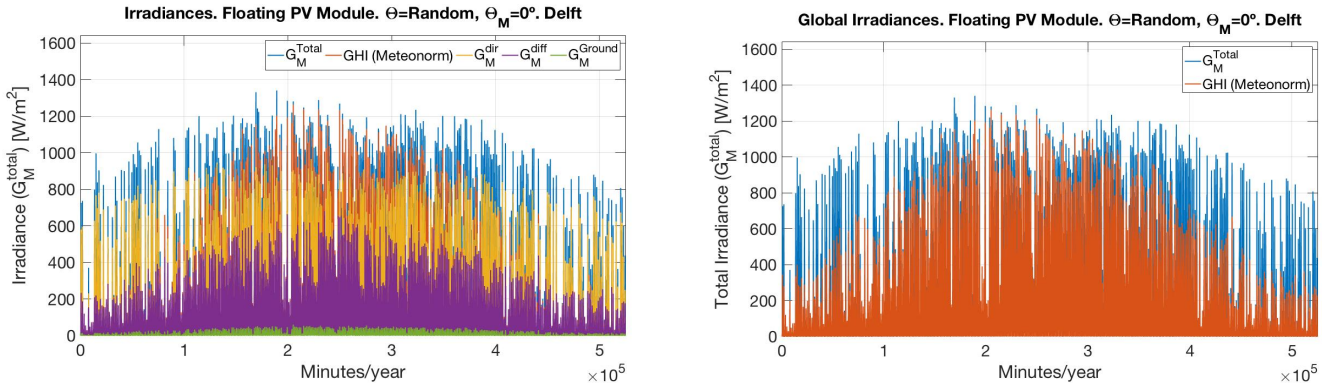

(a) (b)

Figure 6.18: (a)Total, direct, diffuse and ground irradiances calculated vs GHI from KNMI. (b)Total irradiance falling onto the module vs GHI from KNMI file.

Figure 6.19 deploys the information about the AEY incident onto the floating PV module.

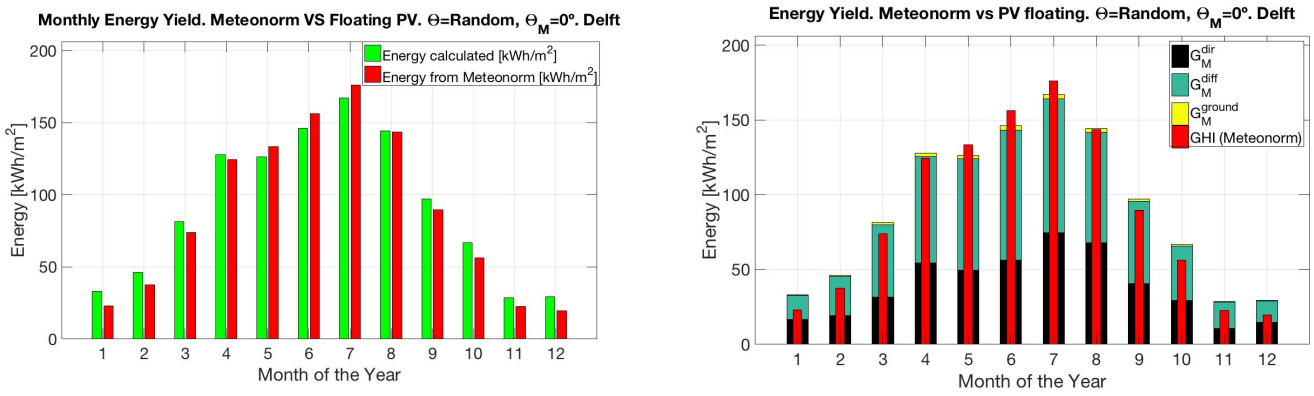

(a) (b)

Figure 6.19: (a)Monthly energy yield incident on the floating PV module in [kWh/m^2] (b)Individual energy yield provided by the direct, diffuse and ground irradiances in [kWh/m^2].

It is clear that even if the random angles caused by the wave can not be predicted, the floating PV module has a surplus in its AEY. Table 6.4 compares the results from the random wave tilting angle vs the ones of the controlled wave tilt scenario. The PV Static at θ_M=0º is also present.

Topology	G_M [kWh/m^2]	G_M^{dir} [kWh/m^2]	G_M^{diff} [kWh/m^2]	G_M^{ground} [kWh/m^2]
PV Static (0º)	**1039**	437	602	0
Float PV, Θ=69º;θ_M=0º	**1160**	540	608	12
Float PV, Θ=45º;θ_M=49º	**1147.5**	519	607	21
Float PV, Θ=Random; θ_M=0º	**1095**	466	610	19
Dif.(Θ=69º vs PV Static) [kWh/m^2]	**+121**	+103	+6	+13
Dif.(Θ=69º vs PV Static) in [%]	**+11.6 %**	+23.6 %	+1 %	N/A
Dif.(Θ=45º vs PV Static)[kWh/m^2]	**+108.5**	+82	+5	+21
Dif.(Θ=45º vs PV Static) in [%]	**+10.4 %**	+18.8 %	+0.83 %	N/A
Dif.(Θ=Random vs PV Static) [kWh/m^2]	**+56**	+29	+8	+19
Dif.(Θ=Random vs PV Static) in [%]	**+5.4 %**	+6.64 %	+1.33 %	N/A

Table 6.4: Individual Energy Yield. Contribution by irradiance. (Floating PV Model: CONTROLLED Tilting and RANDOM Tilting) vs PV Static at θ_M=0º.

Where "Dif." stands for "difference". The first observation is that at a random wave tilting, the floating PV module has a poor increase in its incident AEY (5.4 %). Its direct irradiance is the lowest of the floating scenarios studied in this chapter and curiously, the diffuse irradiance incident on the floating PV module barely changes when compared to the other floating cases.

Of course, since the waving behaviour in this scenario is randomly generated, there could be cases in which the AEY is higher or lesser than any of the cases 'presented in this example. One thing is 100 % true: the AEY in the random wave tilting and a θ_M=0º will always be higher than the PV Static module also with a θ_M=0º (PV module's tilting angle).

6.4.1. Random Wave Scenario. Scenarios With a θ_M>=0º

Table 6.5 describes various scenarios when the floating PV module has any of the tilting angles previously studied in this chapter. The PV static model at θ_M=0º is also shown in the table.

Topology	G_M [kWh/m^2]	G_M^{dir} [kWh/m^2]	G_M^{diff} [kWh/m^2]	G_M^{ground} [kWh/m^2]
PV Static (0º)	**1039**	437	602	0
Float PV, Θ=Random; θ_M=0º	**1095**	466	610	19
Float PV, Θ=Random;θ_M=15º	**1086**	456	611	19
Float PV, Θ=Random;θ_M=30º	**1055**	420	612	23
Float PV, Θ=Random;θ_M=47º	**1005**	360	615	30
Dif.(PVS vs Rand, θ_M=47º)[kWh/m^2]	**-34**	-77	+13	+30
Dif.(PVS vs Rand, θ_M=47º) in [%]	**-3.27 %**	-17.62 %	+2.16 %	N/A

Table 6.5: Individual Energy Yield. Contribution by irradiance. Floating PV Model RANDOM Tilting vs PV Static at θ_M=0º. Different θ_M angles for the Floating PV Module.

Where "Dif." stads for "difference" and "PVS" for "PV Static at θ_M=0º". For the first time in this project, it is found a situation where there is a deficit in the AEY if it is compared with the PV Static at a θ_M=0º. It is observed that there is a general depreciation of 3.3 % and the direct irradiance incident on the PV module was the biggest "loser" with a deficit of almost 18 %. The diffuse and the ground irradiances improved their AEY thanks to the waves movement.

Some relevant observations from Table 6.5 are concluded: the first and most important one is that the optimal tilting angle for a floating PV module offshore under random wave tilting, is 0º.

The second observation is that the higher the θ_M the lower the AEY.

The third one is that the direct irradiance incident on the PV module is the most affected under these circumstances. The possible reason for this, is that the waves randomly generated had angles > 45º (facing the Sun), causing that the final angle of the floating PV module were >90º, causing thus the loss on the direct irradiance. The other option is that there were several cases where the final tilting angle on the module was < 0º, causing, again, more losses in the direct irradiance. Besides, the PV panel's azimuth barely is at its optimal position (180º for this location), affecting thus the incident irradiance.

The fourth observation is that from all the floating scenarios, the one with the highest energy yield coming from the ground irradiance (G_M^{ground}) was when θ_M=47º at a random tilting wave angle. This can be related to the previous point, when Mf (module's final tilting angle, refer to Figure 6.13 to see the variable names) has a very steeped angle in several occasions. In this case, the ground irradiance had a stronger contribution for the final AEY due to the steeped angle of the PV panel, even if the water's albedo is 0.1.

As a fifth point, it can definitely be said that the diffuse irradiance will always be the main contributor for the general AEY for a floating PV for both controlled and random wave tilting angles.

6.4.2. Conclusions Float PV Model, RANDOM Wave Scenario

Several interesting results could be observed, where in general, it was discovered that the best scenario for a floating PV system offshore, with a random tilting angle, is when θ_M=0º (in other words, when the PV module lays at a flat position onto the wave).

6.5. Conclusions. Floating PV MATLAB Model

For the Controlled wave scenario

The ideal scenario for this case is if the waves move as little as possible, generating tiny tilt angles on the final module tilting (Mf). Of course, the perfect scenario would be to have a final tilt angle equal to an optimal tilting angle onshore, but for this, it is necessary that there were no tilting angles on the waves during the entire year (in other words: no waves), which is an impossible scenario.

For the Random wave scenario

For this scenario, the best option for the highest AEY is to always have a θ_M=0º. From Table 6.5 is observed that a tilted PV module only means a decrease in the (already low) AEY.

Once that the results from the simulations of a PV module offshore were calculated, the answers to the research questions of the Section 1.7 are presented next.

What is the irradiance and the AEY incident on a PV module located offshore under a controlled wave scenario and under a random wave scenario?

In general, it can be said that this is the worst topology in terms of incident irradiance and AEY under the scenarios studied so far in this Thesis Project. The diffuse irradiance also showed to have the most constant value in all the floating scenarios with almost no changes in it.

What is the optimal tilting angle under each scenario (controlled and random waving) and why?

Figure 6.16 depicts the different wave tilting angles Θ and their respective θ_M. In general, for the controlled scenario, a θ_M of about 46º is recommended, whereas for a random case scenario, a flat PV module (θ_M=0º) is the best choice.

For the controlled wave scenario, the best performance is found when the waves have a predominantly flat movement and the PV module's tilting angle (θ_M) is around 47º. If compared with the PV Static at θ_M=0º, this means a surplus of 14.92 %. In the next chapter these and other results will be analysed.

For the random wave scenario, it had its best incident AEY when θ_M=0º, which when it is compared with the PV Static at θ_M=0º, this means a low surplus of 5.4 %. When θ_M>0º there are losses in the incident AEY. This can be consulted in Table 6.5.

For the Floating PV System in General

It is important to say the current floating PV plants working today in different locations around the globe, work under controlled conditions and on fresh water. This is due to the current material used in the PV technologies, which are not in conditions to work under a drastic scenario such as the sea.

Besides of the material corrosion, probably another important fact that could be observed here, is that this topology has the lowest incident annual energy yield from all the studied topologies. This means that it would be required to cover a bigger area in the sea in order to achieve the same incident irradiance of that of a PV module on the ground. This means to have higher investment costs for something that probably could perform better on the land.

These reasons could be some of the causes of why this kind of projects are built onshore, on fresh water and under controllable variables (such as the waving behaviour) and not offshore. The economical aspect is one of the most important of all of them, since it is expected an extremely high initial investment cost for offshore PV plants. Moreover, the unpredictable behaviour of the sea makes it even more difficult to foresee a standard scenario which helps to have a more trustworthy sizing of the PV system.

As seen on this chapter, the current MATLAB model can not determine which is the optimal tilting angle when the wave causes a determined inclination on the PV module. Therefore, create a "tilt optimiser" which finds the optimal tilting angle for a float PV module in order to receive the highest incident irradiance per year at a certain wave tilting, would be a good next step.

7

Discussion of the Results

This chapter will summarize the results observed in this thesis project. The final and most relevant values of each topology will be analysed and compared. For the cases in which more than one tilt angle was compared (such as in the PV Static, TRA and Floating PV topologies) only the optimal tilt angle in which the highest incident AEY was calculated is considered.

7.1. Comparison of Annual Energy Yield of all the Topologies

In this section, all the topologies seen in this thesis (the static, tracking and floating PV modules) will be compared and their incident annual energy yield will be discussed. In Table 7.1 all the topologies which were studied here are compared. Table 7.1 deploys, from the highest to the lowest, all the annual energy yields calculated in this project from all the topologies. The contribution of the annual energy yield of each individual irradiance is also shown.

For the case of the floating PV module topology, only the one that got the highest incident energy yield is considered. In this case, when the wave had a tilt of 15º and the module a 47º tilting angle. In the table, M stands for the tilt angle of the floating PV module. Refer to Figure 6.13 to clarify. The case where there was a deficit in the AEY is also included (see Table 6.5 in Section 6.4.1).

Topology	G_M [kWh/m^2]	G_M^{dir} [kWh/m^2]	G_M^{diff} [kWh/m^2]	G_M^{ground} [kWh/m^2]
TRAT	**1573**	867	657	49
TRA (67º)	**1515**	835	615	65
TRT	**1280**	613	634	33
PV Static (52º)	**1218**	567	611	40
Floating PV(Θ=15º, M=47º)	**1194**	568	609	17
Floating PV(Θ=Random, M=0º)	**1095**	466	610	19
PV Static (0º)	**1039**	437	602	0
Float PV, Θ=Random;θ_M=47º	**1005**	360	615	30

Table 7.1: TRAT vs TRA vs TRT vs PV Static vs Floating PV.

Table 7.2 shows the difference of performance of each topology compared against the PV Static model with a θ_M=0º, which is the reference point for these comparisons. If the value is positive in the variable of the topology (+) it means that its value had a surplus if compared with that same variable of the PV Static topology at 0º. If the value is negative (-) then the variable of that topology had a deficit in its performance when compared with that same variable of the PV Static topology at 0º. The table is also in decreasing order of performance. In the table: Θ stands for the wave tilting, "Dif." for "difference" and θ_M=47º for the PV module's tilting angle at 47º.

Topology Comparison	G_M	G_M^{dir}	G_M^{diff}	G_M^{ground}
Difference(TRAT vs PVStatic 0º)[kWh/m^2]	**+534**	+430	+55	+49
Difference (TRAT vs PVStatic 0º)[%]	**+51.4 %**	+98.4 %	+9.14 %	N/A
Difference(TRA 67º vs PVStatic 0º) [kWh/m^2]	**+476**	+398	+13	+65
Difference(TRA 67º vs PVStatic 0º)[%]	**+45.8 %**	+91 %	+2.16 %	N/A
Difference(TRT vs PVStatic 0º) [kWh/m^2]	**+241**	+176	+32	+33
Difference(TRT vs PVStatic 0º)[%]	**+23.2 %**	+40.3 %	+5.32 %	N/A
Difference PVStatic (52ºvs0º) [kWh/m^2]	**+179**	+130	+9	+40
Difference PVStatic (52ºvs0º)[%]	**+17.23** %	+29.75 %	+1.5 %	N/A
FloatPV(Θ=15º,M=47º) vs PVStatic 0º [kWh/m^2]	**+155**	+131	+7	+17
FloatPV(Θ=15º,M=47º) vs PVStatic 0º [%]	**+14.92 %**	+30 %	+1.16 %	N/A
Dif.(FloatPV, Θ Random,θ_M 0º vs PVStatic 0º)[kWh/m^2]	**+56**	+29	+8	+19
Dif.(FloatPV, Θ Random,θ_M 0º vs PVStatic 0º)[%]	**+5.4 %**	+6.64 %	+1.33 %	N/A
Dif.(FloatPV, Θ Random,θ_M 47º vs PVStatic 0º)[kWh/m^2]	**-34**	-77	+13	+30
Dif.(FloatPV, Θ Random,θ_M 47º vs PVStatic 0º)[%]	**-3.27 %**	-17.62 %	+2.16 %	N/A

Table 7.2: TRAT vs TRA vs TRT vs PV Static vs Floating PV. Difference in the annual energy yield incident on the PV module in [kWh/m^2] and in percentage [%].

Table 7.2 demonstrates that for most of the cases, the incident diffuse irradiance on the module is the main contributor for the annual energy yield. Only on the azimuth-tilting tracker (TRAT) and on the azimuth tracking systems (TRA) the direct irradiance is the main contributor. In terms of investment costs, probably the floating PV system offshore would be the most costly and probably with the current technology it would be even more expensive.

The TRA has the highest contribution for the ground irradiance. This is because the azimuth tracker has a high steeped inclination for the PV module, which improves the irradiance coming from the ground.

As it can be observed from the Table 7.1, this topology has the lowest incident irradiance of all the topologies studied here. This is due to the constant movement that the module experiences at every minute throughout the year, causing that the PV panel's tilting angle changes and it will never have an optimized fixed tilting angle. The sea water poor albedo also caused a low energy contribution from reflection.

Table 7.3 describes the rank (from 1 to 7) that each topology has in reference to the PV Static topology at θ_M=0º.

Topology Comparison	G_M	G_M^{dir}	G_M^{diff}	G_M^{ground}
Difference(TRAT vs PVStatic 0º),rank	**1**st	1st	1st	2nd
Difference(TRA 67º vs PVStatic 0º), rank	**2**nd	2nd	3rd	1st
Difference(TRT vs PVStatic 0º), rank	**3**rd	3rd	2nd	4th
Difference PVStatic (52ºvs0º), rank	**4**th	5th	5th	3rd
FloatPV(Θ=15º,M=47º) vs PVStatic 0º, rank	**5**th	4th	7th	7th
Dif.(FloatPV, Θ Random,θ_M 0º vs PVStatic 0º), rank	**6**th	6th	6th	6th
Dif.(FloatPV, Θ Random,θ_M 47º vs PVStatic 0º), rank	**7**th	7th	3rd	5th

Table 7.3: Rank according to performance, compared against the PV Static model at θ_M=0º.

The three previous tables resume in a highly accurate way in which cases the best results are found in each of the seven MATLAB models developed in this project. The graphs of the irradiances and the AEY seem

to match with the results observed in real projects, even if the tilting angles for the models which required a static θ_M differ from some literature and the tilting angles used in locations such as the Netherlands (for the PV Static topology).

The surprise was given by the Floating PV model with a random Θ and a θ_M=47º, which was the third best performance for the G_M^{diff}. Nevertheless, this is useless since its overall performance had a deficit of almost 3.3 % for the G_M and a huge loss of almost -18% for G_M^{dir}.

To conclude this chapter, the results showed what it was expected for each topology, with one or two new results during the development of these models. More studies and on-field research would help to change (or corroborate) the conclusions presented here.

8

Conclusions and Recommendations

In this final chapter of this thesis project, the most important conclusions and the recommendations which could be implemented to improve this project in the future, are discussed and proposed.

8.1. Conclusions

The main goal of the work developed here, was to provide a full and detailed analysis of the contribution of the incident energy yield that each of the three known different irradiances (direct, diffuse and ground) on a PV module. Also, the analysis of a new study case was performed: a floating PV module offshore.

In chapter 2, it was described which were the components to calculate the value of the global irradiance incident on a PV module, thus, what would be the annual energy yield received on it. Several known concepts which are implemented in PV systems projects, such as the PV panel's tilting angle, the sky view factor and the direct, diffuse and ground irradiances were studied and analysed. The formula used in order to calculate the diffuse irradiance incident on the PV module (G_M^{diff}), was the Sandia laboratories' model, whereas SAM uses the Perez model. The decision to use the Sandia formula was because they claim to have the highest accuracy, it was the continuation of a project started by Narayan and because it is a relatively new formula (from 2015) compared to other existent models.

The next important step was seen in chapter 3, in which two known softwares used to simulate and size a PV system have been compared: the NREL's System Advisor Model (SAM) and the PVSyst model. Once the comparison of the results among these applications finished, it was decided to use SAM as a "calibrator", which would help during the developing of a third model using MATLAB. SAM shows the solar azimuth and elevation, and these variables were the main elements that helped to "calibrate" the MATLAB model. In this new model, several sub-models were coded in order to determine the incident irradiance on a PV module under all these topologies, to later calculate the annual energy yield in each of them. A final and new model was introduced and also analysed: an offshore floating PV panel (working on the sea).

It has been demonstrated that the assumption of considering the latitude of the location as the PV module's optimal tilting angle is valid, at least, for locations with a latitude above 50º. This is only valid for the PV static topology. For the PV semi-static configuration, it was proposed that (following the logic from the PV static topology) the PV module has to be tilted to its optimal tilting angle per month. Therefore, the irradiance incident onto the PV module will increase.

For the Tracking topologies, when an azimuth-tilting tracker (TRAT) is programmed to remain flat (θ_M=0º), it prioritizes the diffuse irradiance over the direct one when the day has a poor sunlight. For the azimuth-tracking topology (TRA), it was demonstrated that the PV module's optimal tilting angle in this topology is not the same as the one used in the PV static one. However, a rough approximation to calculate its optimal tilting angle can be performed: determine the average of the inclination angle used on the PV module during the location's winter (the solar calculator [33] can be used to do this). Finally, in the tilting tracking topology (TRT), it was found that the annual average tilting angle for the PV module located in Delft, which is about 36º, is similar to the angle found in different sources and close to the one used by default by SAM and PVSyst (which is 30º). This difference of optimal tilting angles could be due to the use of the Sandia model to determine the (G_M^{diff}) whereas SAM and PVSyst use the Perez model. Nevertheless, for the MATLAB model developed in this project, it was proven that the **average** tilt angle is not equal to the **optimal** tilting angle.

Even if the PV semi-static calculations were not able to be measured, it is expected to have a higher performance than the PV Static at 52º tilting angle and lower than any tracker. Since the panel is optimally tilted by month, hence, it will improve its performance. In the semi-static topology, it is foreseen that the diffuse irradiance will be the main contributor for the annual energy yield incident on the PV module. Moreover, since the panel will have a steeper tilt during winter and autumn, it is expected that the ground irradiance also increases in winter.

In chapter 6, the new model of a floating PV module offshore was analysed. Here, it was discovered that it has the lowest performance from all the topologies studied. Another interesting outcome, is that the optimal tilting angle for a PV module does not significantly change while the tilting caused by the waves movement heavily changes. Nevertheless, this is not the case for the annual energy yield incident on the PV module, since it continuously decreases while the wave tilting increases. In other words: the tilt angle caused by the waves is inversely proportional to the annual energy yield incident on a PV module.

Finally, in chapter 7, once all the calculations were performed, a comparison amongst all the studied topologies was analysed. From those, interesting results were present in the TRA topology, where its steeped tilting angle surprised to be the optimal one for Delft and in which the highest incident annual energy yield (AEY) was calculated for this topology. Also, the high tilting angle for the PV static topology indicated that, as previously mentioned, the best tilting angle for Delft was 52º. This is contrary to what many sources, included the SAM and PVSyst models, indicate. The optimal tilting angles in which the highest performance of a PV System is calculated in these softwares, is found in a range of about 30º-37º. PV Syst finds its higher performance when θ_M=30º and SAM finds it at 37º.

8.1.1. Accuracy of the MATLAB Model

As mentioned in 5, another of the objectives of this model was to make it available to perform analysis of the incident irradiance anywhere in the world. In Appendix A, several cities from all the latitudes and longitudes are shown in order to prove that this objective was satisfactorily fulfilled.

8.2. Recommendations

There are 4 main recommendations to apply on different models in order to improve them and make the even more complete than they are now. The main objective of these proposals of improvement is to complement the work finished here and make it more robust, in order to cover more important aspects which were not covered in this project. Some of the recommendations were already proposed in previous chapters.

1. Make a model which determines what is the optimal tilting angle for the PV module per month, season and semester. Similar to the "PV-Static Finder" described on Section 5.3

2. Make an optimal tilting angle finder model for the azimuth-tracker (TRA). Again, it would be similar to the "PV-Static Finder"

3. For the floating PV module, create another optimal tilting angle finder model

4. Remake the MATLAB models presented here but using the Reindl or Perez model to calculate the diffuse irradiance incident on the module, to later compare those results with the ones presented in this thesis to finally determine if the optimal tilting angles using either of these models are the same as those from SAM or if they are similar to the ones obtained by using the Sandia lab model

Other recommendations can be proposed. This project only determines the irradiance falling onto one PV module, therefore this project can strongly be extended in several ways, such as:

1. (Single Module) Performance of one single PV panel using this incident irradiance (how much energy is produced by the PV module) [kWh]

2. (Array) Irradiance falling on an PV array of several modules

3. Energy produced by this array [kWh]

4. Make a real studio of how the waves affect the module's position and not an assumption where the module's tilting due to the waves is estimated

5. (Materials) Corrosion/damage in the modules and the power electronic devices due to the extreme constant contact with humidity and salty water
6. Make an economical analysis of a PV array offshore to determine if it is economically feasible
7. Effect of shading due to the waves/modules
8. Make a field test
9. Make a 3-D modelling

Moreover, getting information about the behaviour of the waves for the wanted location would be useful (if such data exists). This would help to have a more realistic idea about the PV module's motion and its tilting angle caused by the waves movement. The ideal case would be to work with as little assumptions as possible and more realistic information.

It also would be profitable to recreate these scripts made in MATLAB by using other models; especially for the diffuse irradiance. As previously mentioned, the Perez and/or the Reindl modellings could be used in order to compare their results with the ones implemented in this thesis.

Finally, a field study would be highly recommended in order to see first-hand the results and observe the differences from the simulated data. This proposal probably would be more for a long-term project, such as a PhD or research programme. Nevertheless, the study on field is highly encouraged here.

A

Results on other Locations of the World

In this section, the calculations for other cities around the world have been performed. As mentioned in Section 8.1.1, this is shown in order to corroborate that the model created with MATLAB properly works for any location in the world. Only the graphs of the PV Static MATLAB model are plotted and tabulated in this appendix, since it is the most common configuration for a PV installation.

In order to make more readable the graphs, the Table A.1 indicates what is the value of each angle in terms of the cardinal points:

North	East	South	West
0º	90º	180º	270º

Table A.1: Azimuth of the Sun and its relation with the cardinal points.

The PV module's optimal tilt angles in each city were calculated with the PV Static Finder MATLAB model created in this project. The meteorological information was extracted from the Meteonorm application.

The reader will note that the analemmas of the locations at the Southern hemisphere, have a different shape than those from the Northern one. This is because when the PV module is at the Northern hemisphere, it has to face to the South (180º) in order to get the highest possible irradiance. This means that for the PV module, the sunrise will appear at its left side (East, 90º) and the sunset is at its right side (West, 270º). In the Southern hemisphere is the opposite: the module is facing North (0º), the sunrise is at its left side and the sunset at its right one. Like a mirror effect.

Please note that he black lines and the stars in the middle of the graph at Figure A.3a are origin errors coming from the input files. They don't affect the final results of the analysis.

A.1. Mexico City, Mexico

Location	Longitude [º]	Latitude [º]	PV Module's Optimal Tilting Angle [º]
Mexico City	-99.2	19.4	28

Table A.2: Mexico City information and PV Static optimal tilting angle.

A.1.1. PV Static

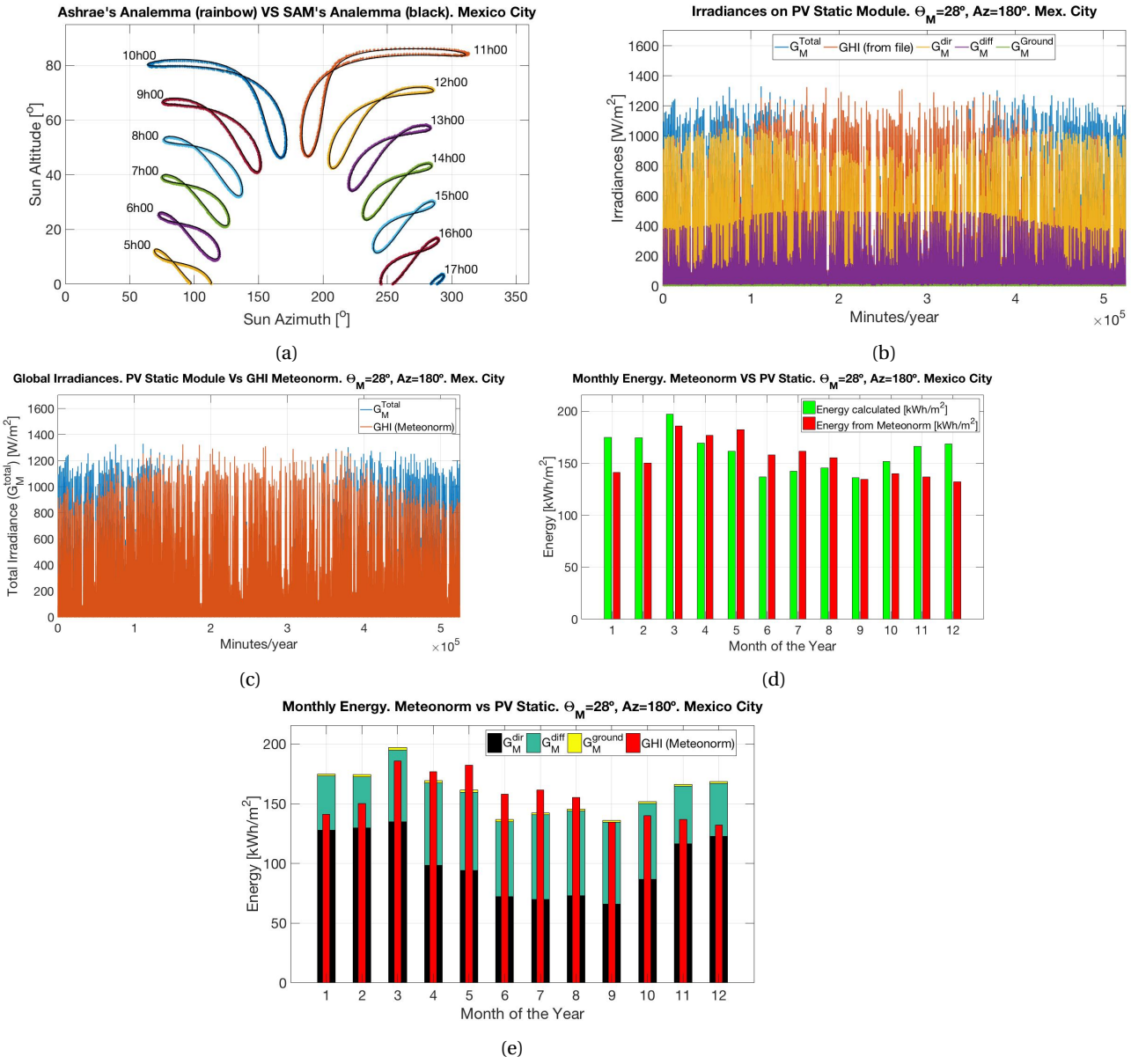

Figure A.1: Mexico City, Mexico. PV Static (a) Mexico City's analemma at different times (b) Irradiances: direct, diffuse and ground (c) Irradiances: MATLAB vs Meteonorm (d) Monthly energy yield. MATLAB vs Meteonorm (e) Individual Energy Yield per irradiance.

$\mathbf{G}_M$ [kWh/m^2]	$\mathbf{G}_M^{dir}$ [kWh/m^2]	$\mathbf{G}_M^{diff}$ [kWh/m^2]	$\mathbf{G}_M^{ground}$ [kWh/m^2]
1926	1191	711	24

Table A.3: Individual Energy Yield. Contribution by irradiance. Mexico City. PV Static topology.

A.2. Phoenix, AZ, USA

Location	Longitude [º]	Latitude [º]	PV Module's Optimal Tilting Angle [º]
Phoenix	-112.017	33.433	39

Table A.4: Phoenix information and PV Static optimal tilting angle.

A.2.1. PV Static

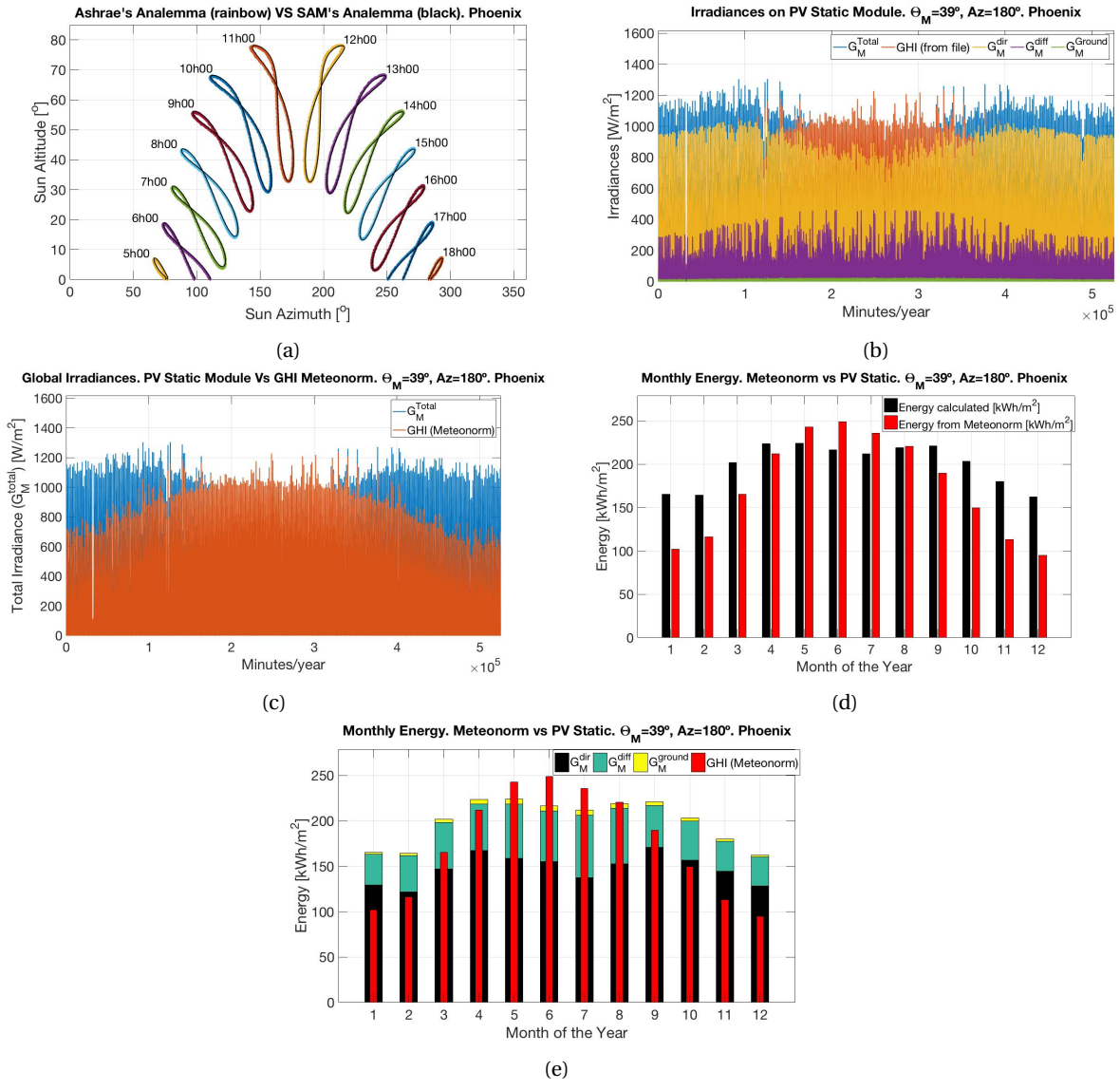

Figure A.2: Phoenix, USA. PV Static (a) Phoenix's analemma at different times (b) Irradiances: direct, diffuse and ground (c) Irradiances: MATLAB vs Meteonorm (d) Monthly energy yield. MATLAB vs Meteonorm (e) Individual Energy Yield per irradiance.

$\mathbf{G}_M$ [kWh/m^2]	$\mathbf{G}_M^{dir}$ [kWh/m^2]	$\mathbf{G}_M^{diff}$ [kWh/m^2]	$\mathbf{G}_M^{ground}$ [kWh/m^2]
2393	1765	579	49

Table A.5: Individual Energy Yield. Contribution by irradiance. Phoenix, USA. PV Static topology.

A.3. Temuco, Chile

Location	Longitude [º]	Latitude [º]	PV Module's Optimal Tilting Angle [º]
Temuco	-72.633	-38.75	37

Table A.6: Temuco information and PV Static optimal tilting angle.

A.3.1. PV Static

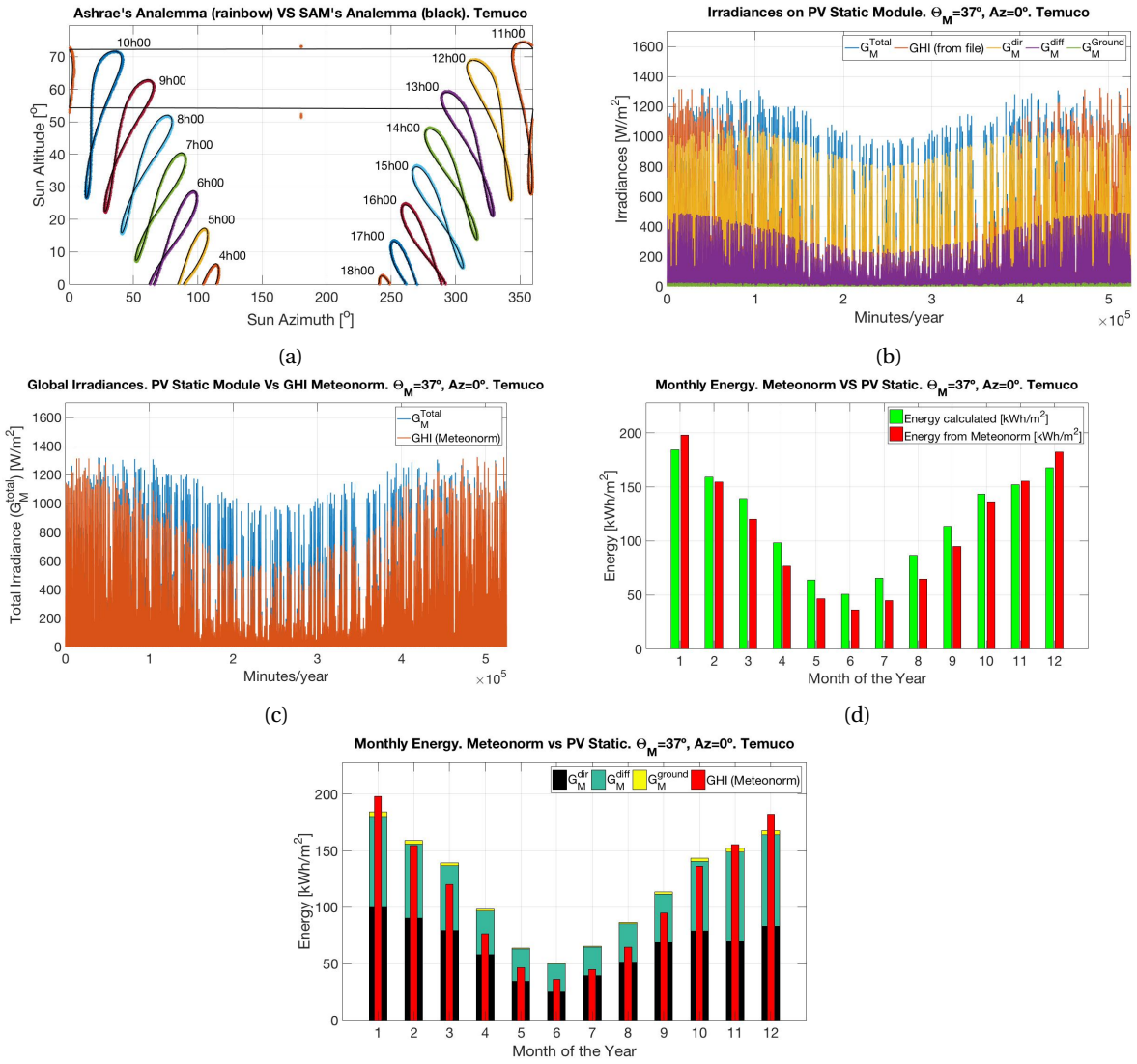

Figure A.3: Temuco, Chile. PV Static (a) Temuco's analemma at different times (b) Irradiances: direct, diffuse and ground (c) Irradiances: MATLAB vs Meteonorm (d) Monthly energy yield. MATLAB vs Meteonorm (e) Individual Energy Yield per irradiance.

$\mathbf{G}_M$ [kWh/m^2]	$\mathbf{G}_M^{dir}$ [kWh/m^2]	$\mathbf{G}_M^{diff}$ [kWh/m^2]	$\mathbf{G}_M^{ground}$ [kWh/m^2]
1425	779	618	28

Table A.7: Individual Energy Yield. Contribution by irradiance. Temuco, Chile. PV Static topology.

A.4. New Delhi, India

Location	Longitude [º]	Latitude [º]	PV Module's Optimal Tilting Angle [º]
New Delhi	77.2	28.583	38

Table A.8: New Delhi information and PV Static optimal tilting angle.

A.4.1. PV Static

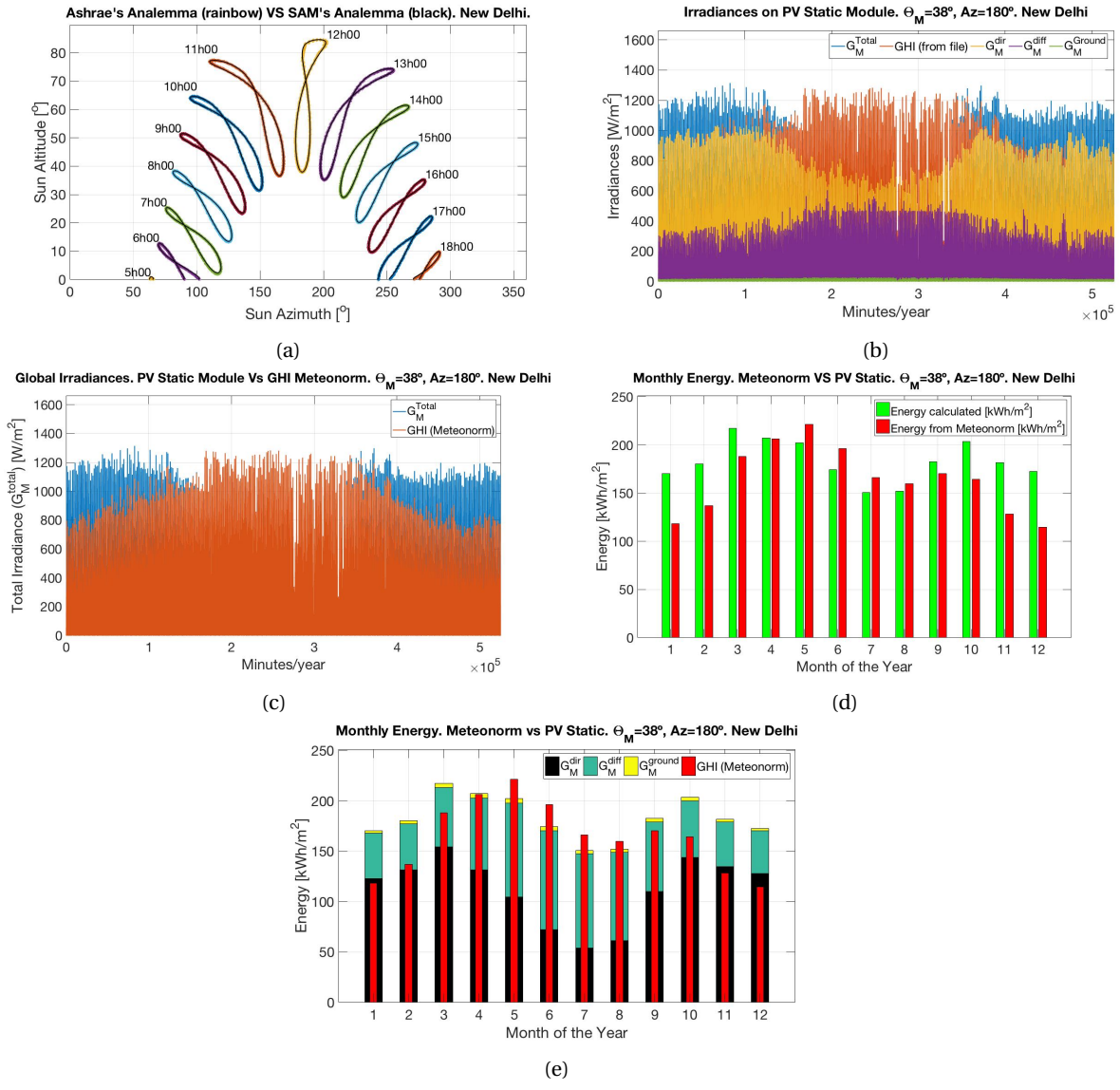

Figure A.4: New Delhi, India. PV Static (a) New Delhi's analemma at different times (b) Irradiances: direct, diffuse and ground (c) Irradiances: MATLAB vs Meteonorm (d) Monthly energy yield. MATLAB vs Meteonorm (e) Individual Energy Yield by each irradiance.

$\mathbf{G}_M$ [kWh/m^2]	$\mathbf{G}_M^{dir}$ [kWh/m^2]	$\mathbf{G}_M^{diff}$ [kWh/m^2]	$\mathbf{G}_M^{ground}$ [kWh/m^2]
2196	1346	806	44

Table A.9: Individual Energy Yield. Contribution by irradiance. New Delhi, India. PV Static topology.

A.5. Christchurch, New Zealand

Location	Longitude [º]	Latitude [º]	PV Module's Optimal Tilting Angle [º]
Christchurch	172.533	-43.830	48

Table A.10: Christchurch information and PV Static optimal tilting angle.

A.5.1. PV Static

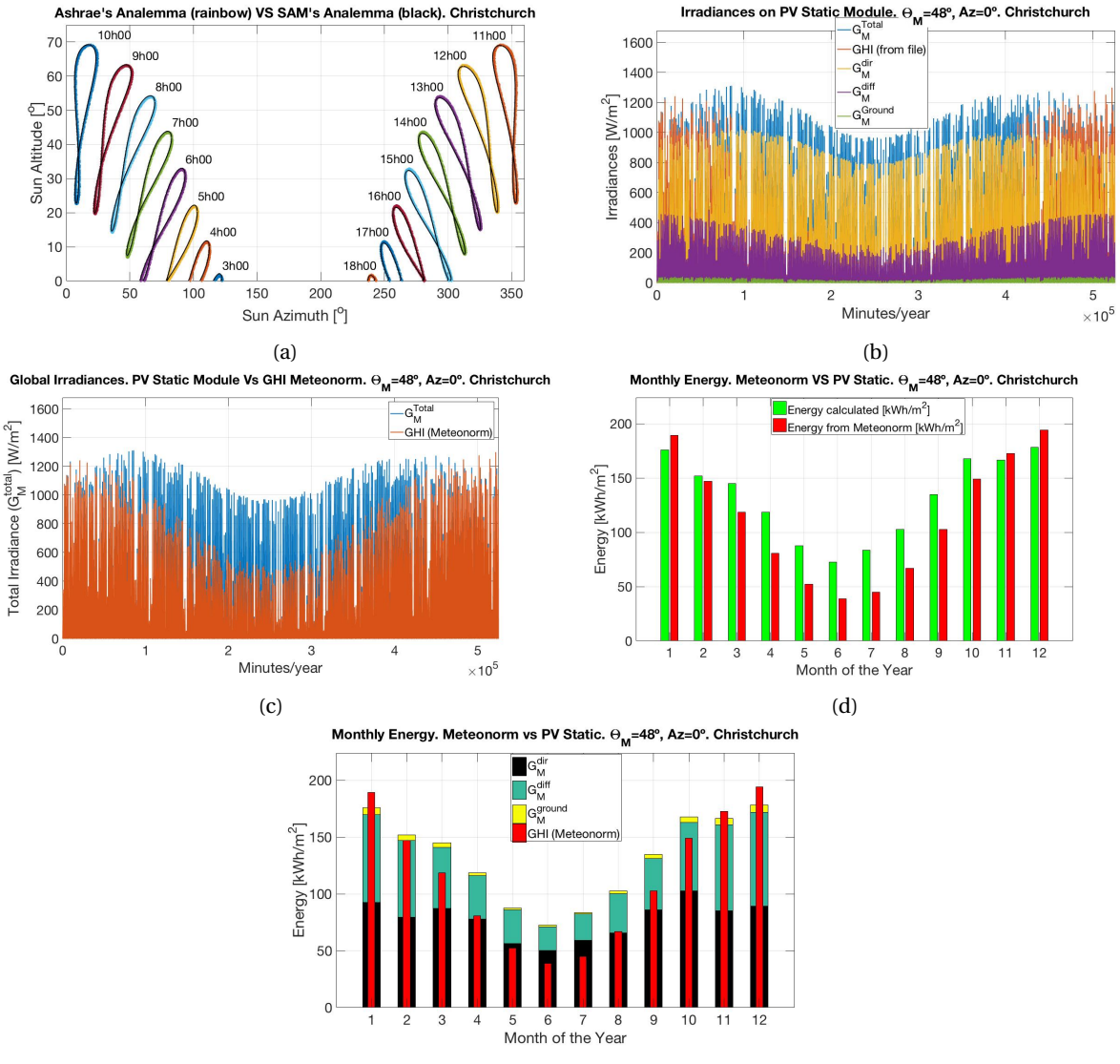

Figure A.5: Christchurch, New Zealand. PV Static (a) Analemma at different times (b) Irradiances: direct, diffuse and ground (c) Irradiances: MATLAB vs Meteonorm (d) Monthly energy yield. MATLAB vs Meteonorm (e) Individual Energy Yield per irradiance.

G_M [kWh/m^2]	G_M^{dir} [kWh/m^2]	G_M^{diff} [kWh/m^2]	G_M^{ground} [kWh/m^2]
1585	929	609	47

Table A.11: Individual Energy Yield. Contribution by irradiance. Christchurch, New Zealand. PV Static topology.

A.6. Quito, Ecuador

Location	Longitude [º]	Latitude [º]	PV Module's Optimal Tilting Angle [º]
Quito	-0.167	-78.483	0

Table A.12: Quito information and PV Static optimal tilting angle.

A.6.1. PV Static

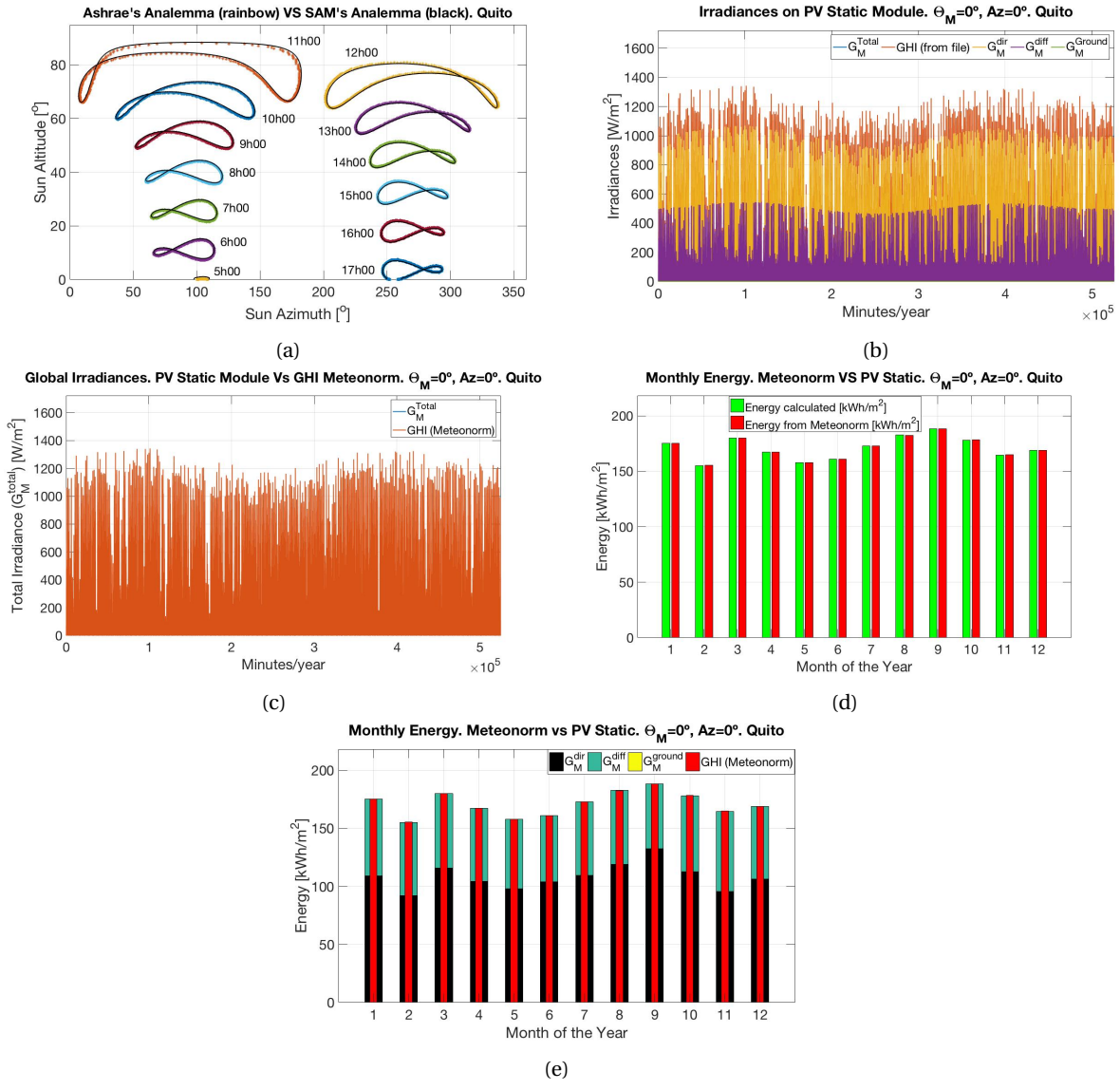

Figure A.6: Quito, Ecuador. PV Static (a) Quito's analemma at different times (b) Irradiances: direct, diffuse and ground (c) Irradiances: MATLAB vs Meteonorm (d) Monthly energy yield. MATLAB vs Meteonorm (e) Individual Energy Yield per irradiance.

$\mathbf{G}_M$ [kWh/m^2]	$\mathbf{G}_M^{dir}$ [kWh/m^2]	$\mathbf{G}_M^{diff}$ [kWh/m^2]	$\mathbf{G}_M^{ground}$ [kWh/m^2]
2053	1300	753	0

Table A.13: Individual Energy Yield. Contribution by irradiance. Quito, Ecuador. PV Static topology.

B

MATLAB Code

This appendix shows the script used to calculate the PV Static topology. The code has all the details about what does each part of the code.

B.1. PV Static model

```
%% Solar Calculator. Fixed Module tilt angle and Module's Azimuth.
% This script determines the total irradiance (G_direct, G_diffuse and
% G_ground (or albedo) that a module recieves minutely per year. The
    module
% has a fixed azimuth (180 degrees for North hemisphere or 0 degrees
    for South one) and a
% fixed tilting angle (the default one depending the region in the
    world
% where the panel wants to be used.
tic

%A=xlsread('03_Final_Delft_NishantInput_20170501.xlsx'); %<---Contains
    the info from Meteonorm.
info_name = 'Christchurch_data_A.mat';
A = load(info_name);

%% First we calculate the Sun's position for every minute of the year:
    solar azimuth and altitude.
% Use this code when it is extracted from an excel file
% latitude = A(1:1,7); % Get the latitude from file. At that row,
    column. %Negative value = it's in the South hemisphere. Positive
    value = North hemisphere.
% longitude = A(1:1,8); % Get the longitude from file. At that row,
    column. %Negative value = it's in the Western. Positive value =
    Eastern.
% DNI = A(3:end,7);
% GHI = A(3:end,6);
% DHI = A(3:end,8);
% minute = A(3:end,5);
% second = 0;
% UTC_orig = A(1:1,9);
% albedo = 0.2;

% Use this one if you use the command: load A = load(filename);
```

```
latitude = A.A(1:1,7); % Get the latitude from file. At that row,
    column. %Negative value = it's in the South hemisphere. Positive
    value = North hemisphere.
longitude = A.A(1:1,8); % Get the longitude from file. At that row,
    column. %Negative value = it's in the Western. Positive value =
    Eastern.
DNI = A.A(3:end,7);
GHI = A.A(3:end,6);
DHI = A.A(3:end,8);
minute = A.A(3:end,5);
second = 0;
UTC_orig = A.A(1:1,9);
albedo = 0.2;
M_tilt = 49; % Module's tilting. Since the file is from Delft, 30
    degrees is the used module's tilting angle.
devia = 0; % Minutes in which there are differences in comparison with
    SAM. It helps to get almost the same analemma from SAM.
a_M = 90-M_tilt; % Module's altitude

if latitude >= 0 % Module's Azimuth. 180 = Facing south; 0 = Facing
    North.
        A_M = 180;
else
        A_M = 0;
end

%% Calculation of the enegy yield according to the data file previously
     read.
% Units: kWh.
E_GHI_file = sum(GHI)/6e4;
E_DHI_file = sum(DHI)/6e4;
E_DNI_file = sum(DNI)/6e4;

% Equivalent Sun Hours. Units: hours.
ESH_GHI_file = E_GHI_file/365;
ESH_DNI_file = E_DNI_file/365;
ESH_DHI_file = E_DHI_file/365;

% Monthly energy from the file
GHI_01_jan = GHI(1:1440*31); % Number of minutes in January (1440 mins
    * 31 days)
GHI_02_feb = GHI(44641:84960);
GHI_03_mar = GHI(84961:129600);
GHI_04_apr = GHI(129601:172800);
GHI_05_may = GHI(172801:217440);
GHI_06_jun = GHI(217441:260640);
GHI_07_jul = GHI(260641:305280);
GHI_08_aug = GHI(305281:349920);
GHI_09_sep = GHI(349921:393120);
GHI_10_oct = GHI(393121:437760);
GHI_11_nov = GHI(437761:480960);
GHI_12_dec = GHI(480961:525600);

%% Calculated Monthly Energy Yield from file [kWh]
E_file_01_jan = sum(GHI_01_jan)/6e4;
E_file_02_feb = sum(GHI_02_feb)/6e4;
```

```
E_file_03_mar = sum(GHI_03_mar)/6e4;
E_file_04_apr = sum(GHI_04_apr)/6e4;
E_file_05_may = sum(GHI_05_may)/6e4;
E_file_06_jun = sum(GHI_06_jun)/6e4;
E_file_07_jul = sum(GHI_07_jul)/6e4;
E_file_08_aug = sum(GHI_08_aug)/6e4;
E_file_09_sep = sum(GHI_09_sep)/6e4;
E_file_10_oct = sum(GHI_10_oct)/6e4;
E_file_11_nov = sum(GHI_11_nov)/6e4;
E_file_12_dec = sum(GHI_12_dec)/6e4;

%% Calculated Monthly Energy Yield from file [kWh]
Energy_file_01_jan = sum(GHI_01_jan)*60/3.6e6;
Energy_file_02_feb = sum(GHI_02_feb)*60/3.6e6;
Energy_file_03_mar = sum(GHI_03_mar)*60/3.6e6;
Energy_file_04_apr = sum(GHI_04_apr)*60/3.6e6;
Energy_file_05_may = sum(GHI_05_may)*60/3.6e6;
Energy_file_06_jun = sum(GHI_06_jun)*60/3.6e6;
Energy_file_07_jul = sum(GHI_07_jul)*60/3.6e6;
Energy_file_08_aug = sum(GHI_08_aug)*60/3.6e6;
Energy_file_09_sep = sum(GHI_09_sep)*60/3.6e6;
Energy_file_10_oct = sum(GHI_10_oct)*60/3.6e6;
Energy_file_11_nov = sum(GHI_11_nov)*60/3.6e6;
Energy_file_12_dec = sum(GHI_12_dec)*60/3.6e6;

% The next line will be used to create a graphic of bars later. The
   monthly
% monthly energy from the file [kWh/m^2]
Energy_monthly_file = [Energy_file_01_jan, Energy_file_02_feb,...
    Energy_file_03_mar, Energy_file_04_apr,Energy_file_05_may,...
    Energy_file_06_jun,Energy_file_07_jul, Energy_file_08_aug,...
    Energy_file_09_sep,Energy_file_10_oct, Energy_file_11_nov,
       Energy_file_12_dec];

E_monthly_file = [E_file_01_jan, E_file_02_feb, E_file_03_mar,
   E_file_04_apr,...
    E_file_05_may, E_file_06_jun,E_file_07_jul, E_file_08_aug,
       E_file_09_sep,...
    E_file_10_oct, E_file_11_nov, E_file_12_dec];

%% Calculated Monthly ESH from file [kWh]
ESH_file_01_jan = E_file_01_jan/365;
ESH_file_02_feb = E_file_02_feb/365;
ESH_file_03_mar = E_file_03_mar/365;
ESH_file_04_apr = E_file_04_apr/365;
ESH_file_05_may = E_file_05_may/365;
ESH_file_06_jun = E_file_06_jun/365;
ESH_file_07_jul = E_file_07_jul/365;
ESH_file_08_aug = E_file_08_aug/365;
ESH_file_09_sep = E_file_09_sep/365;
ESH_file_10_oct = E_file_10_oct/365;
ESH_file_11_nov = E_file_11_nov/365;
ESH_file_12_dec = E_file_12_dec/365;

%% Find the Solar Altitude and Azimuth
% Variables that are calculated per hour.
```

```
days_per_month = [31 28 31 30 31 30 31 31 30 31 30 31];
minutes_past_midnight = zeros(525600,1);
hour_angle = zeros(525600,1);
cos_theta_0 = zeros(525600,1);
theta_0 = zeros(525600,1); %Solar Zenith Angle.
num_of_days = 0; % # of days that have passed in the year.
position = 0; %Counter
LSTM = 15*round(abs(longitude)/15); %local longitude of standard time
    meridian.
DD = zeros(525600,1); % day-to-day with an annual cycle.
ET = zeros(525600,1); % Equation of time.
AST = zeros(525600,1); %Apparent Solar Time.
time_in_hour = zeros(525600,1);
time_in_mins_step1 = zeros(525600,1);
time_in_mins_step2 = zeros(525600,1);
time_in_mins = zeros(525600,1);
decl_angle = zeros(525600,1); % declination angle
sin_altitude_left = zeros(525600,1);
sin_altitude_right = zeros(525600,1);
sin_altitude_sum = zeros(525600,1);
altitude = zeros(525600,1); % Sun's altitude
azimuth_prev = zeros(525600,1);
azimuth = zeros(525600,1); % Sun's azimuth
azim_num = zeros(525600,1);
azim_den = zeros(525600,1);
latitude_kron = kron(latitude,ones(525600,1));

for months_minutely = 1:12
    for day_minutely = 1:days_per_month(months_minutely)
        num_of_days = num_of_days + 1;
        for hours_minutely = 0:23
            for minutes_minutely = 0:59
                position = position + 1;
                %Steps to calculate the hour angle.
                DD(position,1) = 360*(num_of_days - 81)/365; % day-to-
                    day with an annual cycle.
                ET(position,1) = 9.87*sind(2*DD(position,1)) - 7.53*
                    cosd(DD(position,1)) - 1.5*sind(DD(position,1)); %
                    Equation of time.
                AST(position,1) = (hours_minutely*60 + minutes_minutely
                    ) + 4*(LSTM - abs(longitude)) + ET(position,1);
                time_in_hour(position,1) = fix(AST(position,1)./60); %
                    The hours of the day.
                time_in_mins_step1(position,1) = AST(position,1)./60; %
                     Get the hours with decimals, e.g. 7.433
                time_in_mins_step2(position,1) = time_in_mins_step1(
                    position,1) - fix(time_in_mins_step1(position,1));
                    % Get the decimals (7.4333 - 7 = 0.4333)
                time_in_mins(position,1) = fix(time_in_mins_step2(
                    position,1).*60); %Get the minutes of the hours of
                    the day: fix(0.4333*60) = 25

                 % Correction of deviation between SAM and this code
                     check
                 % the variable "devia" to see the time difference. For
                 % Delft it turned to be about 25 minutes
```

```
if time_in_mins(position,1) < devia
    time_in_mins(position,1) = time_in_mins(position,1)
       - devia +60;
    time_in_hour(position,1) = time_in_hour(position,1)
        - 1;
else
    time_in_mins(position,1) = time_in_mins(position,1)
        - devia;
end

%% Here we calculate the sun's altitude and azimuth
% 1st we calculate the "declination angle"
decl_angle(position,1) = 23.45 * sind((num_of_days+284)
   *360/365);

% 2nd is the Calculation of the hour angle
% But first we calculate the minutes past from midnight
minutes_past_midnight(position,1) = time_in_hour(
   position,1).*60+time_in_mins(position,1); %I.E.:
   for 15:25 it'd be: 15*60+25=925

% Hour angle.
hour_angle(position,1) = (minutes_past_midnight(
   position,1)-720)./4;

% 2nd get sun's altitude is calculated
sin_altitude_left(position,1) = cosd(latitude_kron(
   position,1)).*...
    cosd(decl_angle(position,1)).*cosd(hour_angle(
       position,1));
sin_altitude_right(position,1) = sind(latitude_kron(
   position,1)).*...
    sind(decl_angle(position,1));
sin_altitude_sum(position,1) = sin_altitude_left(
   position,1)+...
    sin_altitude_right(position,1);
altitude(position,1) = asind(sin_altitude_sum(position
   ,1));

%3rd get Sun's azimuth angle
azim_num(position,1) = sind(altitude(position,1)).*sind
   (latitude_kron(position,1))...
    -sind(decl_angle(position,1));
azim_den(position,1) = cosd(altitude(position,1)).*cosd
   (latitude_kron(position,1));
azimuth_prev(position,1) = acosd(azim_num(position,1)./
   azim_den(position,1)).*...
    sign(hour_angle(position,1));

% azimuth_prev is given in notation 0 tp 180 and 0 to
   -180.
% This "if-statement" is used to make it from 0 to 360.
if azimuth_prev(position,1) >= 0
    azimuth(position,1) = 180+azimuth_prev(position,1);

else %if azimuth_prev(position,1) < 0
```

```
                    azimuth(position,1) = 180-abs(azimuth_prev(position
                        ,1));
                end

                % Calculate the Solar Zenith.
                theta_0(position,1) = acosd(sind(latitude)*sind(
                    decl_angle(position,1)) + cosd(latitude)*cosd(
                    decl_angle(position,1))*cosd(hour_angle(position,1)
                    )); %Solar Zenith.
                cos_theta_0(position,1) = sind(latitude).*sind(
                    decl_angle(position,1)) + cosd(latitude).*cosd(
                    decl_angle(position,1)).*cosd(hour_angle(position
                    ,1));
            end % minutes_minutely = 0:59
        end %hours_minutely =1:24
    end %end for days_minutely =...
end %end months_minutely = 1:12

%% Calculating direct irradiance (G_dir) on the module
% Calculating cos(gamma). (Angle between the surface normal and the
% incident direction of the sunlight).
cosgamma = zeros(length(DNI),1); %Preallocation for speed.

for j=1:length(DNI)
    cosgamma(j,1) = cosd(a_M)*cosd(altitude(j,1))*cosd(A_M-azimuth(j,1)
        )+...
         sind(a_M)*sind(altitude(j,1));
end %End for

G_dir = zeros(length(DNI),1); % REAL DNI (from file)

for l=1:length(DNI)
    G_dir(l,1) = DNI(l) .* cosgamma(l); % REAL DNI (from file)

    if G_dir(l,1) < 0 % REAL DNI (from file)
        G_dir(l,1) = 0;
    else
        continue
    end %end if G_dir
end %end for

%% Calculating diffuse irradiance on the module (Using the Sandia Model
    )
SVF = (1+cosd(M_tilt))/2;% Sky view factor
G_diff = DHI.*SVF + GHI.*(0.012.*theta_0 - 0.04).*(1-cosd(M_tilt))./2;

%% Calculate G_albedo or G_ground (Albedo Irradiance).
G_ground = GHI.*albedo.*(1-SVF);

%% Total irradiance received by the module per minute (sum of matrices)
    .
G_M_total = G_dir + G_diff + G_ground; %REAL DNI

%% Irradiance per year.
G_dir_final = sum(G_dir); %REAL Total irradiance on the module.
G_dir_max = max(G_dir);
```

```
G_diff_final = sum(G_diff); %Total irradiance on the module.
G_diff_max = max(G_diff);

G_ground_final = sum(G_ground);
G_ground_max = max(G_ground);

G_M_total_final = sum(G_M_total); %REAL DNI
G_M_total_max = max(G_M_total);

%% Calculated Energy yields and ESH.
% Energy on the module [kWh]
E_GHI_module = G_M_total_final/6e4;%REAL DNI

E_DNI_module = G_dir_final/6e4;%REAL DNI

E_DHI_module = G_diff_final/6e4;
E_ground_module = G_ground_final/6e4;

% Equivalent Sun Hours enhanced [hr]
ESH_GHI_module = E_GHI_module/365; % REAL DNI
ESH_DNI_module = E_DNI_module/365; % REAL DNI
ESH_DHI_module = E_DHI_module/365;
ESH_Ground_module = E_ground_module/365;

%% REAL Monthly irradiance falling onto the module [W/m^2] ---------o
   ------------------o------------------o------------------o---------
G_M_total_jan = G_M_total(1:1440*31); % Number of minutes in January
   (1440 mins * 31 days)
G_M_total_feb = G_M_total(44641:84960);
G_M_total_mar = G_M_total(84961:129600);
G_M_total_apr = G_M_total(129601:172800);
G_M_total_may = G_M_total(172801:217440);
G_M_total_jun = G_M_total(217441:260640);
G_M_total_jul = G_M_total(260641:305280);
G_M_total_aug = G_M_total(305281:349920);
G_M_total_sep = G_M_total(349921:393120);
G_M_total_oct = G_M_total(393121:437760);
G_M_total_nov = G_M_total(437761:480960);
G_M_total_dec = G_M_total(480961:525600);

%% Calculated Monthly Energy Yield [kWh]
E_01_jan = sum(G_M_total_jan)/6e4;
E_02_feb = sum(G_M_total_feb)/6e4;
E_03_mar = sum(G_M_total_mar)/6e4;
E_04_apr = sum(G_M_total_apr)/6e4;
E_05_may = sum(G_M_total_may)/6e4;
E_06_jun = sum(G_M_total_jun)/6e4;
E_07_jul = sum(G_M_total_jul)/6e4;
E_08_aug = sum(G_M_total_aug)/6e4;
E_09_sep = sum(G_M_total_sep)/6e4;
E_10_oct = sum(G_M_total_oct)/6e4;
E_11_nov = sum(G_M_total_nov)/6e4;
E_12_dec = sum(G_M_total_dec)/6e4;

% Enhanced Monthly ESH
```

```
ESH_01_jan = E_01_jan/31;
ESH_02_feb = E_02_feb/28;
ESH_03_mar = E_03_mar/31;
ESH_04_apr = E_04_apr/30;
ESH_05_may = E_05_may/31;
ESH_06_jun = E_06_jun/30;
ESH_07_jul = E_07_jul/31;
ESH_08_aug = E_08_aug/31;
ESH_09_sep = E_09_sep/30;
ESH_10_oct = E_10_oct/31;
ESH_11_nov = E_11_nov/30;
ESH_12_dec = E_12_dec/31;

%% REAL Monthly irradiance falling onto the module [W/m^2] ---------o
    ------------------o------------------o------------------o---------
G_module_jan = G_M_total(1:1440*31); % Number of minutes in January
    (1440 mins * 31 days)
G_module_feb = G_M_total(44641:84960);
G_module_mar = G_M_total(84961:129600);
G_module_apr = G_M_total(129601:172800);
G_module_may = G_M_total(172801:217440);
G_module_jun = G_M_total(217441:260640);
G_module_jul = G_M_total(260641:305280);
G_module_aug = G_M_total(305281:349920);
G_module_sep = G_M_total(349921:393120);
G_module_oct = G_M_total(393121:437760);
G_module_nov = G_M_total(437761:480960);
G_module_dec = G_M_total(480961:525600);

%% Total Irradiance falling onto the module per month.
G_M_total_01_jan = sum(G_module_jan);
G_M_total_02_feb = sum(G_module_feb);
G_M_total_03_mar = sum(G_module_mar);
G_M_total_04_apr = sum(G_module_apr);
G_M_total_05_may = sum(G_module_may);
G_M_total_06_jun = sum(G_module_jun);
G_M_total_07_jul = sum(G_module_jul);
G_M_total_08_aug = sum(G_module_aug);
G_M_total_09_sep = sum(G_module_sep);
G_M_total_10_oct = sum(G_module_oct);
G_M_total_11_nov = sum(G_module_nov);
G_M_total_12_dec = sum(G_module_dec);

%% Total Energy falling onto the module per month [kWh/m^2]
total_energy_01_jan = sum(G_module_jan)*60/3.6e6;
total_energy_02_feb = sum(G_module_feb)*60/3.6e6;
total_energy_03_mar = sum(G_module_mar)*60/3.6e6;
total_energy_04_apr = sum(G_module_apr)*60/3.6e6;
total_energy_05_may = sum(G_module_may)*60/3.6e6;
total_energy_06_jun = sum(G_module_jun)*60/3.6e6;
total_energy_07_jul = sum(G_module_jul)*60/3.6e6;
total_energy_08_aug = sum(G_module_aug)*60/3.6e6;
total_energy_09_sep = sum(G_module_sep)*60/3.6e6;
total_energy_10_oct = sum(G_module_oct)*60/3.6e6;
total_energy_11_nov = sum(G_module_nov)*60/3.6e6;
total_energy_12_dec = sum(G_module_dec)*60/3.6e6;
```

```
% The next line will be used to create a graphic of bars later.
E_monthly = [E_01_jan, E_02_feb, E_03_mar, E_04_apr, E_05_may, E_06_jun
    ,...
     E_07_jul, E_08_aug, E_09_sep, E_10_oct, E_11_nov, E_12_dec];

Energy_monthly = [total_energy_01_jan, total_energy_02_feb,...
     total_energy_03_mar, total_energy_04_apr, total_energy_05_may,...
     total_energy_06_jun,total_energy_07_jul, total_energy_08_aug,...
     total_energy_09_sep,total_energy_10_oct, total_energy_11_nov,
        total_energy_12_dec];

%% ----------- 1st.- Creation of CSV files. Irradiances and their
    random tilting angles.-----------
% Collecting all the info needed to create the CSV files with relevant
    information.
% Creation of a table with the content of the Irradiances and optimal
    angles.
% We read again the "month", "day" and "hour" columns from the "A" file
% since they were modified.
month = A.A(3:end,2);
hour = A.A(3:end,4);
day = A.A(3:end,3);
% We create a column with 525600 elements for M_azimuth and M_tilt.
    Otherwise
% it fails when making the concatenation.
M_azimuth = kron(A_M,ones(length(DNI),1));
M_tilt = kron(M_tilt,ones(length(DNI),1));

G_concatenation = [month,day,hour,minute,DHI,G_diff,DNI,G_dir,G_ground,
    GHI,...
     G_M_total,altitude,azimuth,M_tilt,M_azimuth];

%% Now we create the .csv file.
file_name1 = 'PVStatic_Irradiances_and_Angles.csv';
csvwrite(file_name1, G_concatenation);
type 'PVStatic_Irradiances_and_Angles.csv';

%% Now we add the row of each column name to know what is what.
%1st create an array with the format needed for the final file
array_created1 = {'Month','Day','Hour','Minute','DHI (from file)','
    G_diff','DNI (from file)',...
     'G_dir','G_ground','GHI (from file)','G_module (REAL)','
        Sun_Altitude','Sun_Azimuth',...
     'Module_tilt','Module_azimuth'};

%% 2nd we attach the array_created to the file called "Final_Delft.csv
    ".
fid = fopen(file_name1, 'w');
fprintf(fid, '%s,', array_created1{1,1:end-1});
fprintf(fid, '%s\n', array_created1{1,end});
fclose(fid);

%Creation of the file.
dlmwrite(file_name1, G_concatenation, '-append');
```

```
%% ----------- 2nd.- Creation of CSV files. Energy yield from File vs
    Calculated.-----------
% Collecting all the info needed
% Creation of an auxiliar table to create the file.
number = 4;
auxiliar2 = zeros(1,number); % Helps to create an auxiliar of 1 row by
    "number" columns.
M_tilt_str = num2str(M_tilt(1)); % Convert number to string because for
     some reason it fails to pass the number directly into the created
    file.
UTC_orig_str = num2str(UTC_orig);
G_diff_max_str = num2str(G_diff_max);

%% Now we create the .csv file.
file_name2 = 'PVStatic_Energy_Yield_And_ESH.csv'; % Name given to the
    created file.
csvwrite(file_name2,auxiliar2); % It helps to create the file. There is
     no calculated data.
type 'PVStatic_Energy_Yield_And_ESH.csv';

%% Now we add the row of each column name to know what is what.
%1st create an array with the format needed for the final file
array_created2 = {'latitude','longitude','Module''s_Tilting','UTC';...
    latitude,longitude,double(M_tilt_str),double(UTC_orig_str);...
    'Info of the place',',',',',',',';... %+3
    ',',',',',',',',';... % White space in the file

    'E_GHI_module [kWh/m^2]','E_DNI_module [kWh/m^2]','E_DHI_module [
       kWh/m^2]',...
    'E_ground_module [kWh/m^2]';...
    E_GHI_module,E_DNI_module,E_DHI_module,E_ground_module;...
    'Energy calculated in the code',',',',',',',';... % Energy calculated
        in this code. 9
    ',',',',',',',',';... % White space in the file

    'E_01_jan [kWh/m^2]','E_02_feb [kWh/m^2]','E_03_mar [kWh/m^2]','
       E_04_apr [kWh/m^2]';...
    E_01_jan,E_02_feb,E_03_mar,E_04_apr;...
    ',',',',',',',',';...% Monthly Energy calculated in this code. 24
    'E_05_may [kWh/m^2]','E_06_jun [kWh/m^2]','E_07_jul [kWh/m^2]','
       E_08_aug [kWh/m^2]';...
    E_05_may,E_06_jun,E_07_jul,E_08_aug;...
    ',',',',',',',',';... % Monthly Energy calculated in this code. 27
    'E_09_sep [kWh/m^2]','E_10_oct [kWh/m^2]','E_11_nov [kWh/m^2]','
       E_12_dec [kWh/m^2]';...
    E_09_sep,E_10_oct,E_11_nov,E_12_dec;...
    'Monthly Energy calculated in the code','REAL',',',',',';... %
       Monthly Energy calculated in this code. 30
    ',',',',',',',',';... % White space in the file

    'G_diff_max [W/m^2]','G_diff_final [W/m^2]','G_M_dir_max [W/m^2]','
       G_M_dir_total [W/m^2]';...
    double(G_diff_max_str),G_diff_final,G_dir_max,G_dir_final;...
    'Diffuse and Direct Irradiances  [W/m^2]',',',',',',',';... %+12
    'G_M_ground_max [W/m^2]','G_M_ground_total [W/m^2]','G_M_total_max
       [W/m^2]','G_M_total [W/m^2]';...
```

```
G_ground_max,G_ground_final,G_M_total_max,G_M_total_final;...
'Albedo or Ground Irradiance and Total irradiance [W/m^2]',',','
   REAL DNI',',';... %+15
',',',',',',',',';... % White space in the file

'E_GHI_file [kWh]','E_DNI_file [kWh]','E_DHI_file [kWh]','
   E_GHI_calculated [kWh]';...
E_GHI_file,E_DNI_file,E_DHI_file,'N/A';...
'Energy calculated from the file',',',',',',';... % Energy
   calculated from the file 3
'ESH_GHI_file [h]','ESH_DNI_file [h]','ESH_DHI_file [h]','
   ESH_Ground_file [h]';...
ESH_GHI_file,ESH_DNI_file,ESH_DHI_file, 'N/A';...
'ESH calculated from the file',',',',',',';... % ESH calculated
   from the file 6
',',',',',',',';... % White space in the file

'ESH_GHI_module [h]','ESH_DNI_module [h]','ESH_DHI_module [h]',...
'ESH_Ground_module [h]'; ...
ESH_GHI_module,ESH_DNI_module,ESH_DHI_module,ESH_Ground_module;...
'ESH calculated in the code',',',',',',';...  % ESH calculated in
   this code. 12
',',',',',',',';... % White space in the file

'E_file_01_jan [kWh/m^2]','E_file_02_feb [kWh/m^2]',...
'E_file_03_mar [kWh/m^2]','E_file_04_apr [kWh/m^2]';...
E_file_01_jan,E_file_02_feb,E_file_03_mar,E_file_04_apr;...
',',',',',',',';... % Monthly Energy calculated from the file. 15
'E_file_05_may [kWh/m^2]','E_file_06_jun [kWh/m^2]',...
'E_file_07_jul [kWh/m^2]','E_file_08_aug [kWh/m^2]';...
E_file_05_may,E_file_06_jun,E_file_07_jul,E_file_08_aug;...
',',',',',',',';... % Monthly Energy calculated from the file. 18
'E_file_09_sep [kWh/m^2]','E_file_10_oct [kWh/m^2]',...
'E_file_11_nov [kWh/m^2]','E_file_12_dec [kWh/m^2]';...
E_file_09_sep,E_file_10_oct,E_file_11_nov,E_file_12_dec;...
'Monthly Energy REAL [kWh/m^2]',',',',',',';... % Monthly Energy
   FROM THE FILE. 21
',',',',',',',';... % White space in the file

'ESH_file_01_jan [h]','ESH_file_02_feb [h]','ESH_file_03_mar [h]','
   ESH_file_04_apr [h]';...
ESH_file_01_jan,ESH_file_02_feb,ESH_file_03_mar,ESH_file_04_apr;...
',',',',',',',';... % Monthly ESH calculated from the file. 33
'ESH_file_05_may [h]','ESH_file_06_jun [h]','ESH_file_07_jul [h]','
   ESH_file_08_aug [h]';...
ESH_file_05_may,ESH_file_06_jun,ESH_file_07_jul,ESH_file_08_aug;...
',',',',',',',';...% Monthly ESH calculated from the file. 36
'ESH_file_09_sep [h]','ESH_file_10_oct [h]','ESH_file_11_nov [h]','
   ESH_file_12_dec [h]';...
ESH_file_09_sep,ESH_file_10_oct,ESH_file_11_nov,ESH_file_12_dec;...
'Monthly ESH calculated from the file',',',',',',';...% Monthly ESH
    calculated from the file. 39
',',',',',',',';... % White space in the file

'ESH_01_jan [h]','ESH_02_feb [h]','ESH_03_mar [h]','ESH_04_apr [h]'
   ;...
```

```
    ESH_01_jan,ESH_02_feb,ESH_03_mar,ESH_04_apr;...
    'Monthly ESH calculated from the code','REAL',',',',';... % Monthly
        ESH calculated from the code. 42
   'ESH_05_may [h]','ESH_06_jun [h]','ESH_07_jul [h]','ESH_08_aug [h]';
      ...
    ESH_05_may,ESH_06_jun,ESH_07_jul,ESH_08_aug;...
    ',',',',',',',',';... % Monthly ESH calculated in this code. 45
    'ESH_09_sep [h]','ESH_10_oct [h]','ESH_11_nov [h]','ESH_12_dec [h]'
       ;...
    ESH_09_sep,ESH_10_oct,ESH_11_nov,ESH_12_dec;...
    'Monthly ESH calculated in the code','REAL',',',',',};% Monthly ESH
       calculated in this code. 48

%% 2nd we attach the array_created to the file called "Final_Delft.csv
    ".
fid = fopen(file_name2, 'w');
for array_line = 1:length(array_created2)
    fprintf(fid, '%s,', array_created2{array_line,1:end-1});
    fprintf(fid, '%s\n', array_created2{array_line,end});
end
fclose(fid);

dlmwrite(file_name2,auxiliar2,'-append'); %Creation of the file.

%% Here the plots of the calculations are done.
%% Figure 1
fntsze = 30; %FontSize on the all the graphics.
fntsze_legend = 22; %FontSize in the graph's legend.
figure(1)
plot(G_M_total); % FROM REAL DNI
hold on

plot(GHI) % GHI from file (original unmodified data)
hold on

plot(G_dir); % FROM REAL DNI
hold on

plot(G_diff);
hold on

plot(G_ground);
hold on
grid on

title('\fontsize{30}Irradiances on PV Static Module. Tilt=49 degrees,
   Azimuth=0 degrees. Christchurch')
xlabel('Minutes/year','FontSize',fntsze)
ylabel('Irradiances [W/m^2]','FontSize',fntsze)
legend({'G_M^{Total}','GHI (from file)','G_{M}^{dir}','G_M^{diff}','G_M
   ^{Ground}'},'FontSize',fntsze_legend)
axis([0 length(DNI) 0 max(GHI)+380]);

% The next line changes the Axis numbers' size.
ax = gca; % current axes
ax.FontSize = fntsze;
```

```
ax.TickLength = [0.02 0.02];


%% Figure 2
figure(2)
plot(G_M_total); % FROM REAL DNI
hold on

plot(GHI) % GHI from file (original unmodified data)
hold on
grid on

title('\fontsize{30}Global Irradiance PV Static Module (G_M^{total}) Vs
    GHI from file. Tilt=49 degrees, Azi=0 degrees. Christchurch')
xlabel('Minutes/year','FontSize',fntsze)
ylabel('Total Irradiance (G_M^{total}) [W/m^2]','FontSize',fntsze)
legend({'G_M^{Total}','GHI (Meteonorm)'},'FontSize',fntsze_legend)
axis([0 length(DNI) 0 max(GHI)+380]);

% The next line changes the Axis numbers' size.
ax = gca; % current axes
ax.FontSize = fntsze;
ax.TickLength = [0.02 0.02];

%% Figure 3
figure (3)
%This configuration code is to generate a side-by-side graphic
E_monthly_comb = [E_monthly;E_monthly_file]'; % Creation of a 12 rows x
    2 columns matrix

hb = bar(E_monthly_comb);
set(hb(1), 'FaceColor','green'); % REAL DNI
set(hb(2), 'FaceColor','red')
grid on

title('\fontsize{30}Monthly Energy from Meteonorm VS PV module. Tilt=49
    degrees, Azimuth=0 degrees. Christchurch')
xlabel('Month of the Year','FontSize',fntsze)
ylabel('Energy [kWh/m^2]','FontSize',fntsze)
legend({'Energy calculated [kWh/m^2]','Energy from Meteonorm [kWh/m^2]'
   },'FontSize',fntsze_legend)
% Lenght for X axis (from 0 to length(E_monthly)+1) and Y axis (from 0
   to max(E_monthly)+20).
axis([0 length(E_monthly)+1 0 max(E_monthly_file)+30]);

% The next line changes the Axis numbers' size.
ax = gca; % current axes
ax.FontSize = fntsze;
ax.TickLength = [0.02 0.02];

%% Figure 4
figure (4)
%This configuration code is to generate a side-by-side graphic
E_monthly_comb = [Energy_monthly;Energy_monthly_file]'; % Creation of a
    12 rows x 2 columns matrix
```

```
hb = bar(E_monthly_comb);
set(hb(1), 'FaceColor','black'); % REAL DNI
set(hb(2), 'FaceColor','red')
grid on

title('\fontsize{30}Energy from the file vs PV module. Tilt=49 degrees,
    Azimuth=0 degrees. Christchurch')
xlabel('Month of the Year','FontSize',fntsze)
ylabel('Energy [kWh/m^2]','FontSize',fntsze)
legend({'Energy calculated [kWh/m^2]','Energy from Meteonorm [kWh/m^2]'
   },'FontSize',fntsze_legend)
% Lenght for X axis (from 0 to length(E_monthly)+1) and Y axis (from 0
   to max(E_monthly)+20).
axis([0 length(Energy_monthly)+1 0 max(Energy_monthly_file)+30]);

% The next line changes the Axis numbers' size.
ax = gca; % current axes
ax.FontSize = fntsze;
ax.TickLength = [0.02 0.02];

%% Figure 5
% Stacked plot to see the contribution of G_dir, G_diff and G_ground vs
    the
% GHI from the input file.
% Monthly energy calculated from G_dir
G_dir_01_jan = G_dir(1:1440*31); % Number of minutes in January (1440
   mins * 31 days)
G_dir_02_feb = G_dir(44641:84960);
G_dir_03_mar = G_dir(84961:129600);
G_dir_04_apr = G_dir(129601:172800);
G_dir_05_may = G_dir(172801:217440);
G_dir_06_jun = G_dir(217441:260640);
G_dir_07_jul = G_dir(260641:305280);
G_dir_08_aug = G_dir(305281:349920);
G_dir_09_sep = G_dir(349921:393120);
G_dir_10_oct = G_dir(393121:437760);
G_dir_11_nov = G_dir(437761:480960);
G_dir_12_dec = G_dir(480961:525600);

% Calculated Monthly Energy Yield from G_dir [kWh]
E_G_dir_01_jan = sum(G_dir_01_jan)/6e4;
E_G_dir_02_feb = sum(G_dir_02_feb)/6e4;
E_G_dir_03_mar = sum(G_dir_03_mar)/6e4;
E_G_dir_04_apr = sum(G_dir_04_apr)/6e4;
E_G_dir_05_may = sum(G_dir_05_may)/6e4;
E_G_dir_06_jun = sum(G_dir_06_jun)/6e4;
E_G_dir_07_jul = sum(G_dir_07_jul)/6e4;
E_G_dir_08_aug = sum(G_dir_08_aug)/6e4;
E_G_dir_09_sep = sum(G_dir_09_sep)/6e4;
E_G_dir_10_oct = sum(G_dir_10_oct)/6e4;
E_G_dir_11_nov = sum(G_dir_11_nov)/6e4;
E_G_dir_12_dec = sum(G_dir_12_dec)/6e4;

%%
```

```
Energy_monthly_G_dir = [E_G_dir_01_jan,E_G_dir_02_feb,E_G_dir_03_mar,
    ...
     E_G_dir_04_apr,E_G_dir_05_may,E_G_dir_06_jun,E_G_dir_07_jul,...
     E_G_dir_08_aug,E_G_dir_09_sep,E_G_dir_10_oct,E_G_dir_11_nov,
        E_G_dir_12_dec];

%% Monthly energy calculated from G_diff
G_diff_01_jan = G_diff(1:1440*31); % Number of minutes in January (1440
    mins * 31 days)
G_diff_02_feb = G_diff(44641:84960);
G_diff_03_mar = G_diff(84961:129600);
G_diff_04_apr = G_diff(129601:172800);
G_diff_05_may = G_diff(172801:217440);
G_diff_06_jun = G_diff(217441:260640);
G_diff_07_jul = G_diff(260641:305280);
G_diff_08_aug = G_diff(305281:349920);
G_diff_09_sep = G_diff(349921:393120);
G_diff_10_oct = G_diff(393121:437760);
G_diff_11_nov = G_diff(437761:480960);
G_diff_12_dec = G_diff(480961:525600);

% Calculated Monthly Energy Yield from G_diff [kWh]
E_G_diff_01_jan = sum(G_diff_01_jan)/6e4;
E_G_diff_02_feb = sum(G_diff_02_feb)/6e4;
E_G_diff_03_mar = sum(G_diff_03_mar)/6e4;
E_G_diff_04_apr = sum(G_diff_04_apr)/6e4;
E_G_diff_05_may = sum(G_diff_05_may)/6e4;
E_G_diff_06_jun = sum(G_diff_06_jun)/6e4;
E_G_diff_07_jul = sum(G_diff_07_jul)/6e4;
E_G_diff_08_aug = sum(G_diff_08_aug)/6e4;
E_G_diff_09_sep = sum(G_diff_09_sep)/6e4;
E_G_diff_10_oct = sum(G_diff_10_oct)/6e4;
E_G_diff_11_nov = sum(G_diff_11_nov)/6e4;
E_G_diff_12_dec = sum(G_diff_12_dec)/6e4;

%%
Energy_monthly_G_diff = [E_G_diff_01_jan,E_G_diff_02_feb,
    E_G_diff_03_mar,...
     E_G_diff_04_apr,E_G_diff_05_may,E_G_diff_06_jun,E_G_diff_07_jul,
        E_G_diff_08_aug,...
     E_G_diff_09_sep,E_G_diff_10_oct,E_G_diff_11_nov,E_G_diff_12_dec];

%% Monthly energy calculated from G_ground
G_ground_01_jan = G_ground(1:1440*31); % Number of minutes in January
    (1440 mins * 31 days)
G_ground_02_feb = G_ground(44641:84960);
G_ground_03_mar = G_ground(84961:129600);
G_ground_04_apr = G_ground(129601:172800);
G_ground_05_may = G_ground(172801:217440);
G_ground_06_jun = G_ground(217441:260640);
G_ground_07_jul = G_ground(260641:305280);
G_ground_08_aug = G_ground(305281:349920);
G_ground_09_sep = G_ground(349921:393120);
G_ground_10_oct = G_ground(393121:437760);
G_ground_11_nov = G_ground(437761:480960);
G_ground_12_dec = G_ground(480961:525600);
```

```
% Calculated Monthly Energy Yield from G_ground [kWh]
E_G_ground_01_jan = sum(G_ground_01_jan)/6e4;
E_G_ground_02_feb = sum(G_ground_02_feb)/6e4;
E_G_ground_03_mar = sum(G_ground_03_mar)/6e4;
E_G_ground_04_apr = sum(G_ground_04_apr)/6e4;
E_G_ground_05_may = sum(G_ground_05_may)/6e4;
E_G_ground_06_jun = sum(G_ground_06_jun)/6e4;
E_G_ground_07_jul = sum(G_ground_07_jul)/6e4;
E_G_ground_08_aug = sum(G_ground_08_aug)/6e4;
E_G_ground_09_sep = sum(G_ground_09_sep)/6e4;
E_G_ground_10_oct = sum(G_ground_10_oct)/6e4;
E_G_ground_11_nov = sum(G_ground_11_nov)/6e4;
E_G_ground_12_dec = sum(G_ground_12_dec)/6e4;

%%
Energy_monthly_G_ground = [E_G_ground_01_jan,E_G_ground_02_feb,
    E_G_ground_03_mar,...
     E_G_ground_04_apr,E_G_ground_05_may,E_G_ground_06_jun,
        E_G_ground_07_jul,...
     E_G_ground_08_aug,E_G_ground_09_sep,E_G_ground_10_oct,
        E_G_ground_11_nov,...
     E_G_ground_12_dec];

%%
Energy_monthly_G_module = [Energy_monthly_G_dir;Energy_monthly_G_diff;
    ...
     Energy_monthly_G_ground]'; % Creation of a 12 rows x 3 columns
        matrix

%% Final part: the plotting.
figure(5)
hb = bar(1:12, Energy_monthly_G_module, 0.5,'stack');
set(hb(1),'FaceColor','k');
%legend('G_{dir}', 'G_{diff}', 'G_{ground}')
hold on

hb2 = bar(Energy_monthly_file,0.2);
set(hb2(1),'FaceColor','red');
grid on
%
title('\fontsize{30}Energy from Meteonorm vs PV Static. Tilt=49 degrees
    , Azimuth=0 degrees. Christchurch')
xlabel('Month of the Year','FontSize',fntsze)
ylabel('Energy [kWh/m^2]','FontSize',fntsze)
legend({'G_M^{dir}', 'G_M^{diff}', 'G_M^{ground}','GHI (Meteonorm)',...
     'GHI (Meteonorm)'},'FontSize',fntsze_legend)
% Lenght for X axis (from 0 to length(E_monthly)+1) and Y axis (from 0
    to max(E_monthly)+20).
axis([0 13 0 max(Energy_monthly_file)+30]);

% The next line changes the Axis numbers' size.
ax = gca; % current axes
ax.FontSize = fntsze;
ax.TickLength = [0.02 0.02];
```

```
%% Plot of analemma
% figure 6
% figure(6)
% info_name2 = 'SAM_Alti_Azim_data_A.mat';
% B = load(info_name2);
% %SAM=xlsread('SAMs_SolarAltitudesAndAzimuths.xlsx'); %<---Contains
    the info from SAM.
% SAM_alt = B.SAM(:,1);
% SAM_azim = B.SAM(:,2);
%
% fntsze = 18;
% ix = 180:1440:525600;
% n = 60;
% c = 0;
% for hr_Counter = 3:23
%     c = c+1;
%     plot(azimuth(ix+n*c),altitude(ix+n*c),'*')
%     hold on
% end
%
% c=0;
% for hr_Counter = 3:23
%     c = c+1;
%     plot(SAM_azim(ix+n*c),SAM_alt(ix+n*c),'k')
%     hold on
% end
% grid on
%
% title('\fontsize{18}Ashrae''s Analemma (rainbow) VS SAM''s Analemma (
    black). Delft')
% xlabel('Sun Azimuth [^o]','FontSize',fntsze)
% ylabel('Sun Altitude [^o]','FontSize',fntsze)
% legend({'3h00 Analemma','4h00 Analemma','5h00 Analemma',...
%     '6h00 Analemma','7h00 Analemma','8h00 Analemma','9h00 Analemma
    ',...
%     '10h00 Analemma','11h00 Analemma','12h00 Analemma','13h00
    Analemma',...
%     '14h00 Analemma','15h00 Analemma','16h00 Analemma','17h00
    Analemma',...
%     '18h00 Analemma','19h00 Analemma','20h00 Analemma','21h00
    Analemma',...
%     '22h00 Analemma','23h00 Analemma'},'FontSize',fntsze)
% % Lenght for X axis (from 0 to length(E_monthly)+1) and Y axis (from
    0 to max(E_monthly)+20).
% axis([0 max(azimuth) 0 max(altitude)+5]);
%
% % The next line changes the Axis numbers' size.
% ax = gca; % current axes
% ax.FontSize = fntsze;
% ax.TickLength = [0.02 0.02];
toc
```

Bibliography

[1] H. D. R. . United Nations Development Programme, *Informe sobre desarrollo humano 2015,* (2015), accessed: 2017-07-10.

[2] O. Isabella, K. Jäger, A. Smets, R. van Swaaij, and M. Zeman, *Solar Energy: The Physics and Engineering of Photovoltaic Conversion, Technologies and Systems* (UIT Cambridge Ltd., 2016).

[3] J. A. Fuentes Casillas, *Ilkerin Kenya: Design of a Hybrid Renewable System Using a PV System and Biomass Digesters and Feasibility Analysis for a Solar Water Pump in the Ilkerin-Loita Integral Devel- opment Programme*, Tech. Rep. (TU Delft, 2015).

[4] rs-online, *Charge controller,* (2016), accessed: 2017-07-11.

[5] L. Edge, *Battery bank,* (2016), accessed: 2017-07-11.

[6] M. Hankins, *Stand-alone Solar Electric Systems: The Earthscan Expert Handbook for Planning, Design and Installation*, Vol. I (Earthscan, 2010) pp. 19–21.

[7] T. Korea, *Rooftop semi-static tracker,* (2017), accessed: 2017-07-11.

[8] A. Expo, *Static roof mounting system,* (2017), accessed: 2017-07-11.

[9] S. Choice, *Solar trackers,* (2010), accessed: 2017-07-11.

[10] T. of Malta, *Solaqua floating solar panels project nears completion,* (2016), accessed: 2017-08-07.

[11] S. Baker, *The benefits of floating solar panels,* (2017), accessed: 2017-08-07.

[12] KNMI, *Koninklijk nederlands meteorologisch instituut,* (2017), accessed: 2017-07-12.

[13] Meteotest, *Meteonorm: Irradiation data for every place on earth,* (2017), accessed: 2017-07-13.

[14] J. Remund, S. Müller, S. Kunz, B. Huguenin-Landl, C. Studer, D. Klauser, C. Schilter, and R. Lehnher, *Meteonorm Handbook Part II: Theory*, Tech. Rep. (Meteotest, Bern, Switzerland, 2015).

[15] Time and D. AS, *Time zone map,* (2017), accessed: 2017-07-12.

[16] R. American Society of Heating and I. Air-Conditioning Engineers, *2011 ASHRAE HANDBOOK: Heating, Ventilating, and Air-Conditioning APPLICATIONS*, Vol. SI Edition (ASHRAE, 2011) pp. 497–498.

[17] R. American Society of Heating and A.-C. Engineers, *About ashrae,* (2017), accessed: 2017-07-12.

[18] A. a Mathematician / Ask a Physicist., *Q: Why isn't the shortest day of the year also the day with the earliest sunset?* (2010), accessed: 2017-08-06.

[19] V. Energy, *What is direct normal irradiance?* (2017), accessed: 2017-07-12.

[20] V. Energy, *What is diffuse horizontal irradiance?* (2017), accessed: 2017-07-12.

[21] D. T. Reindl, W. A. Beckman, and J. A. Duffie, *Evaluation of hourly tilted surface radiation models,* Solar Energy **45**, 9 (1990).

[22] A. Luque and S. Hegedus, *Handbook of Photovoltaic Science and Engineering*, edited by A. Luque and S. Hegedus (John Wiley & Sons, Ltd, Chichester, UK, 2011).

[23] O. Isabella, *Sky models,* PV Systems Course **3**, 31 (2014).

[24] P. G. Loutzenhiser, H. Manz, C. Felsmann, P. A. Strachan, T. Frank, and G. M. Maxwell, *Empirical validation of models to compute solar irradiance on inclined surfaces for building energy simulation,* Solar Energy **81**, 254 (2007).

[25] S. Dervishi and A. Mahdavi, *Computing diffuse fraction of global horizontal solar radiation: A model comparison,* Solar Energy **86**, 1796 (2012).

[26] NREL, *System Advisor Model (SAM).*, Tech. Rep. (NREL, 2017).

[27] R. Perez, P. Ineichen, R. Seals, J. Michalsky, and R. Stewart, *Modeling daylight availability and irradiance components from direct and global irradiance,* Solar Energy **44**, 271 (1990).

[28] S. N. Laboratories, *Simple sandia sky diffuse model,* (2014), accessed: 2017-07-12.

[29] A. P. C. W. H. M. Lave, W. Hayes, *Evaluation of Global Horizontal Irradiance to Plane-of-Array Irradiance Models at Locations Across the United States,* Solar Energy **5**, 597 (2015).

[30] PVSyst, *Albedo Coefficient,* (2015), accessed: 2017-07-19.

[31] N. Snow and I. D. Center, *All about sea ice. thermodynamics: Albedo,* (2017), accessed: 2017-07-12.

[32] M. Boxwell, *Solar Electricity Handbook - 2017*, Vol. I (Earthscan, 2017) p. 177.

[33] T. S. E. H. website, *Solar angle calculator,* (2017), accessed: 2017-07-14.

[34] N. R. E. Laboratories, *System advisor model (sam),* (2017), accessed: 2017-07-13.

[35] N. R. E. Laboratories, *About,* (2017), accessed: 2017-08-10.

[36] P. Software, *About us. we hope you will enjoy pvsyst!* (2017), accessed: 2017-08-10.

[37] http://cimss.ssec.wisc.edu, *What is matlab?* (2017), accessed: 2017-07-14.

[38] P. Software, *Pvsyst photovoltaic software,* (2017), accessed: 2017-07-14.

[39] Mathworks, *Math. graphics. programming.* (2017), accessed: 2017-07-14.

[40] A. S. Bosch, *Photovoltaic system feasibility study Designing a blueprint for sustainable schools in India*, Vol. I (TU Delft, 2015) p. 89.

[41] K. E. Holbert, *Solar calculations,* (2007), accessed: 2017-05-28.

[42] K. E. Holbert, *Solar calculations,* (2007), accessed: 2017-05-28.

[43] E. GOODE, *New solar plants generate floating green power,* (2016), accessed: 2017-07-19.